

1. Report No.		2. Government Accession No.		3. Recipient's Catalog No.	
4. Title and Subtitle AUTOMOBILE ACCIDENT RECONSTRUCTION BY DYNAMIC SIMULATION				5. Report Date May 1983	
				6. Performing Organization Code	
7. Author(s) Walter S. Reed				8. Performing Organization Report No. Research Report 302-1F	
9. Performing Organization Name and Address Center for Transportation Research The University of Texas at Austin Austin, Texas 78712-1075				10. Work Unit No.	
				11. Contract or Grant No. Research Study 3-18-80-302	
12. Sponsoring Agency Name and Address Texas State Department of Highways and Public Transportation; Transportation Planning Division P. O. Box 5051 Austin, Texas 78763				13. Type of Report and Period Covered Final	
				14. Sponsoring Agency Code	
15. Supplementary Notes Study conducted in cooperation with the Texas State Department of Highways and Public Transportation					
16. Abstract <p>The overall motivation for this study is to improve the safety of automobile travel through a better understanding of the predominant characteristics which lead to an accident and influence injury severity. Quantification of conditions of accidents and vehicle and occupant behavior have currently led to many improvements in the design of vehicles and roadways, as well as aiding our legal system in administrating justice. Simulation of vehicle collisions has played an important role in this progress. Yet, substantial potential for further improvement exists. The focus of this report pertains to the approach being taken in the development of new dynamic computer simulation techniques by a research team at The University of Texas at Austin.</p> <p>The work presented herein represents only the beginning of a very extensive program of research. The progress to date has been quite good and represents a significant step in accomplishing our goals.</p>					
17. Key Words automobile accident, reconstruction, simulation, safety, computer, modularized algorithms, impact, trajectory			18. Distribution Statement No restrictions. This document is available to the public through the National Technical Information Service, Springfield, Virginia 22161.		
19. Security Classif. (of this report) Unclassified		20. Security Classif. (of this page) Unclassified		21. No. of Pages 222	22. Price

AUTOMOBILE ACCIDENT RECONSTRUCTION
BY DYNAMIC SIMULATION

by

Walter S. Reed

Research Report Number 302-1F

Automobile Accident Reconstruction
by Dynamic Simulation

Research Project 3-18-80-302

conducted for

Texas

State Department of Highways and Public Transportation

in cooperation with the
U. S. Department of Transportation
Federal Highway Administration

by the

CENTER FOR TRANSPORTATION RESEARCH
BUREAU OF ENGINEERING RESEARCH
THE UNIVERSITY OF TEXAS AT AUSTIN

May 1983

The contents of this report reflect the views of the authors, who are responsible for the facts and the accuracy of the data presented herein. The contents do not necessarily reflect the official views or policies of the Federal Highway Administration. This report does not constitute a standard, specification, or regulation.

There was no invention or discovery conceived or first actually reduced to practice in the course of or under this contract, including any art, method, process, machine, manufacture, design or composition of matter, or any new and useful improvement thereof, or any variety of plant which is or may be patentable under the patent laws of the United States of America or any foreign country.

ACKNOWLEDGEMENTS

I would like to first express my sincere appreciation to all those members of the Governor's Office of Traffic Safety and later the Office of Traffic Safety, Texas Department of Highways and Public Transportation who interacted with me and supported this work. I am deeply indebted to these people who were kind enough to support my work for many years and provide a basis for my professional development in this field. Without their help, my work in this area would not have been possible and the current support for my work would not have been forthcoming.

I would also like to thank Dr. Craig Smith whose contributions to this project were substantial. His leadership in developing the MASS concept laid the foundation for much of what the current system has evolved into. I also would like to thank all of the dedicated students who have put the pieces of this system together and made our concept a reality.

SUMMARY

The overall motivation for this study is to improve the safety of automobile travel through a better understanding of the predominant characteristics which lead to an accident and influence injury severity. Quantification of conditions of accidents and vehicle occupant behavior have currently lead to many improvements in the design of vehicles and roadways, as well as aiding our legal system in administrating justice. Simulation of vehicle collisions has played an important role in this progress. Yet, substantial potential for further improvement exists. The focus of this report pertains to the approach being taken in the development of new dynamic computer simulation techniques by a research team at The University of Texas at Austin.

The work presented herein represents only the beginning of a very extensive program of research. The progress to date has been quite good and represents a significant step in accomplishing our goals.

TABLE OF CONTENTS

Acknowledgement	iii
Chapter I - Introduction	1
Chapter II - Vehicle Collision Reconstruction	13
Impact Phase: Principle of Impulse and Momentum	14
Impact Phase: Conservation of Mechanical Energy	18
Trajectory Phase: Conservation of Mechanical Energy	20
Simulation Techniques	21
Computer Simulation of Vehicle Collisions: A Survey	28
Modular Accident Simulation System	31
Chapter III - Trajectory Analysis Algorithm	35
Derivation of Vehicle Equations of Motion	35
Tire Model	42
Speed Dependency	43
Tire Forces	44
Wheel Slip Angle	47
Tire Force Direction	48
Friction Circle Concept	49
Tire Lateral Force Model	53
Chapter IV - Impact Phase Analysis	57
General Impact Equations	58
Linear Momentum Impact Equations	58

Angular Momentum Impact Equations	61
Impact Analysis Equation Systems	63
Classification of Linear Momentum Equation Variables	65
Classification of Angular Momentum Equation Variables	68
Solution of Impact Analysis Equation Systems	70
Chapter V - A Computer Hardware/Software System	75
MASS Operating System	77
Graphic Input Device	77
Control and Execution of Analysis Modules	84
Graphic Output Device	85
Output File Management	87
Reconstruction Example	91
Description of Accident	91
Collection of the Data	93
Scale Drawing	93
Vehicle and Zone Properties	95
Input of Data to MASS	101
Display of Post-Crash Output	110
Impact Analysis	113
Pre-Crash Analysis	115
Miscellaneous Information	116
Chapter VI - Measurement of Road/Tire Friction Characteristics	119
General Considerations	119
The Coefficient of Friction	127

Measurement Techniques	134
Accelerometer	146
Micro-Computer	152
Computer Mode Operations	159
Calibration	160
Execution	163
Tape Dump	165
Display G's	166
Fifth Wheel	166
System Testing and Data Evaluation	167
Testing Procedure	169
Test Results	171
Chapter VII - Summar and Current Work	203
References	205

CHAPTER I

INTRODUCTION

A great number of papers have appeared related to the characteristics of automobile collisions. The overall motivation for pursuing these studies is to improve the safety of automobile travel through a better understanding of the predominant characteristics which lead to an accident and influence injury severity. Quantification of conditions of accidents and vehicle and occupant behavior have currently led to many improvements in the design of vehicles and roadways, as well as aiding our legal system in administering justice. Simulation of vehicle collisions has played an important role in this progress. Yet, substantial potential for further improvement exists. The focus of this report pertains to the approach being taken in the development of new dynamic computer simulation techniques by a research team at The University of Texas at Austin.

Before discussing the alternative simulation approaches the goals of accident reconstruction require further elaboration. A discussion of reconstruction goals, as related to potential injury severity studies, requires an understanding of the factors affecting occu-

pant injury in automobile collisions. Marquardt [1]^{*} has organized these factors into groups of vehicle-related factors, relating to the collision external to the occupant compartment, and occupant-related factors, which relate to occupant compartment interactions. The analysis presented shows the actual injury incurred is determined by occupant-related factors for a given Peak Contact Velocity (PCV). Peak Contact Velocity is defined as the maximum relative velocity with which the occupant can contact the vehicle interior. The PCV is essentially the velocity change of the vehicle during the crushing phase, when the vehicles are brought from their original velocities to a common velocity in the forward phase of impact. Consequently, the determination of velocity changes in vehicle accidents is an important step in quantifying injury severity potential. The actual injury is a function of many occupant-related factors and Marquardt has concluded that a statistically valid sample of the random occupant variables is necessary to draw conclusions about the correlation of injuries to accident conditions.

Although staged accidents with test dummies present a method to generate statistical data, a large number of accidents would be required to draw viable conclusions. However, a large number of field accidents

^{*} Brackets will be used to cite references in the attached bibliography.

occur on our nation's highways every year which could serve as the basis for a statistical study, given simulation techniques applicable to field accident reconstruction. The National Highway and Traffic Safety Administration has sponsored a National Crash Severity Study to obtain the first such statistical data using a computer simulation program to reconstruct a large number of accidents across the nation. The particular computer simulation program used in this study will be discussed later in this report. Although the National Crash Severity Study includes accidents from rural as well as urban and city settings, the settings are confined to areas where an organization with sufficient technical expertise in accident reconstruction is located. This may prove sufficient for the initial statistical study; however, in the future a broader accident base may be desirable.

In order to facilitate broader use, future dynamic computer simulation techniques should be developed with the non-technically educated user in mind and should be as simple and compact as possible in order to utilize smaller more inexpensive computers.

The preceding general statement regarding simulation techniques can also be justified by looking at the other motivation for automobile collision studies pertaining to understanding the characteristics leading to an accident. Although there are many characteristics

which attribute to automobile collisions which do not involve the dynamic state of the vehicles involved, this report and the simulation techniques discussed only pertain to the dynamic characteristics of automobile collisions. Quantification of the characteristics leading to an accident can be useful in designing safer roadways and aiding our legal system in administering justice. For the most part, these activities are state and local government functions and, therefore, the ability to reconstruct accidents on a local level with non-technical people could also prove beneficial from these standpoints.

Another purpose of automobile collision analysis is to provide a uniform method of investigating collisions. This uniform method is necessary for two reasons.

The first reason is to provide an automobile collision technology. This technology can serve as a base of information from which investigators can draw information to aid in the reconstruction of collisions or to critically evaluate the analysis of other automobile collision investigators. This ability to evaluate the work of other investigators is especially important in the courtroom where the qualifications of expert witnesses must be established.

The second reason is to provide a method with which technically educated people can be trained as collision investigators or by which veteran collision inves-

tigators can refresh their knowledge. At the present time, there is a shortage of qualified collision investigators and the resulting gap is too often made up by less qualified investigators. In the courtroom, it is difficult for judges and juries to determine the difference between these two types of investigators.

In order for dynamic computer simulation techniques to facilitate use by non-technical people as well as simplifying the complexity of reconstruction by technical people, a simple, logical approach to reconstruction needs to be implemented in the form of a computer simulation. The computer simulation techniques must also be adaptive to an educational role, whereby local non-technical people can be trained to use the computer simulation.

Several constraints severely limit the implementation of automobile collision analysis. The main difficulty lies in the fact that if the investigator begins with incorrect or invalid data, the results will almost always be invalid regardless of the type of analysis used. Several factors contribute to incorrect data.

Lack of training for people assigned the responsibility for taking measurements at the scene of an accident is one contributing factor to incorrect data. It is very often the case where information such as the impact point of the vehicles, final resting position of

the vehicles or the locations of skid marks are measured incorrectly or are not measured at all.

Lack of proper equipment for making these measurements also contributes to inaccuracies. For example, the coefficient of friction at the scene of an accident is usually measured by a standard skid test. In this skid test, the investigating officer brings his automobile from a known velocity to rest in a locked-wheel skid. The length of the skid marks determines the average coefficient of friction. This technique works reasonably well as long as the skid marks are clearly visible and the coefficient of friction is not a strong function of velocity. Often however, this method yields results that are inaccurate when used with a simple work-energy formula. An alternative to this system might be to provide an automated system which could measure the coefficient of friction through tachometers and accelerometers.

It is my belief that a modular algorithm approach can best meet the overall goals of the computer simulation. A modular approach may require more user training before the user can make intermediate decisions regarding the use of individual algorithms. However, once the user is acquainted with the system and acquires an understanding of vehicle accident processes, a logical approach to accident reconstruction should be obtainable.

Once trained, a modular approach will allow the investigator to interact more with the computer throughout the reconstruction process, enhancing the investigator's ability to input insights and decisions with respect to any particular accident. In addition, a modular package of reconstruction algorithms will allow implementation on smaller mini- and micro-computers. Use of smaller and, consequently, less expensive computers would enable local governments and other small organizations to acquire the required facilities for computer aided accident reconstruction.

This approach varies somewhat from the general approach taken by Calspan Corporation, which to date has been the predominant developer of dynamic accident reconstruction computer programs. The computer reconstruction programs in most widespread use in this country today were created by Calspan and will be discussed in further detail later in this report. In general, the Calspan programs can be classified as general algorithms for application to a wide spectrum of accidents. However, the generality required in one large algorithm in order to facilitate its broad use eliminates the capability of the accident investigator to interact with the computer algorithm in such a way as to simplify the accident reconstruction. Not only will a modularized package of reconstruction algorithms allow interactive input,

allowing the investigator to check his insights regarding the accident at various phases in the accident without restarting the simulation at the beginning, but modules appropriate to different classes of accidents can take advantage of applicable simplifying assumptions valid for that particular accident. Through a process of trial and error with small module algorithms, the trained investigator should be able to piece the accident together in a shorter period of time at a tremendously lower cost. In essence, the modular algorithm approach should serve as a much better learning device for accident reconstruction in total, as well as for determining the events in any particular automobile accident.

This report also consists of a presentation of the dynamic principles applicable to automobile accident reconstruction and a survey of the current literature available with respect to simulation techniques. Once the fundamentals have been discussed, a critique of the application of computer simulation techniques to accident reconstruction is presented. Through the following survey and discussion, a basic insight into the development of modularized algorithms for accident reconstruction should be gained.

Before discussing dynamic principles and simulation techniques, the reader is referred to reference [2] for insight into the reconstruction problem. For the

two-vehicle collision model, Wilson presents one possible set of system parameters (40 in this particular case) which could be used to define the impact and post-impact trajectory phases of an accident. Depending upon the particular accident, the available evidence (i.e., tracking data, post-collision inspections), and the mechanical principles used to simulate or reconstruct the accident, the set of system parameters may be altered. However, Wilson's classification of the system parameters into subsets classified as most certain, less certain, least certain, and definite unknowns defines the logical process utilized in this work for evaluating parameters for any given accident.

The body of work required to accomplish the above defined goals is, of course, enormous. The work accomplished to date which forms the basis of this report is a beginning only. While our progress has been substantial, the task of assembling a low cost computer based collision reconstruction system will progress for many, many years to come.

Work on this system has provided topics for six completed theses (Master of Science in Mechanical and Electrical Engineering) with three more in various stages of completion. The work of Olson [3] and Self [4] formed the foundation of the Modular Accident Simulation System (MASS). Their work provided the basic analysis

algorithms for analyzing vehicle dynamics during a collision scenario.

The work of Kroeger [5] in designing and building a microcomputer based, graphical input, hardware/software system followed by Dobbins [6] in developing and implementing a microcomputer operating system for MASS provided the physical manifestation of the collision reconstruction system.

Current work by several students, combined with current major computer upgrades, are already reshaping the nature of the MASS system. Video graphic output of analysis results is nearing completion as is the prospect for substantially reduced analysis execution times on new dedicated hardware.

As an outgrowth of numerous collision reconstructions, an awareness of the sensitivity of the analysis to road/tire friction characteristics was developed. This awareness spawned a parallel effort to develop portable field equipment for accurately measuring and transmitting the actual coefficient of friction from the accident site. The work of Reid [7] in developing a portable transducer and Edmiston² in developing and building a portable microcomputer system integrated with the transducer formed the basis for field measurements

²Thesis currently in preparation

of the coefficient of friction. The work of Coke [3] extended the transducer to provide a sophisticated computer based field data acquisition device capable of providing stored empirical data. He then designed and implemented an extension to the MASS system to permit integration of the empirical data into the analysis algorithms.

The following chapters will attempt to discuss all of this work in some degree of detail. It is impossible, however, to even begin to expose the enormity of work contained in references [3] to [8]. The reader is encouraged therefore to pursue those references and the additional work to be published in the near future for a more detailed insight into the subject matter of this report.

CHAPTER II

VEHICLE COLLISION RECONSTRUCTION

The reconstruction of vehicle collisions utilizing the principles of rigid body dynamics is certainly nothing new. With the introduction of the digital computer, the capability to substantially increase the complexity of the reconstruction exists, and has been the focus of enormous effort during the past decade. However, regardless of the complexity introduced, a basic understanding of the principles of impulse-momentum and conservation of mechanical energy with applicable assumptions is needed by the investigator. Although there are different approaches for analyzing an accident, in general, vehicle accident reconstruction is separated into the distinct phases of 1) pre-impact trajectory, 2) impact, and 3) post-impact trajectory. Consequently, the principles as applied to the individual phases will be discussed separately. Note should be made that with the division of the analysis into separate phases (events) as presented here, the impact phase is modeled assuming that tire forces are negligible during that phase. Although this assumption is reasonable for most collisions as noted in references [9, 10], McHenry [10] indicates significant

errors have resulted for moderate-speed intersection collisions in which multiple contacts occur.

Impact Phase: Principle of Impulse and Momentum

Most introductory dynamics texts will present a discussion of the application of the principle of impulse-momentum (conservation of momentum) to the basic input problem. Beer and Johnson [11] present introductory discussions for both central and eccentric impact. A more complete yet fundamental treatment of the principle of impulse-momentum with specific reference to vehicle collision impact can be found in reference [12]. More detailed presentations of the principle applied to the impact problem can be found in references [13, 14].

Several assumptions are made in the application of the principles of rigid bodies to vehicle collisions. In traffic accidents, the bodies (vehicles) undergo elastic and plastic deformations. Although the centers of gravity of the bodies are affected, their locations do not change radically during the impact phase and, therefore, are assumed to be constant. The mass moments of inertia of the vehicles are also assumed to be constant during and following deformation. Due to the substantial crushing involved in severe collisions, portions of the body structure (i.e., occupant compartment) take an appreciable, though still short time to reach a common velocity. Consequently, portions of the body structure or mass

may undergo a change in velocity before the rest of the vehicle. This effect is not modeled in detail and all of the mass of the vehicle is assumed to have the same velocity at all times. In current simulations, only two-dimensional vehicle motion has been included. Although pitching and rolling are present in essentially "planar" accidents, their effects are typically small and are, therefore, neglected. The influence of the preceding assumptions are considered in reference [9].

The impact phase of a collision can be further broken down into periods or subphases. Immediately following collision, the relative velocities of two masses will tend to be equalized as the masses continue along their initial trajectories interacting by impulsive forces. Once a common velocity is reached, the forward impact or period of deformation of the collision terminates. At this instant, reaction forces acting to separate the masses are present if at least one of the masses is elastic to some degree. This period of the impact is commonly called the period of restitution or rebound. It ends when the reaction force reduces to zero at vehicle separation.

The ratio of the integrals of the forces acting during the period of restitution to those during the period of deformation is called the coefficient of restitution. This ratio may also be viewed as the momentum

transfer at rebound to the momentum transfer during crush. The coefficient of restitution varies between zero for a perfectly plastic collision to one for a perfectly elastic collision. The principle of conservation of momentum is valid regardless of the value of the coefficient of restitution. In general, total mechanical energy is not conserved in impact problems except where the impact is perfectly elastic. Therefore, the coefficient of restitution serves as a measure of energy loss as previously noted.

In application to vehicle collision, the coefficient of restitution tends to be small depicting the almost inelastic behavior of crushing automobiles. The coefficient of restitution is typically on the order of 0.05 to 0.1 for symmetric head-on collisions of two automobiles [9]. Consequently, it is common to assume perfectly plastic collisions which result in a common velocity after impact. Confirmation of the assumption of small coefficients of restitution is found in reference [1] where it has been determined that a change of the coefficient from 0 to 0.1 would only change the amount of energy absorbed by 1 percent.

Given ample evidence, the assumption of an a priori coefficient of restitution is not required and it is possible to calculate the coefficient. This also provides a subjective check on the accuracy of the inter-

pretation of the available evidence. The validity of the assumption of a perfectly plastic collision may be subjectively evaluated by considering the final relative positions of the vehicles involved [15]. Caution must be taken in considering the final distance between two vehicles as representative of the degree of elastic behavior as many variables which enter into the post-trajectory phase of a collision, affect final rest positions.

Another treatment of the impact phase of a vehicle collision concentrating on an approach using the equations of impulse and momentum is presented by Brach [15]. Due to the inability of locating the exact point of application of the resultant force impulses in vehicle collisions, Brach contends the resultant of the total surface contact forces should consist of both force and moment impulses to accurately formulate the equations of impact. For a physical interpretation, the moment can be considered to be generated by the mechanical interlocking of parts of the deforming vehicles. In including moment impulse into the formulation, an impulse moment coefficient, similar to the coefficient of restitution, is introduced corresponding to angular velocities. The moment coefficient ranges between negative and positive one. At negative one, the angular impact is elastic, at zero the vehicles have zero relative angular velocity following impact, and at positive one, no moment is transmitted at impact relating to the direct central impact problem.

Brach's paper is the only known reference to consider surface moment impulse in the context of vehicle collisions. As little work has been done with this concept, it would be difficult to establish a priori values for the moment coefficient in vehicle collision analysis. When ample collision evidence is known, the moment coefficient can be treated as an unknown and the analysis accuracy can be improved. Brach presented one example where the moment coefficient was treated as an unknown and calculated to equal 0.70. The relatively high moment coefficient value, approaching the direct central impact value, as well as the accuracy of collision analyses by others while ignoring the moment impulse, would lead one to question the need for this approach and the additional complexity introduced. However, the theory offers improved accuracy and additional work in this area appears warranted.

Impact Phase: Conservation of Mechanical Energy

Another approach to the analysis of the impact phase of vehicle collisions is to use the principle of conservation of mechanical energy. The summation of the initial kinetic energies before impact and the energy absorbed (negative) by plastic deformation during the period of deformation, for the vehicles involved, must equal the summation of the kinetic energies of the vehicles at the instant the period of restitution ends.

In order to use this balance of mechanical energy to reconstruct vehicle collisions, a method for determining deformation energy terms from post-collision crush profiles is needed. In reference [2], vehicle-to-vehicle crush data [16] showing that the mean vehicle crush deformation is linearly correlated to vehicle impact speed, is used to calculate the plastic work. An identical linear correlation based on barrier test data for frontal impact is presented by Campbell [17] to calculate what he refers to as an "Equivalent Barrier Speed" (EBS) for estimation of the energy absorbed by plastic deformation. Equivalent Barrier Speed is commonly defined as the speed at which equivalent vehicle damage (based on equivalent energy absorption) is produced in a fixed barrier test of the same vehicle. Campbell tabulates the coefficients of a linear equation and the standard weight at which these coefficients were determined for four classifications of vehicles. A linear force-deflection model is also developed which reproduces the barrier test linear relationship using the same coefficients. The tabulated data is only applicable for frontal impact due to the limited availability of additional test data, however, the concept is applicable for all types of collisions. Campbell proposes the factors involved in a collision could be used to classify collisions into categories where EBS formulations applicable for the particu-

lar categories could be used. To arrive at the additional EBS formulations, test programs supplemented by accident simulations are needed.

Trajectory Phases: Conservation of Mechanical Energy.

The trajectory phases of an accident can be reconstructed on the basis of conservation of mechanical energy. Following vehicle separation at the end of the period of restitution of the impact phase, the kinetic energy levels possessed by the individual vehicles are reduced to zero by frictional work between the vehicle and roadway. Thus, the summation of translational and rotational kinetic energy following impact and the frictional work (always negative work) during the post-collision trajectory must equal zero. Brief presentations of the principle and a means of calculating the total frictional work can be found in references [2, 18].

Another presentation of post-impact trajectory analysis based on energy dissipation by frictional work between vehicle separation and rest positions is found in [24]. Although this presentation is not a unique solution based on the theory, more detail of the development is provided. Steering is not considered in a detailed sense and in the initial development, a piecewise linear idealization of the linear and angular velocity time histories is assumed with abrupt changes in deceleration rates between linear and angular motion. In other words, when the

vehicle slides laterally, the angular velocity is assumed constant while the linear velocity is decelerated and conversely when the direction of linear velocity is aligned with the longitudinal axis of the vehicle. By approximate integrations of the idealized velocity versus time plots and rigid body mechanics, approximate linear and angular deceleration times are found. Assuming the linear and angular phases of motion end at approximately the same time, equations relating the separation velocities to displacements, the friction coefficient, and vehicle geometry are derived. Although this initial development has been found to have several shortcomings, it is a fairly uncomplicated approach and offers an alternative method for trajectory analysis. This general approach, as well as a method based on integration of equations of motions, will be discussed further later in this report.

Note that although the discussion has been focused on post-impact trajectory analysis, the principles can as easily be applied to pre-impact trajectories in order to find initial velocities prior to braking or skidding. Typically, pre-impact trajectory analysis is simplified as angular velocities are negligible.

Simulation Techniques

In this section, a discussion of several simulation techniques combining available evidence and the mechanical principles are presented. As depicted in the

previous section, alternative methods for developing simulation techniques exist and the techniques presented in the following discussion will re-emphasize this fact.

However, the simulation techniques discussed are not limited to the general approaches previously presented.

Vehicle collisions have been reconstructed for some time with hand calculations using the dynamic principles of rigid bodies as previously discussed. Given accident layouts with tire tracks, impact point, and rest positions, an investigator can estimate accident conditions. The velocity of each vehicle at the termination of the period of restitution can be approximated by using conservation of mechanical energy and assuming friction factors. With further assumptions and the principle of impulse and momentum, the impact phase can be analyzed to approximate initial contact velocities. If tire tracks indicate braking or skidding before impact, conservation of mechanical energy can again be used to approximate initial velocities. By varying the assumed values in the calculations (e.g., friction coefficients) a sensitivity study can be made and, for most accidents, a reasonably accurate reconstruction is obtainable. In reference [12], several vehicle collisions are reconstructed with hand calculations.

In reference [2], Wilson outlines two individual algorithms applicable to the estimation of initial speeds and the post-impact trajectory lengths of an accident.

The algorithms are not designed to be used together as modules, as the input and outputs between them are not consistent.

The first algorithm has outputs of initial velocities, post-impact linear and angular velocities, and the force impulse. The algorithm is based on the conservation of mechanical energy in combination with the impulse-momentum principle. The basis is different from those discussed previously in that the force impulse is left as an unknown and the coefficient of restitution is not introduced. A numerical example of an oblique impact is used to illustrate the algorithm. Another example of a central impact is also presented, however, in this case the algorithm as previously presented was not implemented. Instead, Wilson uses the conservation of mechanical energy in combination with the conservation of linear momentum where the force impulse has been eliminated as a variable. The assumption of a coefficient of restitution is not noted, although its use is implicit in the assumption of a common post-impact velocity which is equivalent to assuming a coefficient of restitution equal to zero.

The second algorithm for trajectory estimation uses a vector equation describing the locations of the vehicles in combination with equations common with the first algorithm to arrive at admissible solutions. In this case, the definite unknowns are the post-impact

trajectory lengths. Initial velocities are classified as least certain and are input with lower and upper bounds. Numerical examples for the second algorithm are not presented.

Calspan Corporation appears to have done more in the area of accident reconstruction by computer simulation than anyone else [10, 19, 20, 21, 22]. It is Calspan's CRASH computer program which was used in a National Crash Severity Study. The Calspan Reconstruction of Accident Speeds on the Highway (CRASH) program is actually a refinement of a routine (START) used to generate initial approximations for a much more detailed simulation program called SMAC for Simulation Model for Automobile Collisions.

The SMAC program is an algorithm which predicts a time history response and corresponding evidence (i.e., rest positions, damage, and tire marks and tracks) when supplied with initial approximations of the collision conditions. In the reconstruction of accidents, successive iterative runs are performed until an acceptable match with real accident evidence is obtained.

In general, the uniqueness of SMAC is in its generality and the extent of analytical detail. Equations based on the fundamental physical laws and empirical relations are used to balance the applied and inertial forces and moments acting on vehicles throughout an accident. Empirical laws are introduced in order to treat collision and tire forces simultaneously. The analytical

assumptions which are made for the collision force aspect of the impact which differ substantially from those previously discussed are outlined by McHenry in [10].

1. The vehicles are treated as rigid bodies, each surrounded by a layer of isotropic, homogeneous material exhibiting elastic-plastic behavior.
2. The dynamic pressure in the peripheral layer increases linearly with the depth of penetration relative to the initial boundary of the deflected surface.
3. The adjustable, nonlinear coefficient of restitution varies as a function of maximum deflection.

The "friction circle" concept for introducing tire forces, which is a method for limiting tire forces to those obtainable by Coulomb friction, is also introduced in this reference.

The SMAC predicted time histories of vehicle responses during impact and spinout trajectories are generated by step-by-step integration of continuous equations of motion over the time interval of the accident. A derivation of the equations implemented in SMAC is outlined in reference [20]. A simpler presentation of equations of motion applicable to vehicle collisions is outlined in Appendix 2 of the paper by Grime and Jones [9]. Although SMAC is obviously more complex in its treatment of colli-

sion and tire forces [20] than the presentation in [9], the integration of equations of motion to generate time responses should be readily apparent from either reference.

The SMAC program has been found to yield ± 5 percent accuracy in velocity estimation [19] in certain test cases. However, a sufficiently detailed definition of the accident is required to obtain this level of accuracy and to take advantage of the benefits provided by SMAC predictions. Examples of application of SMAC appear in [10, 20, 21, 23]. The development of the CRASH program was prompted by a need to reconstruct accidents where a detailed definition of the accident is lacking. Although the range of accuracy with CRASH is decreased to about ± 12 percent [19], a 75 percent cost savings per run is obtained and the program inputs are less detailed. These factors provide for a broader application potential. A discussion of CRASH and comparative results from CRASH and SMAC appears in [19].

The CRASH program contains two methods of analyzing accident evidence. The first method is an extension of the trajectory analysis, based on energy dissipation by frictional work [19], introduced earlier in this paper. Application of this trajectory analysis to SMAC generated spinout trajectories revealed shortcomings existed due to assumptions and idealizations in the original derivation. Modifications were introduced in order to avoid the assumption that linear and angular motion terminated simul-

taneously, the errors introduced in the integration of the velocity plots, and the assumptions that deceleration rates between linear and angular motions changed abruptly. Although the details of the modification are sketchy, it is apparent that SMAC was implemented to generate empirical relationships used in the resulting equations. By combining this trajectory analysis with an impact phase analysis based on the impulse-momentum principle, the change in velocity during impact and initial impact velocities are obtained.

The second analysis method in CRASH is an extension of Campbell's damage analysis technique. The linear damage analysis is based on a spring-mass-dissipator system using potential energy relationships and conservation of momentum to derive expressions for velocity changes during the impact phase as a function of the absorbed energy in crushing deformation. The absorbed energy calculation is based on Campbell's work where gross approximations are made for the empirical coefficients for side and rear collisions. The computation of the absorbed energy is accomplished by integration of the energy equations by trapezoidal approximations where coefficients are shown in tables.

The impact phase velocity changes calculated with the two analysis methods contained in the CRASH program are comparable, although the trajectory analysis must be used

in both cases in order to calculate initial impact velocities.

Computer Simulation of Vehicle Collisions: A Survey.

The first computer program to be used on a large scale for accident reconstruction was Calspan's SMAC program. As previously noted, the SMAC program was designed to be very general, thus allowing its application to a large spectrum of accidents assuming sufficient detailed evidence exists. The generality, however, causes several problems. First, the program is of significant size requiring a large computer for storage and computation. At The University of Texas where the program has been used to reconstruct field accidents, it is advantageous to store SMAC and do computation on a CDC 6600 while input and output was handled with a PDP 11/40. Calspan used a similar approach to handle the program at one time as depicted in reference [21]. Second, it is likely the complexity and analytical detail incorporated into the program is not required to obtain comparable accuracy for certain accidents. The second point is especially true when detailed evidence is not available. For instance, in frontal impact accidents at high speeds, a simplified reconstruction using the assumption of a coefficient of restitution equal to zero is likely to be of sufficient complexity to obtain suitably accurate results.

Some of the drawbacks noted above for the SMAC program contributed to Calspan's reasoning to develop CRASH as previously noted. The alternative methods for approximating impact phase speed change provided with CRASH make it possible for the user to select the results based on the most reliable evidence available. At the same time, comparison of results from the alternative methods provides a check on the compatibility of the various evidence items. The drawback encountered with the CRASH program is the loss in accuracy.

The accuracy loss in the CRASH trajectory analysis routine is due to the use of approximations leading to idealized velocity versus time plots for the derivation of the energy balance equations representing the trajectory phase, instead of direct integration of equations of motion during this phase. In SMAC, the equations of motion are integrated directly over the trajectory phase as well as the impact phase. Integration of the equations of motion over the impact phase introduce a number of disadvantages due to the short impact time interval during which rapid changes take place, as the integration time steps must be very small to maintain accuracy. Additionally, SMAC requires a great deal of computational effort at each time step during the impact phase to balance the pressures acting on the vehicles across the impact interface. Therefore, the impact phase analysis used in the CRASH program, which is based on the impulse-momentum principle, is a worth-

while trade-off for simplification. However, for the trajectory phase large time steps are appropriate and interface pressures need not be calculated making the trade-off to a less accurate solution such as the CRASH program trajectory analysis questionable.

For the damage based approximations of the CRASH program, based on Campbell's work [17], the main drawback as previously noted is the lack of experimental data for other than frontal impacts. For this reason, it may be desirable to rely more heavily on other methods of approximation, such as impulse-momentum solutions. However, there are classes of accidents where impulse-momentum methods are not applicable (e.g., accidents at slower speeds), and a method based on damage analysis is the only attractive alternative. In this case, the CRASH program damage analysis is as good as one may expect do to with a simplified approach, and in most cases is suitable as depicted by the accuracy obtained [19].

The two algorithms developed by Wilson [2] are similar in nature to the CRASH program. However, both of these algorithms rely on calculating the total plastic work using a linear correlation between vehicle impact speed and mean vehicle crush [16]. It is not evident in the literature that the validity of the algorithms has been substantiated, and it is extremely doubtful the results could be any more accurate than those of CRASH.

In summary, it appears that a number of different algorithms or modules appropriate to different classes of accidents with different types of evidence would be an attractive alternative to a general algorithm for application to a wide spectrum of accidents. By using a modular approach extended to apply to different stages of any particular accident, the complexity of the total package could be reduced while taking advantage of the specific evidence available and appropriate simplifying assumptions. As a proposed scheme, an algorithm package including a trajectory analysis based on the integration of equations of motion and an impact analysis based on the principles of impulse and momentum could be used to reconstruct accidents with full impacts.

Modular Accident Simulation System.

The Modular Accident Simulation System, hereafter referred to as MASS, is basically composed of a system of computer analysis modules connected with input and output devices. Each of these analysis modules are concerned with only one particular aspect of a vehicle collision. The user of MASS has the ability to use each of these modules independent of the others. The input and output devices are basically designed to improve the communication between the user and the computer based analysis modules. The two main goals were considered in the design of MASS.

The first goal was to provide a computer simulation system based on several independent analysis modules as discussed in the previous section. The position held during the course of the project was that modular approaches to automobile collision simulation hold significant advantages over unified approaches like SMAC.

One advantage of a modular approach is the inclusion of the human element in the computational process. Automobile collision reconstruction using a computer basically involves an iterative solution technique. Because of the large number of input variables, the iteration in these programs is left with the investigator. With a modular system such as MASS, the user deals with only one aspect of the collision at a time. Since the collision processes modeled by individual modules are usually straightforward, the user should quickly gain insight into the use of these modules. When the investigator begins to recognize certain patterns of automobile collisions, he will be able to draw on that intuition to reduce the number of iterations needed to form a complete reconstruction.

Another advantage of the modular approach is that computer programs based on a modular analysis scheme are individually much simpler and much shorter than a program which is based on a continuous analysis approach. This means that these modules can be implemented on lower

cost equipment such as mini-computers and micro-computers. The cost of operating these programs could potentially then be brought within the means of nearly all collision investigators.

One more advantage of the modular approach would be in the versatility of a system based on modules. Such a system could be augmented by simply adding additional modules. If the inputs and outputs of each module follow some general format, new modules could be designed as to minimize any modifications that must be made to the overall system.

The second goal in the development of MASS is to provide a simulation system with user oriented input and output. It has been noted from experience using SMAC that a great deal of time is lost when the user is forced to deal with large amounts of input and output data in a numerical format.

The first step in reaching this goal was to use an interactive scheme for inputting of data. In the interactive scheme, the system will ask the user for information and then wait for a response. After the user inputs the information, the system either verifies the information or tells the user that the information was in error. Such an interactive scheme reduces the possibility of input errors since the user has immediate confirmation of the information just entered. An interactive program can also check

for certain types of input errors that would cause the analysis modules to fail. An interactive scheme also facilitates changes in the data file necessary with the iterative procedure employed by MASS. Finally, an interactive scheme reduces the time that a person must spend to become accustomed to the operation of the system.

The second step in reaching the goal of a user oriented system was to provide both alphanumeric and graphic methods of displaying input and output. This allows the user to study the accident in terms of quantities, positions, velocities and accelerations; and in terms of graphic diagrams. The graphic capabilities of the system enables a user to quickly evaluate the results of a simulation and decide on the proper modifications to the input data for the next iteration. The graphic display feature also provides a meaningful method for communicating the results of the simulation to parties not directly involved with the analysis.

With the development of these modular algorithms in mind, the basic theoretical considerations are now discussed in the following two chapters.

CHAPTER III

TRAJECTORY ANALYSIS ALGORITHM

The trajectory analysis algorithm developed in this chapter utilizes the integration of general equations of motion. The discussion of the trajectory analysis algorithm will be divided into two major sections. The first section pertains to the development of vehicle equations of motion, while the second discusses the tire road interface.

This chapter serves as the basis for analyzing both the pre-impact and post-impact phases of a collision.

Derivation of Vehicle Equations of Motion.

Referring to Fig 3-1, the velocity components of the contact patch for each wheel of a four-wheeled vehicle can be written as follows:

$$\begin{array}{ll} \text{Wheel \#1} & \dot{x}_{W1} = \dot{x} - r_f \dot{\theta} \sin(\theta - \phi_f) \\ \text{(right front)} & \dot{y}_{W1} = \dot{y} + r_f \dot{\theta} \cos(\theta - \phi_f) \\ \\ \text{Wheel \#2} & \dot{x}_{W2} = \dot{x} - r_f \dot{\theta} \sin(\theta + \phi_f) \\ \text{(left front)} & \dot{y}_{W2} = \dot{y} + r_f \dot{\theta} \cos(\theta + \phi_f) \\ \\ \text{Wheel \#3} & \dot{x}_{W3} = \dot{x} + r_3 \dot{\theta} \sin(\theta + \phi_3) \\ \text{(right rear)} & \dot{y}_{W3} = \dot{y} - r_3 \dot{\theta} \cos(\theta + \phi_3) \end{array}$$

$$\begin{aligned}
 \text{Wheel \#4} & \quad \dot{x}_{W4} = \dot{x} + r_4 \dot{\theta} \sin(\theta - \phi_4) \\
 \text{(left rear)} & \quad \dot{y}_{W4} = \dot{y} - r_4 \dot{\theta} \cos(\theta - \phi_4) \quad (3-1)
 \end{aligned}$$

where $\dot{x} = u$ and $\dot{y} = r$ in Figure 3-1.

In the above equations, the orientation of the front wheels (r_f, ϕ_f) with respect to the vehicle center of gravity and the vehicle longitudinal axis are constants dependent on vehicular geometry. Front wheel steering, ψ_i , is a result of wheel rotation about nodes located by these parameters. If the rear axle of the vehicle were fixed perpendicular to the longitudinal axis of the vehicle, similar parameters (r_r, ϕ_r) could also be used to locate the rear wheels. However, in order to allow an input for rear axle rotation, ψ_r , to compensate for vehicle damage, independent rear wheel radii and angles are required. Referring to Fig. 3-1 the radii, r_3 and r_4 and angles ϕ_3 and ϕ_4 can be expressed as follows:

$$r_i = \frac{(c/2) \cos \psi_r}{\sin \phi_i} \quad i = 3, 4 \quad (3-2)$$

$$\tan \phi_3 = \frac{(c/2) \cos \psi_r}{b - (c/2) \sin \psi_r} \quad (3-3)$$

$$\tan \phi_4 = \frac{(c/2) \cos \psi_r}{b + (c/2) \sin \psi_r} \quad (3-4)$$

The values for r_f , r_r , ϕ_f , and ϕ_r are easily calculated given vehicle parameters a , b , and c .

Considering each wheel independently, a free body diagram of the wheel with the resultant longitudinal and lateral components of force created at the tire-roadway interface can be drawn as shown in Fig. 3-2.

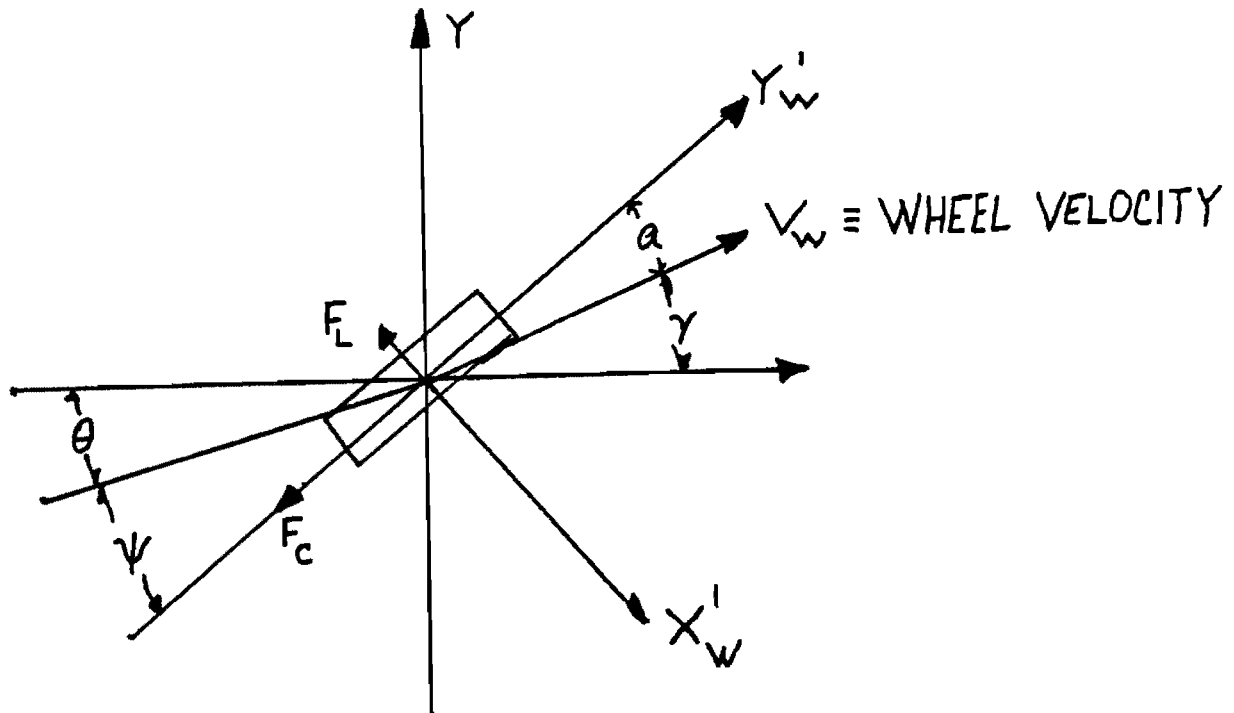


Figure 3-2

Wheel Free Body Diagram

The details of the tire model used to calculate the longitudinal or circumferential and lateral tire forces, F_C and F_L , respectively, will be presented in the next section of this chapter. Consequently, a detailed discussion of Fig. 3-2 will be left until later. Of pri-

mary importance at this point in the derivation of equations of motion for the vehicle is the ability to calculate tire forces in the wheel centered coordinate system (x'_W, y'_W) .¹

Given the tire forces, linear equations of motion for the vehicle can readily be derived by summing forces in the x and y directions and using the momentum principle (Newton's Second Law). Likewise, an angular equation of motion results from summing moments about the vehicle center of gravity and using the angular momentum principle. Referring to Fig. 3-3 the following equations of motion can be written:

$$\sum F_x = \sum_{i=1}^4 [F_{Ci} \cos(\theta + \psi_i) + F_{Li} \sin(\theta + \psi_i)] = m\ddot{x} \quad (3-5)$$

$$\sum F_y = \sum_{i=1}^4 [F_{Ci} \sin(\theta + \psi_i) - F_{Li} \cos(\theta + \psi_i)] = m\ddot{y} \quad (3-6)$$

$$\sum M_{c.g.} = (F_{L1} \sin \psi_1 + F_{C1} \cos \psi_1) \frac{c}{2} + (-F_{L1} \cos \psi_1 + F_{C1} \sin \psi_1) a - (F_{L2} \sin \psi_2 + F_{C2} \cos \psi_2) \frac{c}{2} + (-F_{L2} \cos \psi_2 + F_{C2} \sin \psi_2) a + (F_{L3} \sin \psi_3 +$$

¹The use of primed coordinate systems throughout this report indicate body centered coordinate systems. In their use for both wheels and the vehicle the y' axis will always be along the longitudinal axis of the body (circumferential axis for wheel) with the positive direction toward the front of the vehicle. All coordinate systems are right-handed coordinate systems.

$$\begin{aligned}
 & F_{L3} \cos \psi_3) r_3 \sin \phi_3 - (-F_{L3} \cos \psi_3 + \\
 & F_{C3} \sin \psi_3) r_3 \cos \phi_3 - (F_{L4} \sin \psi_4 + \\
 & F_{C4} \cos \psi_4) r_4 \sin \phi_4 - (-F_{L4} \cos \psi_4 + \\
 & F_{C4} \sin \psi_4) r_4 \cos \psi_4 = I_2 \ddot{\theta} . \quad (3-7)
 \end{aligned}$$

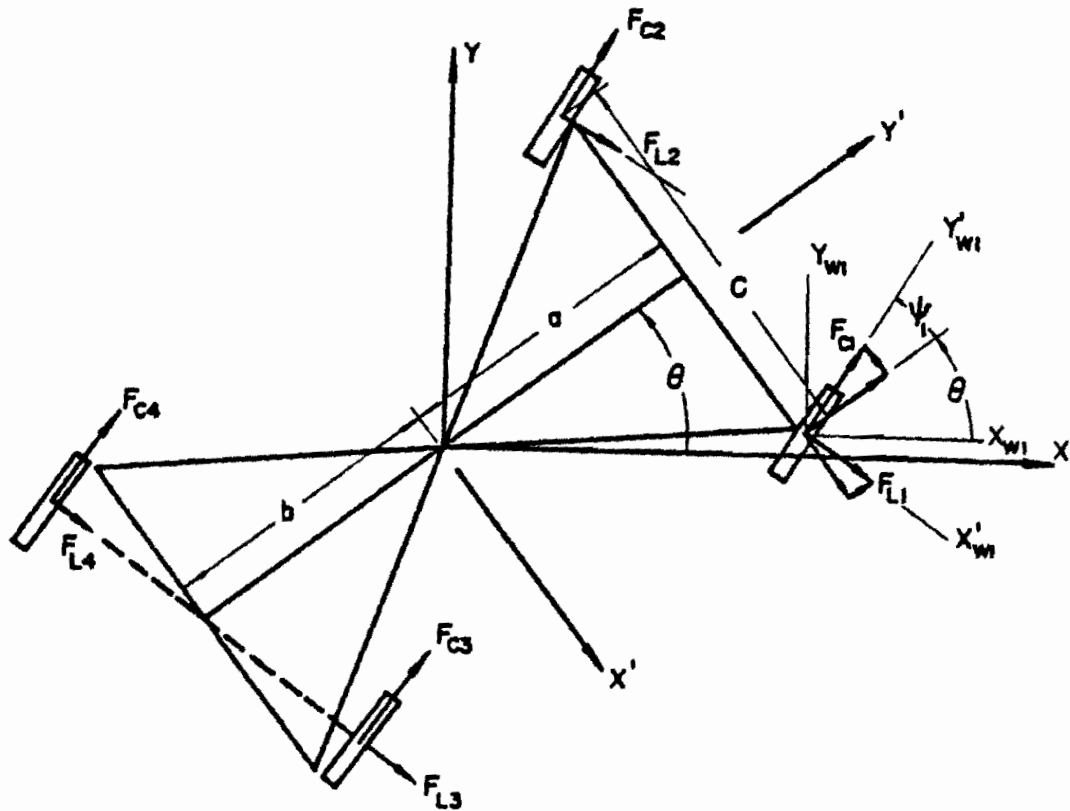


Figure 3-3. Tire Forces Acting on Vehicle Model

Expressing the preceding equations of motion in a first order ordinary differential state vector form results in the following system of equations:

$$\begin{bmatrix} \dot{x} \\ \dot{y} \\ \dot{\theta} \\ \dot{u} \\ \dot{v} \\ \dot{\Omega} \end{bmatrix} = \begin{bmatrix} u \\ v \\ \Omega \\ \frac{1}{m} \sum_{i=1}^4 [F_{Ci} \cos(\theta + \psi_i) + F_{Li} \sin(\theta + \psi_i)] \\ \frac{1}{m} \sum_{i=1}^4 [F_{Ci} \sin(\theta + \psi_i) - F_{Li} \cos(\theta + \psi_i)] \\ \frac{1}{I_z} [(F'_{x1} - F'_{x2}) \frac{c}{2} + (F'_{y1} + F'_{y2}) a + F'_{x3} r_3 \sin \phi_3 \\ - F'_{x4} r_4 \sin \phi_4 - F'_{y3} r_3 \cos \phi_3 - F'_{y4} r_4 \cos \phi_4] \end{bmatrix} \quad (3-8)$$

where the bracketed expressions in equation (3-7) have been replaced with force components expressed in the vehicle centered primed coordinate system as expressed by the following equations.

$$\begin{aligned} F'_{xi} &= F_{Li} \sin \psi_i + F_{Ci} \cos \psi_i \\ F'_{yi} &= -F_{Li} \cos \psi_i + F_{Ci} \sin \psi_i. \end{aligned} \quad (3-9)$$

Tire Model

The forces and moments acting on the vehicle, which were introduced in the derivation of equations of motion in the previous section, result from cornering and tractive forces present in the tire-roadway interface. There are a great number of papers and books which discuss the aspects of tire performance. Rather than attempt to treat all the aspects in this report, the majority of which do not concern us, only a general introduction to the items of concern will be presented.

The tire model which is presented below is constructed to model the steady-state response of the vehicle tires. Although the nonsteady-state response of pneumatic tires can be drastically different from their steady-state behavior, the effects on the path and heading curves of the vehicle, which is what we are concerned with, due to the delays in actual tire force build-up are judged to be slight and unimportant [24]. Aside from tire construction, the most important factors affecting steady-state tire performance are: normal force, inflation pressure, frictional coefficient, tractive effort, camber angle, and speed [29].

The three degree of freedom vehicle model used in this study (Fig. 3-1) does not consider pitch or roll motion. Consequently, the normal force on each tire will be considered constant, where:

$$W_1 = W_2 = \frac{bmg}{2(a + b)} \quad (3-10)$$

$$W_3 = W_4 = \frac{amg}{2(a + b)} \quad (3-11)$$

Tire inflation pressure and camber angle will not be treated as variables in this study. However, the tire cornering stiffness will be treated independently for each of the four tires of a particular vehicle. At least theoretically this will allow simulation of tire construction type, damaged tires, etc. The speed dependency and tractive effort effects on tire performance will be introduced in the following sections.

Speed Dependency.

The speed or velocity of each vehicle wheel can be calculated using equations (3-1). The effect of the magnitude of wheel velocity on tire forces is through an adjustment to the frictional coefficient. The speed adjusted frictional coefficient, μ_{Si} , is determined by the following equation:

$$\mu_{Si} = \mu_i (1.0 + C_\mu |V_{Wi}|) \quad (3-12)$$

where μ_i is the static frictional coefficient for a particular tire-roadway interface, C_μ is the velocity coefficient of friction (always negative), and $|V_{Wi}|$ is the absolute wheel velocity calculated using the following equation:

$$|V_{Wi}| = \sqrt{\dot{x}_{Wi}^2 + \dot{y}_{Wi}^2} \quad (3-13)$$

Because of the sensitivity of the analysis algorithm to errors in μ_{Si} , a substantial effort has been devoted to this project to develop techniques to empirically arrive at μ_S as a function of V_W . Chapter VI discusses this work in detail.

The velocity direction of a given wheel with respect to the wheel heading contributes to the direction of tire circumferential and lateral or cornering forces. This effect will be discussed in depth with an introduction to wheel slip angle in later sections.

Tire Forces.

The remaining factor of importance affecting steady-state tire performance is tractive effort. Circumferential tire force, F_{Ci} , is a function of tractive effort and is limited by the product of the tire-roadway friction coefficient and normal wheel load. The calculation of circumferential tire forces is discussed in depth later with the introduction of the friction circle concept.

The other tire force component, the lateral (cornering) force, introduced in Fig. 3-2, is in one sense or another a function of all the factors presented thus far. However, the most significant aspects become apparent on reviewing Fig. 3-4. Since the normal force is a constant for any given vehicle wheel of our model, the family of curves presented in Fig. 3-4 for any given tire can be reduced to a single curve as shown in Fig. 3-5.

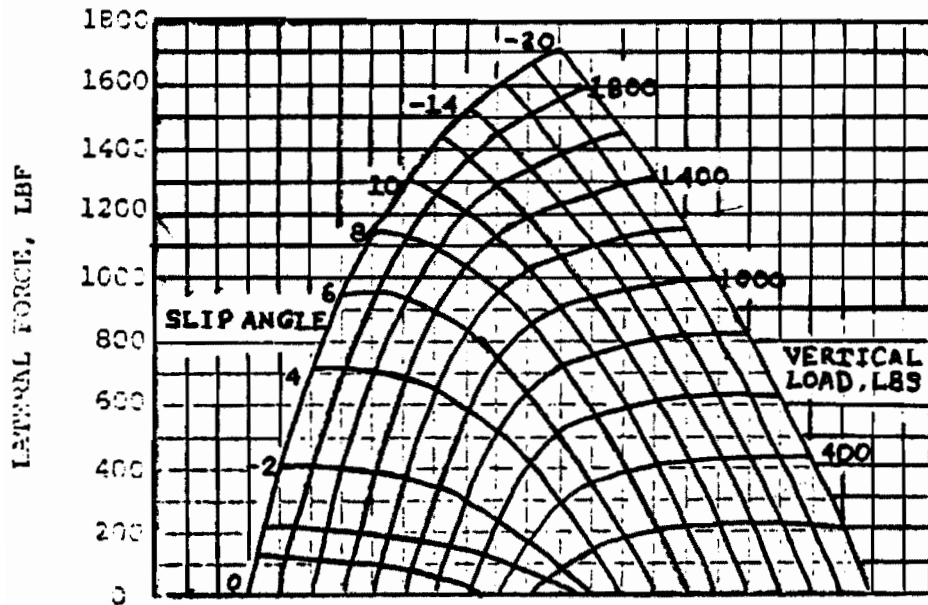


Figure 3-4

Carpet Graph of Lateral Force, F_{Li} , Versus Slip Angle and Normal Force (Reference [26])

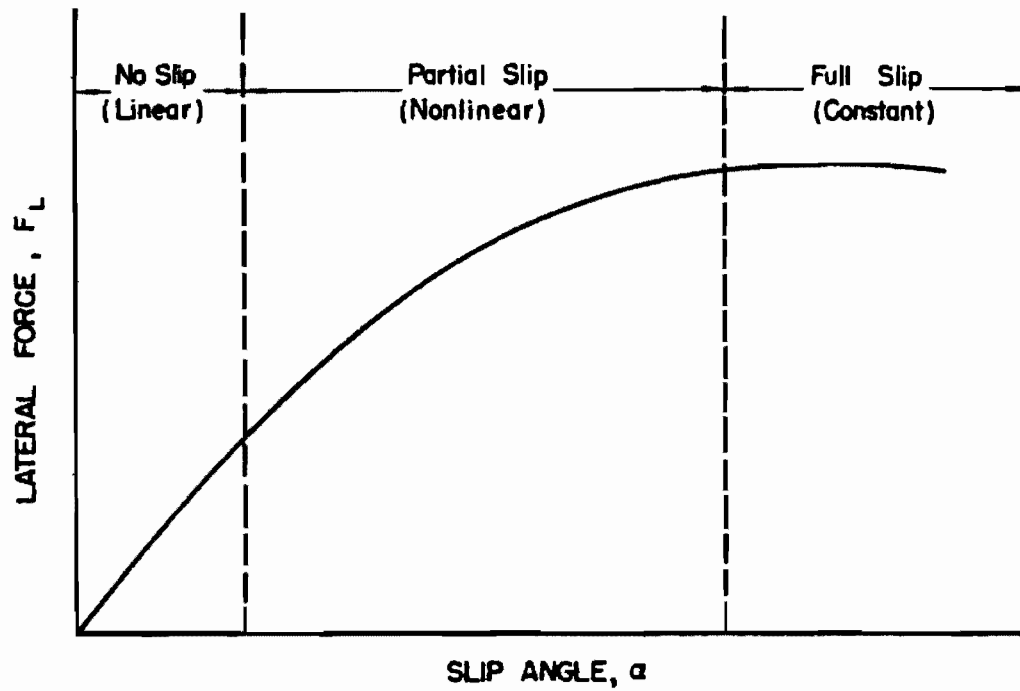


Figure 3-5

Lateral Force As A Function of Tire Slip Angle

Consequently, given a curve such as shown in Fig. 3-5 for a particular vehicle tire, the lateral tire force could be determined as a function of slip angle.

Wheel Slip Angle.

Once the wheel velocities for each vehicle wheel have been calculated using Equations (3-1), the individual wheel slip angles, α_i , can be calculated.* Referring to Fig. 3-2, the slip angle is the measure of the orientation of the wheel circumferential direction with respect to the vector sum of wheel velocity components. In its simplest form, the slip angle can be expressed as:

$$\alpha_i = \theta + \psi_i - \gamma_i \quad (3-14)$$

$$\text{where } \gamma_i = \text{arctangent } (\dot{y}_{Wi} / \dot{x}_{Wi}). \quad (3-15)$$

Gamma, γ_i , ranges from 0 to 2π radians and is positive in the counter-clockwise direction.** The slip angle is limited to an absolute value less than or equal to $\pi/2$ radians. This limitation implies that the slip angle is measured from the total wheel velocity vector to the circumferential wheel axis such that the slip angle is mini-

*The reader may find it beneficial to refer to the fortran listing of the trajectory analysis algorithm in the "TIRE" subroutine found in Appendix D of reference [3] through the following discussion.

** All the angles used in this report are positive in the counter-clockwise direction with the exception of the slip angle, α_i , which will be discussed later.

mized. To accomplish the bounds on the slip angle, multiples of π radians are either added or subtracted from the value calculated in Equation (3-14). The $\pi/2$ radian bound is imposed on the slip angle in order to prevent slip angle saturation of the lateral tire force calculation. This should be apparent from the following equation:

$$F_{Li} = C_i \alpha_i \quad (3-16)$$

which holds for the linear portion of the curve in Fig. 3-5, where the cornering stiffness, C_i , equals:

$$C_i = \left. \frac{\partial F_{Li}}{\partial \alpha_i} \right|_{\alpha_i=0} . \quad (3-17)$$

Tire Force Direction.

The slip angle sign must be determined such that the lateral tire force always opposes the motion of the wheel. For this reason, the sign of the slip angle is not always positive when measured in the counter-clockwise direction from the wheel velocity vector to the circumferential wheel axis.

As an additional check on the direction of the lateral tire force, F_{Li} , and to determine the correct direction for the circumferential tire force, F_{Ci} , the wheel velocity components in a right-handed wheel centered coordinate system are calculated for each wheel. As noted above, the lateral tire force will always oppose the lateral motion of the tire. However, the direction of the

circumferential tire force depends on the mode of tractive effort. In the driving mode (positive traction), the tire circumferential force will be in the forward or positive direction regardless of the tire motion direction. With braking (negative tractive effort), the tire circumferential force will again, always oppose the tire motion direction.

Friction Circle Concept.

Having introduced the primary characteristics of pneumatic tires which are applicable to our tire model, we can now focus our attention on the actual tire "friction circle" model where tire circumferential and lateral forces are calculated. The "friction circle" concept is a method for limiting tire forces to those obtainable by Coulomb friction. In other words, the maximum resultant force is limited such that:

$$F_{Ri} = \sqrt{F_{Ci}^2 + F_{Li}^2} \leq \mu_i W_i. \quad (3-18)$$

A larger resultant force, F_{Ri} , cannot occur due to the occurrence of slippage as the tire-roadway contact patch can only support a maximum friction force equal to $\mu_i W_i$ (saturation limit). If we let $\mu_i W_i$ be the radius of a circle, the so called "friction circle" may be drawn as shown in Fig. 3-6. In actuality, when cornering is superimposed on the tractive effort, the resultant circumferential and lateral components of force combine in such a way the

resultant curve is approximately elliptical in shape. The curve is elliptical since the application of tractive effort to the tire reduces the magnitude of the maximum lateral cornering force as depicted in Fig. 3-7.

Referring to Fig. 3-6, the tire friction circle model can be described as follows. If there is no tractive effort and the wheel is free rolling, no circumferential tire force will exist. If the tractive effort is positive (driving mode) but less than or equal to the saturation limit, $\mu_i W_i$, the magnitude of the tire circumferential force equals the tractive effort input. If the

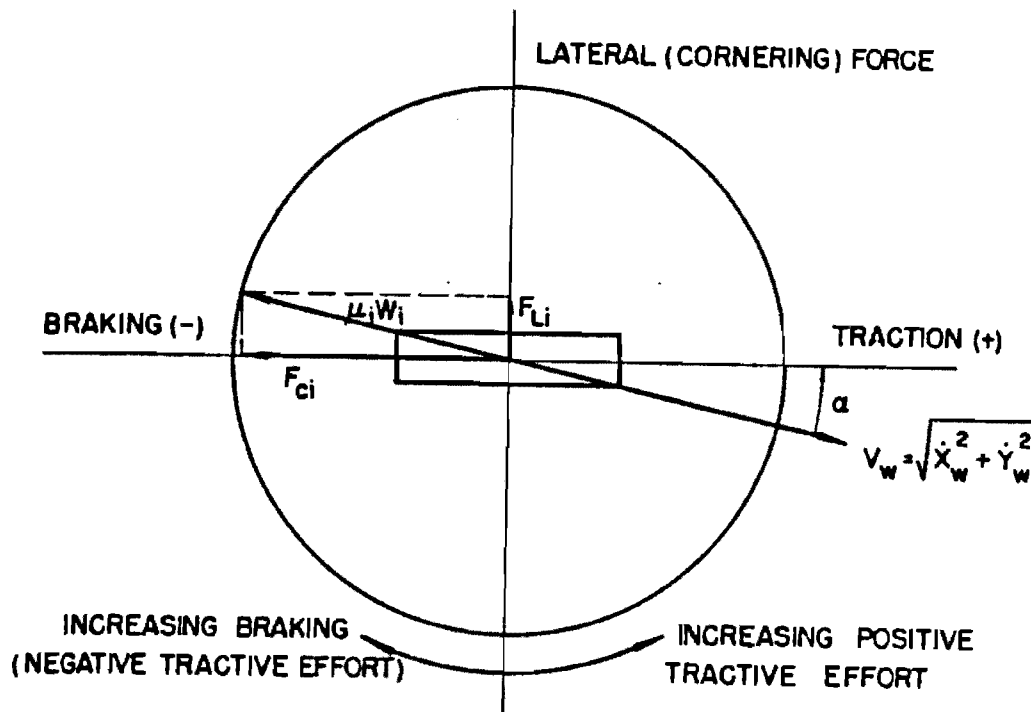


Figure 3-6

Friction Circle

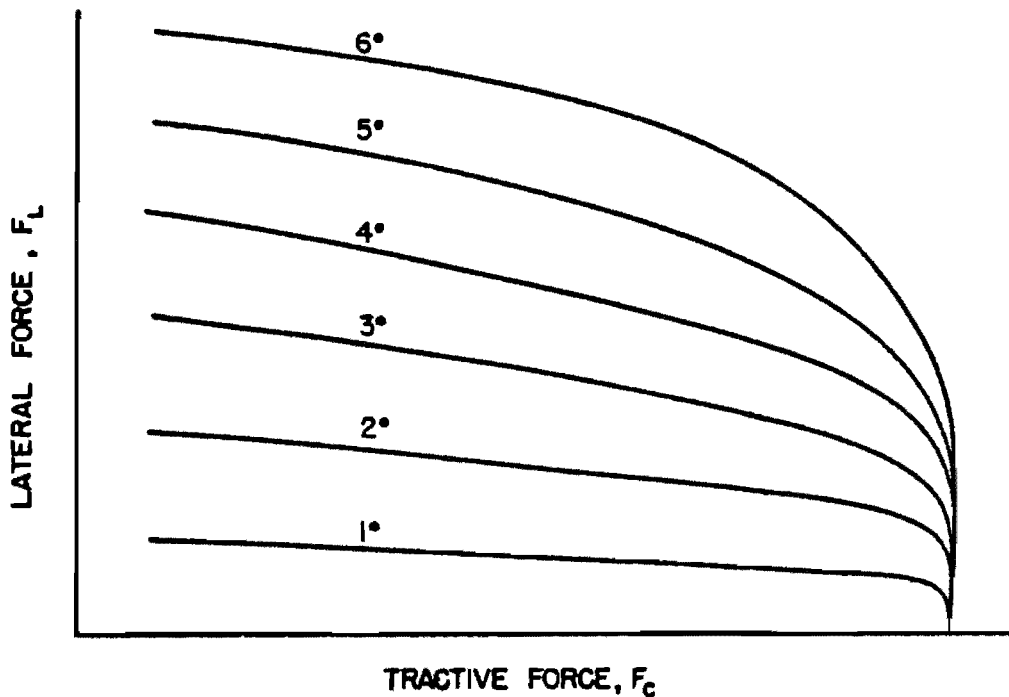


Figure 3-7

Lateral (Cornering) Force As A Function of Circumferential (Tractive) Force For Given Slip Angles (Reference [25])

tractive effort is greater than the saturation limit, the limit is taken as the circumferential force. In the braking mode, the circumferential force saturation limit is equal to the saturation limit, $\mu_i W_i$, times the cosine of the tire slip angle as shown in Fig. 3-6. Otherwise, as before, the circumferential force is equal in magnitude to the tractive effort.

A difference in the way positive and negative tractive effort is treated should be noted above. In the driving mode (positive traction effort) the saturation limit

equals the product $\mu_i W_i$, while in the brake mode (negative tractive effort) the saturation limit equals the product $\mu_i W_i \cos(\alpha_i)$. The reason for this difference stems from the rotation of the wheel. In braking the wheel is locked at the limit and, therefore, has no angular velocity. However, with a positive tractive effort large enough to reach the saturation limit, when slippage occurs at the tire-roadway contact patch, the wheel will spin with an angular velocity, ω . In this circumstance, the velocity of the tire in contact with the roadway is the vector sum of the wheel velocity and the velocity of the tire contact patch with respect to the wheel (i.e., wheel spindle). Consequently, it might be suggested that wheel velocity should not be used solely to determine the direction of the applied forces on the tire but rather use should be made of the vector sum of \vec{V}_W and $\vec{\omega} \times \vec{r}_t$, where \vec{r}_t is the tire radius vector locating the contact patch relative to the wheel spindle. However, in the case where positive traction produces slippage, resulting in wheel spin, the tractive effort dominates and any steering control associated with a lateral force which would result from the direction of the wheel velocity vector, \vec{V}_W , is lost ($F_{Li} \rightarrow 0$). In other words, the wheel velocity, \vec{V}_W , becomes insignificant in comparison to the velocity of the tire contact patch with respect to the wheel spindle, $\vec{\omega} \times \vec{r}_t$. The result is a circumferential tire force equal to the saturation limit, $\mu_i W_i$. Although the preceding

phenomena does not actually occur instantaneous as slip-page occurs, it is initiated rapidly and our steady-state treatment is appropriate.

As noted above, given a positive traction effort of sufficient value to reach the saturation limit the tire lateral force will be set equal to zero. The tire lateral force will also be zero if the slip angle is very small in conjunction with a braking force large enough to lock up the wheels, where the circumferential tire force approaches the limit, $\mu_i W_i (\cos\alpha_i \rightarrow 1.0)$. Consequently, what remains to be shown is a method of calculating lateral tire forces when the saturation limit is not reached with a positive tractive effort where $\cos\alpha_i \neq 1.0$ with a braking effort.

Tire Lateral Force Model.

Referring again to Fig. 3-5, the relationship between the tire lateral force and slip angle is divided into three general regions; linear no slip, nonlinear partial slip, and constant full slip regions. The constant full slip region will only be reached through a combination of circumferential and lateral tire forces whose vector sum exceeds the limiting saturation value of the friction circle, $\mu_i W_i$. Therefore, once the tire circumferential force has been determined as discussed above, the constant full slip lateral tire force value can be determined using the following equation:

$$F_{Li} = \sqrt{(\mu_i W_i)^2 - F_{Ci}^2} . \quad (3-19)$$

The slope of the linear no slip region is equal to the tire cornering stiffness at zero slip angle introduced with Equation (3-17). This cornering stiffness value is a program input parameter. Since we know the initial slope and the constant value at saturation, it remains to be shown how to determine intermediate partial slip lateral force values in the nonlinear region of Fig. 3-5.

In reference [27] it has been shown that a third order polynomial model is the simplest adequate model for determining cornering stiffness values. Consequently, it would be desirable to use a cubic fit for the nonlinear partial slip lateral tire force region between the end conditions discussed above. However, to do so requires knowledge of the slip angle at which the constant lateral force is attained. The method used for determining the saturation slip angle in the trajectory analysis algorithm has been taken from Calspan Corporation's tire model described in reference [20] for their SMAC program. The method uses a linear relationship between slip angle and the saturation lateral force of Equation (3-19), depicted by the following equation:

$$F_{Li \text{ saturation}} = \left[\frac{C_i |_{\alpha_i=0}}{3.0} \right] \alpha_i \quad (3-20)$$

For different tire cornering stiffness values and different roadway and vehicle parameters affecting the product $\mu_i W_i$ and the tractive effort, the intersection of the line described by Equation (3-20) and a family of slip angle versus lateral force curves similar to Fig. 3-5 is shown in Fig. 3-8.

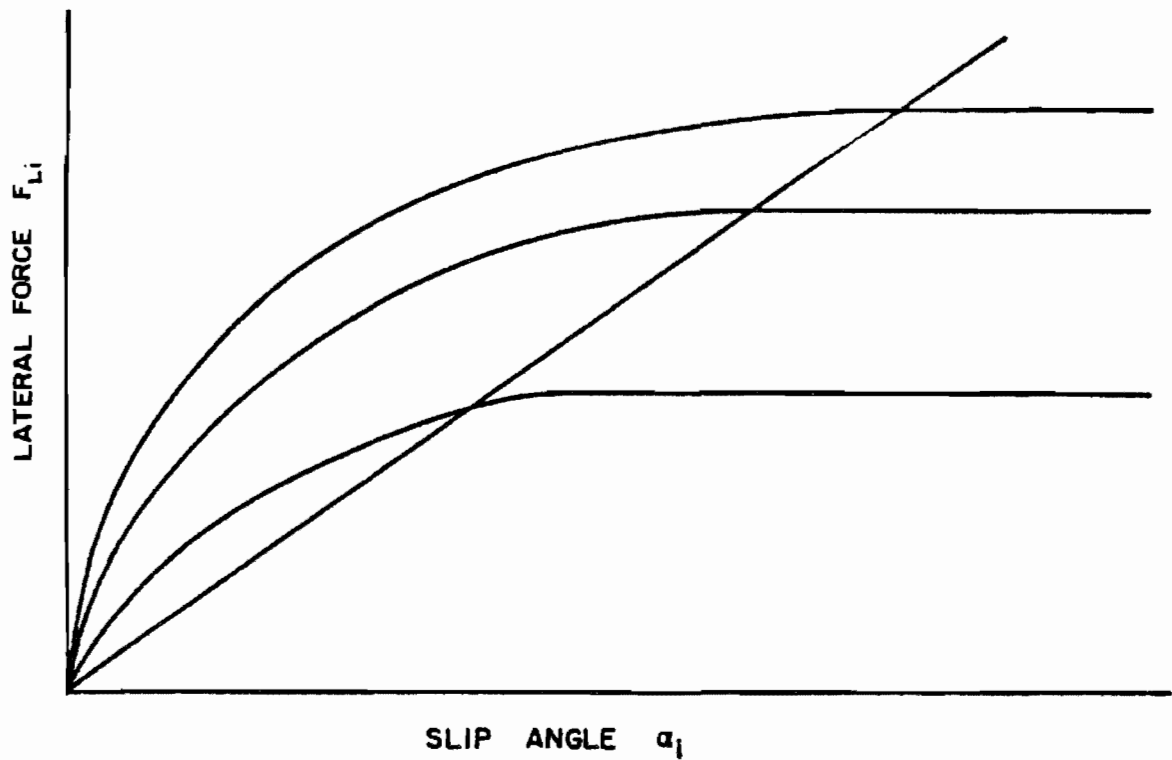


Figure 3-8

Lateral Tire Force Saturation
Points for Family of Lateral
Force Versus Slip Angle Curves

By defining a nondimensional slip angle, β_i , as:

$$\beta_i = \frac{C_i \alpha_i}{\sqrt{(\mu_i W_i)^2 - F_{Ci}^2}}, \quad (3-21)$$

the constant lateral tire force is attained for $|\beta_i| \geq 3.0$. The partial slip region is then modeled with the following equation:

$$F_{Li} = \sqrt{(\mu W_i)^2 - F_{Ci}^2} \left[\beta_i - \frac{1}{3} \beta_i |\beta_i| + \beta_i^3 \right]$$

for $|\beta_i| < 3.0$. (3-22)

As previously noted, the lateral tire force will always oppose the lateral velocity component of the tire. This completes our discussion of the tire model.

CHAPTER IV

IMPACT PHASE ANALYSIS

The discussion of collision impact analysis techniques which is presented in this chapter is divided into four major sections. The first section is comprised of the derivation of a system of general equations, based on linear and angular momentum principles, which are applicable to the vehicle impact phase of an accident. Once the derivation of general equations is complete, the equation variables will be discussed and classified with respect to their certainty in the second section of this chapter. Assumptions applicable to vehicle accidents which are needed in order to reduce the general equations derived in the first section into a system of n equations and n unknowns which can be solved explicitly are also discussed in the second section. The second section is concluded with the brief discussion of an example of a variable classification for a particular accident. Using the variable classification example of the second section, the third section presents the derivation of an explicit solution for the equation system which has been implemented in an impact analysis algorithm.

General Impact Equations.

In the derivation of vehicle impact equations which follows, the vehicles are taken to be rigid bodies with mass, m , and moment of inertia, I_z , about a vertical axis through their center of gravity, analogous to the values used in the trajectory analysis presented in Chapter III. Figure 4-1 depicts the general impact problem, where 4-1(a) illustrates the actual impact and 4-1(b) and (c) are individual free body diagrams for the vehicles.

Linear Momentum Impact Equations.

Integrating the mathematical formulation of the principle of linear momentum:

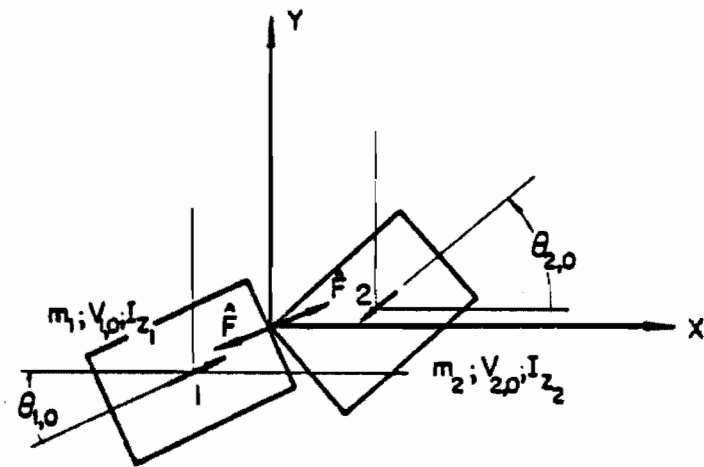
$$F = m \frac{d^2x}{dt^2} = m \frac{dV}{dt} \quad (4-1)$$

once yields:

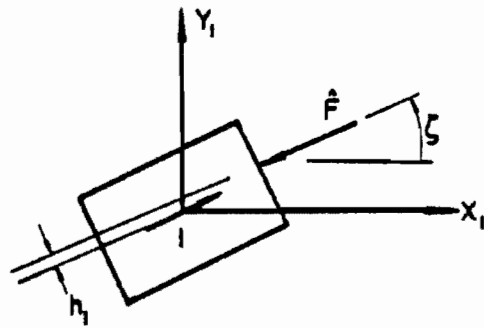
$$\hat{F} = \int_0^{\tau} F dt = m \int_{V_0}^{V_{\tau}} dV = m(V_{\tau} - V_0) , \quad (4-2)$$

where \hat{F} is the force impulse acting on a body and V_0 and V_{τ} are the vehicle initial and final impact linear velocities, respectively.

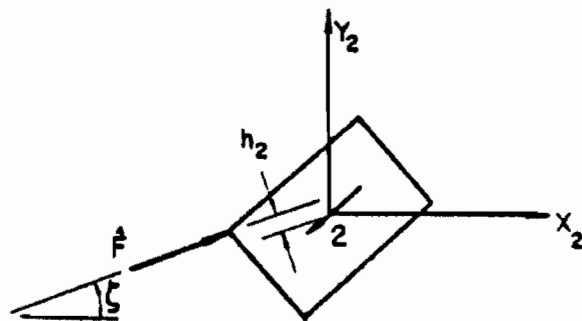
Applying Equation (4-2) to each vehicle with respect to the x and y directions yields the following four equations:



(a) Impact Between Two Vehicles



(b) Free Body Diagram for Vehicle #1



(c) Free Body Diagram for Vehicle #2

Figure 4-1

$$\begin{array}{l}
 \text{Vehicle \#1} \\
 \text{Vehicle \#2}
 \end{array}
 \left\{ \begin{array}{l}
 - \hat{F} \cos \zeta = m_1 (u_{1,\tau} - u_{1,o}) \\
 - \hat{F} \sin \zeta = m_1 (v_{1,\tau} - v_{1,o}) \\
 \\
 F \cos \zeta = m_2 (u_{2,\tau} - u_{2,o}) \\
 F \sin \zeta = m_2 (v_{2,\tau} - v_{2,o}) , \quad (4-3)
 \end{array} \right.$$

where u and v are linear velocities in the x and y directions, respectively.

Recognizing the following vector relationships:

$$u_{j,o} = v_{j,o} \cos \theta_{j,o}$$

$$v_{j,o} = v_{j,o} \sin \theta_{j,o} \quad (4-4)$$

between the initial velocity components, $u_{j,o}$ and $v_{j,o}$, and the initial total vehicle velocity, $V_{j,o}$, and the vehicle orientation, $\theta_{j,o}$, allows Equation (4-3) to be written in another form. Before expressing Equation (4-3) in a new form, relationships between the force impulse, \hat{F} , the angle of application of the force impulse, ζ , and force impulse components in the x and y directions, \hat{F}_x and \hat{F}_y , respectively, will be introduced as follows:

$$\begin{array}{l}
 \hat{F}_x = \hat{F} \cos \zeta \\
 \hat{F}_y = \hat{F} \sin \zeta . \quad (4-5)
 \end{array}$$

Substituting Equations (4-4) and (4-5) into Equation (4-3) results in the following equations:

$$\begin{aligned}
 \text{Vehicle \#1} & \begin{cases} - \hat{F}_x = m_1 (u_{1,\tau} - V_{1,o} \cos \theta_{1,o}) \\ - \hat{F}_y = m_1 (v_{1,\tau} - V_{1,o} \sin \theta_{1,o}) \end{cases} \\
 \text{Vehicle \#2} & \begin{cases} \hat{F}_x = m_2 (u_{2,\tau} - V_{2,o} \cos \theta_{2,o}) \\ \hat{F}_y = m_2 (v_{2,\tau} - V_{2,o} \sin \theta_{2,o}) \end{cases} \quad (4-6)
 \end{aligned}$$

The advantages of the form of Equations (4-6) over that of Equations (4-3) in the application of the principle of linear momentum to vehicle accidents will become evidence later.

Angular Momentum Impact Equations.

Integrating the mathematical formulation of the principle of angular momentum,

$$M = I_z \frac{d^2 \theta}{dt^2} = I_z \frac{d\Omega}{dt} \quad (4-7)$$

yields

$$\hat{M} = \int_0^\tau M dt = I_z \int_{\Omega_0}^{\Omega_\tau} d\Omega = I_z (\Omega_\tau - \Omega_0) , \quad (4-8)$$

where \hat{M} is a moment impulse around the vehicle center of gravity and Ω_0 and Ω_τ are vehicle initial and final impact angular velocities, respectively. The moment impulse, \hat{M} , is attributable to the force impulse, \hat{F} , acting about the vehicle center of gravity. This results in the following equation:

$$\hat{M} = \hat{F}h = I_z (\Omega_\tau - \Omega_0) , \quad (4-9)$$

where h is the moment arm of the force impulse, \hat{F} , shown in Fig. 4-1.

The application of Equation (4-9) to each vehicle yields one equation for each vehicle, as follows:

$$\begin{aligned} \text{Vehicle \#1} \quad & |\hat{F}|h_1 = I_{Z1}(\Omega_1, -\Omega_{1,0}) \\ \text{Vehicle \#2} \quad & |\hat{F}|h_2 = I_{Z2}(\Omega_2, -\Omega_{2,0}) \end{aligned} \quad (4-10)$$

The presence of an absolute value of the force impulse in Equations (4-10) requires elaboration. The sign convention for the force impulse, \hat{F} , introduced in Equations (4-3) is arbitrary, with only a requirement of opposing signs of the force impulse for the two different vehicles. The solution, discussed later in this chapter, yields the appropriate sign for the force impulse, which is nonconsequential as far as the objectives of an impact analysis algorithm is concerned. However, in order to guarantee the proper sign convention for the moment about the vehicle center of gravity caused by the force impulse,^{*} the absolute value of the force impulse is used in Equations (4-10). Thus, the sign of the moment arm, h , dictates the sign of the resulting force impulse moment and the user or investigator need only determine the sign of the moment arm in order to determine or specify the resulting moment.

* Moments are taken positive in the counter-clockwise direction.

Impact Analysis Equation Systems.

The six equations of Equations (4-6) and (4-10) constitute a general system of algebraic equations describing the impact phase of a vehicle accident involving two vehicles in a collision. Consequently, to solve this system of equations not more than six variables can remain unknown. To evaluate the possible systems of equations and unknowns, the variables will be classified according to their certainty as suggested by Wilson [2]. With some thought, the twenty variables in Equations (4-6) and (4-10) can be classified as presented in Table 4-1 for the most general case.

TABLE 4-1
GENERAL CLASSIFICATION OF VARIABLES
IN EQUATIONS (4-6) AND (4-10)

Most Certain:	$m_j; I_{zj}; j = 1, 2$ (vehicle no.)	4 variables
Less Certain:	$u_{j,\tau}; v_{j,\tau}; \Omega_{j,\tau}$	6 variables
Least Certain:	$v_{j,o}; \theta_{j,o}; \Omega_{j,o}; h_j$	8 variables
Definite unknowns:	$\hat{F}_x; \hat{F}_y$	2 variables

The classification of vehicle mass and moment of inertia values as most certain should be apparent. The classification of vehicle linear and angular velocities at

the end of the impact phase in the less certain category, assumes accurate velocity estimations are obtainable from post impact trajectory analysis or at least are assumed for a preliminary impact analysis. Contrary to the first two categories, the classification of the variables in the least certain and definite unknown categories, between the later two categories, is rather arbitrary. Excluding the force impulse components, \hat{F}_x and \hat{F}_y , it is conceivable that any of the rest of the variables in the last two categories, could be in either category for any particular accident. In fact, in some, if not the majority of cases the variables classified as least certain in Table 4-1 would all be definite unknowns unless simplifying assumptions are made.

If it is not apparent already, the number of definite unknowns is typically greater than six and, therefore, the system of Equations (4-6) and (4-10) is normally unsolvable without simplifying assumptions. In other words, assumptions are required in order to classify enough variables as least certain so the number of definite unknowns is equal to six and a solvable system of six equations and six unknowns is obtained.* Therefore, a discussion of possible simplifying assumptions and resulting systems of equations and unknowns is in order. The

* If angular momentum is neglected completely, a system of four equations (4-6) and four unknowns would be sought. In general, a system of n equations and n unknowns is required.

eight variables under question with respect to their classifications between least certain and definite unknowns in Table 4-1 are listed below. The variables are divided into two groups associated with the linear and angular momentum equations. The classification of the two groups of variables will be discussed separately in the following two sections.

$$V_{j,o}; \theta_{j,o}$$

$$\Omega_{j,o}; h_j \quad (j = 1,2)$$

Classification of Linear Momentum Equation Variables.

Of the variables under question with respect to their classification between least certain and definite unknowns, the initial vehicle linear velocities, $V_{j,o}$, and angular orientations, $\theta_{j,o}$, are associated with the linear momentum equations.

At least one of the two initial linear velocities, $V_{j,o}$, will be a definite unknown or else we really do not have an accident reconstruction problem of consequence. Typically, both initial linear velocities will be definite unknowns.

If the system of linear momentum Equations (4-6) had been left in the original form derived, Equations (4-3), four initial linear velocity components would have required classification instead of two total velocities.

By using the variable transformation Equations (4-4), the four linear velocity components were replaced with two total initial velocities, $V_{j,o}$, and initial vehicle angles of orientation, $\theta_{j,o}$. The initial angular orientation of vehicles involved in accidents is often known with fair certainty and can, therefore, be classified as least certain. At a minimum, bounds can be placed on the initial vehicle angular orientations. By performing a transformation of variables on the linear momentum equations using Equations (4-4) it has been possible to simplify the application of the linear momentum principle to vehicle accidents by expressing the equations in terms of variables for which a greater certainty is known.

Based on the thought process for classification of initial linear total velocities and vehicle angular orientations just discussed, it is possible to arrive at a system of four equations (4-6) and four unknowns where only linear momentum is considered. A typical variable classification for this simple system of equations, neglecting angular momentum is shown in Table 4-2. Note, the classification presented in Table 4-2 is not the only possible classification.

Before continuing with a discussion of the classification of the variables under question with respect to angular momentum; $\Omega_{j,o}$, h_j ; additional comments with respect to the linear momentum system of equations

TABLE 4-2
 FOUR EQUATIONS (4-6) - FOUR UNKNOWN VARIABLES
 CLASSIFICATION CONSIDERING
 ONLY LINEAR MOMENTUM

Most Certain	m_j	$(j = 1, 2)$
Less Certain	$u_{j,\tau}; v_{j,\tau}$	
Least Certain	$\theta_{j,o}$	
Definite Unknowns	$\hat{F}_x; \hat{F}_y; V_{j,o}$	

and unknowns are in order. Referring back to our previous discussion, Equations (4-5) were used to transform linear momentum equation variable \hat{F} and ζ into \hat{F}_x and \hat{F}_y . This particular variable transformation was performed primarily to obtain a linear set of equations (4-6).^{*} If ζ was an unknown in Equations (4-3), the equations are nonlinear and a numerical solution would be required. Using the variable transformations, Equations (4-5), a linear set of equations which can be solved explicitly as will be shown later result. However, there may exist cases where the angular orientation of the force impulse, ζ , can be estimated with good certainty (e.g., head-on collisions). In such cases, the use of Equations (4-5) to transform variables would be undesirable. By retaining ζ as a known

^{*} Equations (4-6) are linear only if the initial vehicle angular orientations, $\theta_{j,o}$, are classified as knowns as shown in Table 4-2.

variable another variable of less certainty could be classified as an unknown. When ζ is known, Equations(4-3) are linear with respect to $\sin\zeta$ and $\cos\zeta$.

Similarly, if a particular vehicle's initial angular orientation, $\theta_{j,o}$, cannot be classified as least certain, it would be desirable to leave that particular vehicle's velocity in components ($u_{j,o}$; $v_{j,o}$) and not introduce the initial angular orientation variable using Equations (4-4). Otherwise, the resulting equations are nonlinear with respect to $\sin\theta_{j,o}$ and $\cos\theta_{j,o}$, requiring numerical solution.

Classification of Angular Momentum Equation Variables.

As previously noted, the initial vehicle angular velocities, $\Omega_{j,o}$, and the force impulse moment arms, h_j , associated with the angular momentum equations require classification between least certain and definite unknown categories.

Independent of vehicle heading or the trajectory direction, it is often possible to assume zero initial angular velocities, $\Omega_{j,o}$. In fact, the classification of initial angular velocities as least certain (e.g., $\Omega_{j,o} = 0$) should be possible in the majority of cases.

Under certain conditions of central impact the force impulse moment arm, h_j , of one or both vehicles may be zero with good certainty. However, in a majority of

accidents the force impulse moment arms will both be classified as definite unknowns.

This completes our discussion of possible assumptions which can be used to reduce the general equations of impact into a solvable system of equations. Although the possible assumptions discussed cannot conceivably be used with success in obtaining an adequate system of equations for all possible vehicle accidents, they certainly meet the requirement for the vast majority of accidents. In addition, the preceding discussions have hopefully revealed the thorough process required to arrive at such assumptions.

To close this section, another example of a possible equation-variable classification will be presented combining both linear and angular momentum equations and variables. The following example will rely on earlier discussions and Table 4-2 as well as the preceding discussion in this section.

Assume the particular accident impact phase in question is illustrated in Fig. 4-1. Furthermore, assume it is apparent from pre-impact trajectory paths and tire marks that it is reasonable to believe that vehicles had zero initial angular velocities and initial angular orientations can be estimated with fair certainty. With the assumptions proposed above, a solvable system of equations has been obtained since four of the eight questionable least variables ($v_{j,0}$; $\theta_{j,0}$; $\Omega_{j,0}$; h_j) have been classi-

fiable as least certain having six equations and six definite unknowns. The final variable classification discussed is shown in Table 4-3. The equations which would be implemented, with the variable classification made, are Equations (4-6) and (4-10).

TABLE 4-3
PROPOSED CLASSIFICATION OF VARIABLES FOR IMPACT
ILLUSTRATED IN FIGURE 4-1 USING
EQUATIONS (4-6) AND (4-10)

Most Certain	m_j, I_{Zj}	$j = 1, 2$
Less Certain	$u_{j,\tau}, v_{j,\tau}, \Omega_j,$	
Least Certain	$\theta_{j,o}, \Omega_{j,o}$	
Definite Unknowns	$\hat{F}_x, \hat{F}_y, v_{j,o}, h_j$	

The variable-classification made, are Equations (4-6) and (4-10).

The variable classification presented in Table 4-3 will be used in the next section, where explicit expressions for the definite unknowns are derived in terms of the known (most certain, less certain, least certain) variables.

Solution of Impact Analysis Equation Systems.

For impact analysis equations expressed in the form of Equations (4-6) and (4-10) and the variable classification shown in Table 4-3, a system of six linear equa-

tions and six unknowns is obtained. Given this system of equations or any other system of linear equations resulting from different variable classifications, explicit solutions for the unknowns can be derived.

In this section, the solution of the system of equations resulting from the combination of Equations (4-6) and (4-10) with the variable of classification in Table 4-3 is discussed. This system of equations is believed to be the most suitable system applicable to the reconstruction of the impact phase of the majority of vehicle accidents. The system of six equations and six unknowns in question can be divided into subsystems. Equations (4-6) with the unknowns, \hat{F}_x , \hat{F}_y , and $V_{j,o}$ ($j = 1, 2$) is a subsystem for four equations and four unknowns which can be solved simultaneously to obtain the following expressions for the unknowns:

$$v_{1,o} = \frac{m_2(u_{2,\tau} \sin \theta_{2,o} - v_{2,\tau} \cos \theta_{2,o}) + m_1(u_{1,\tau} \sin \theta_{2,o} - v_{1,\tau} \cos \theta_{2,o})}{m_1 \sin(\theta_{2,o} - \theta_{1,o})}$$

$$v_{2,o} = \frac{m_2 u_{2,\tau} + m_1(u_{1,\tau} - v_{1,o} \cos \theta_{1,o})}{m_2 \cos \theta_{2,o}}$$

$$\hat{F}_x = m_2(u_{2,\tau} - v_{2,o} \cos \theta_{2,o})$$

$$\hat{F}_y = m_2(v_{2,\tau} - v_{2,o} \sin \theta_{2,o}) . \quad (4-11)$$

Adding the force impulse components in the x and y directions vectorially, the resultant force impulse acting on the vehicles can be expressed by:

$$\hat{F} = \sqrt{\hat{F}_x^2 + \hat{F}_y^2} . \quad (4-12)$$

Using Equation (4-5), the angle of application of the force impulse can also be calculated.

Once the resultant force impulse is obtained using Equation (4-12), the angular momentum impact Equations (4-10) can be solved independently for the force impulse moment arms; h_j , $j = 1, 2$; for each vehicle resulting in the following equations:

$$h_1 = \frac{I_{Z1}\Omega_{1,\tau}}{|\hat{F}|}$$

$$h_2 = \frac{I_{Z2}\Omega_{2,\tau}}{|\hat{F}|} . \quad (4-13)$$

The explicit expressions for the unknowns of the impact analysis equation system, Equations (4-11) through (4-13) are easily coded into an impact analysis algorithm which reads the impact phase known variables, calculates the unknowns using the explicit expressions, and creates an output file. Due to the simplicity of the algorithm, further discussion of the algorithm is unwarranted. A listing of an algorithm corresponding to the particular impact analysis equation system just discussed is presented in Appendix E of reference [3].

Due to the simplicity with which a system of linear impact analysis equations can be solved and coded into an impact analysis algorithm for any particular classification of variables, further solutions of other possible impact analysis equation systems will not be presented in this report. This is not meant to imply other algorithms for different systems of impact analysis equations and variable classifications may not be required in a complete package of impact analysis algorithms.

CHAPTER V

A COMPUTER HARDWARE/SOFTWARE SYSTEM

The design of a computer system and associated system software which permits an optimum operating environment for the reconstructionist is a problem with many options. As such, the computer hardware/software system has evolved through many stages. Throughout the evolution of this system, a set of criteria have been developed and include the following primary considerations.

1. The system must be capable of solving the equations modeling the trajectory and impact phases of an accident with accuracy and as much speed as possible.
2. The input should be straightforward (preferably graphic in nature) allowing ease of checking and easy editing.
3. The output format should be dynamic graphics with the option of alphanumeric and permit real-time operator interaction.
4. The hardware system should be low cost, if possible, to permit duplication in governmental agencies.
5. The overall system should be interactive in

nature permitting an iterative solution methodology by the operator.

An early prototype system (MASS) was developed utilizing a CDC 6600 computer linked to a PDP 11/40 with an attached IMLAC PDS-1 graphic mini-computer. The analysis algorithms included SMAC and CRASH executing on the CDC 6600 with an extensive graphic post-processor executing on the PDP 11/40. The post-processor permitted a dynamic display of a vehicle collision reconstruction in several modes including graphic and alphanumeric. While the system was accurate, it lacked the speed necessary to make the overall system interactive in nature. This was due, in part, to the timesharing nature of the link between the CDC 6600 and PDP 11/40 computers. In addition, the large input file required by the analysis programs often required in excess of an hour to create and edit with errors being difficult to detect. Because of the lack of modularity in the analysis programs, a single simulation was quite expensive. A single simulation might require three hours to complete during a period of high demand on the CDC 6600 at a cost of approximately \$10. Considering the fact that thirty simulations might be required to iterate to a successful reconstruction, the prototype system was far from optimum.

From the initial prototype system, a modular hardware/software architecture has evolved into what is now called MASS. The MASS software is composed not only

of the basic modular analysis algorithms discussed previously, but of an extensive set of operating system software supporting input, output, and function control by the investigator. The MASS analysis algorithms have been written for execution on a PDP 11/40 (currently being upgraded to a PDP 11/44) or on a Z80 based micro-computer system. The operating system with attached graphic input/output hardware has been implemented on a Z80 based micro-computer system.

The operating system software comprising this system will be discussed in the following sections of this chapter. In addition, the hardware will be presented as well as a detailed example illustrating the nature of the man machine interaction required to perform a collision reconstruction with the MASS system.

MASS Operating System

The Modular Accident Simulation System Operating System (MASS O.S.) has been developed to link the various modules of MASS. The main responsibilities of the MASS O.S. include the management of input data files, control and execution of the analysis modules and the management and display of output files.

Graphic Input Device

Most all data used by the MASS O.S. is input to the system through a digitizing tablet (see Fig. 5-1).

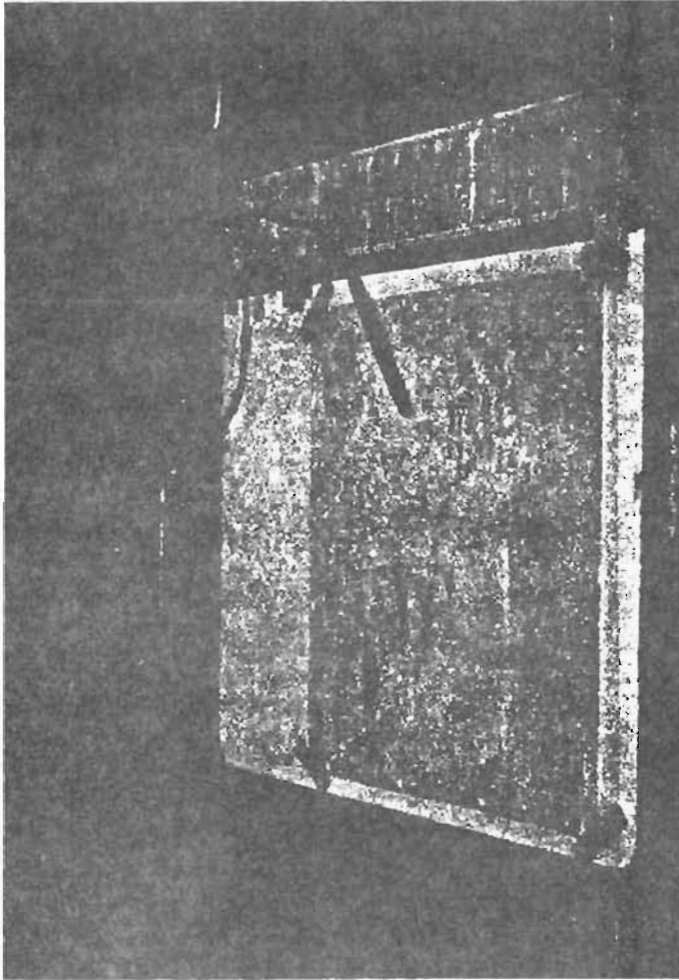


Figure 5-1. Graphic Input Device

The user can select a certain point on the surface of the digitizing tablet with a stylus. The digitizer then determines the coordinates of that position and transmits those coordinates to a micro-processor based controller connected to the S-100 bus of the Z80 micro-computer.

The controller or personality module decides whether the coordinates on the selected point represent a data control command or actual data. A data control command is used to identify the type and quantity of data to follow. The data is collected by the controller, placed in a specific format and transmitted to the central processing unit of MASS (i.e. the Z80 CPU).

The advantage of this type of system lies in the ease of inputting graphic information. A scale drawing of the scene of the accident showing the initial and final positions of the vehicles and the locations of all road surface boundaries is first placed directly on the surface of the digitizing tablet. Graphic information can then be input by selecting strategic points on the drawing using the stylus.

The disadvantage of this system of inputting data is that numeric information is slightly harder to enter. One part of the tablet surface is reserved for an area containing the digits zero through nine. Numbers are entered by selecting each of these digits, one at a time corresponding to the digits of the number as read from left to right. Since the numbers are selected with a stylus

instead of a standard keypad, the user has to take more care to insure that the numbers are entered properly. Once the user becomes accustomed to this method of inputting numbers, this disadvantage is less noticeable.

For a detailed description of the micro-processor based tablet interface, controlled software and tablet hardware, the reader is referred to the work by Kroeger [5].

Data File Management.

Data file management commands will generally be input from the graphic input device. These include commands for creating, editing, saving, displaying and deleting the data files to be used as input to the analysis modules. Table 5-1 gives a list of the graphic input device commands while Table 5-2 discusses specific input data commands.

The create file command signals MASS O.S. to begin with creation of a new data file to be identified with a particular number which is specified by the user. The data files in the MASS contain a post-crash and a pre-crash data area corresponding to pre-impact and post-impact phases of the accident. A data in mode command allows the user to select either post-crash or pre-crash data areas in the data file.

The old file command allows the user to select a previously saved file by its unique number and read it

TABLE 5-1
 GRAPHIC INPUT DEVICE CONTROL COMMANDS

Command Byte	No. of Data Bytes	Range of Parameter	Description of Command
44H	1	0 - 255	Old file
43H	1	0 - 255	New file
42H	1	0 - 255	Delete file
41H	1	0 - 255	Save file
40H	1	0 - 255	Display file library
3EH	0	-	Pre-crash mode
3DH	0	-	Post-crash mode
3BH	0	-	Execute pre-crash
3AH	0	-	Execute crash
39H	0	-	Execute post-crash

into memory from mass storage. The user can then edit any or all portions of the file including pre-crash and post-crash areas through the various commands as given at the graphic input device. The edited version of the file becomes permanent upon the input of the save file command.

The save file command saves the current version of the data file under the specified file number onto the mass storage system. The save file command can also be used to rename an existing data file and save it on mass storage under a new file number. No change to a file becomes permanent until the save command is given.

When an old file is being edited or a new file is being created, the menu commands on the graphic input device can be used to input data to the system. This data will be displayed through the graphic output device as it

TABLE 5-1
GRAPHIC INPUT DEVICE COMMANDS (3)

Command Byte	Number of Data Bytes	Type of Input ¹	No. of Parameters	Units on Parameter ²	Range of Parameter	Comments
35H	1	G	1	in	0:22	Define image area = A
34H	1	N	1	ft/in	0:265	Define scale
32H	2	N	1	-	1:2	No. of Vehicles
31H	2	N	1	sec*1000	-32.768:32.767	Initial time
30H	2	N	1	sec*1000	-32.768:32.767	Final time
2FH	2	N	1	sec*1000	-32.768:32.767	Integration time step
2DH	n x 4	G	n	$\frac{X*2000}{A}, \frac{Y*2000}{A}$	0:2000	Define background graphics
28H	3	N	1	in x 10	-3276.8:3276.7	C.G. to front axle
27H	3	N	1	in x 10	-3276.8:3276.7	C.G. to rear axle
26H	3	N	1	in x 10	-3276.8:3276.7	Tread width
25H	3	N	1	lb*sec ² /in x 100	-327.68:327.67	Vehicle mass
24H	3	N	1	in x 10	-3276.8:3276.7	C.G. to front bumper
23H	3	N	1	in x 10	-3276.8:3276.7	C.G. to rear bumper
22H	3	N	1	in x 10	-3276.8:3276.7	Vehicle width
20H	4	G	1	ft x 100 (X',Y')	-327.68:327.67	Impact point
1FH	5	G	1	ft x 100 (x,y)	-327.68:327.67	Initial position
1EH	3	G	1	deg	-32768:32767	Initial direction
1DH	3	G	1	deg	-32768:32767	Initial velocity direction
1CH	3	N	1	mph x 10	-3276.8:3276.7	Initial velocity
1BH	3	N	1	deg*10/sec	-3276.8:3276.7	Initial angular velocity
19H	5	G	1	ft*10 (x,y)	-327.68:327.67	Final position
18H	3	G	1	deg	-32768:32767	Final direction

TABLE 5-1, Cont.

Command Byte	Number of Data Bytes ⁴	Type of Input ¹	No. of Parameters	Units on Parameter ²	Range of Parameter	Comments
14H	2	N	1	-	1 : 2	No. steering zones
13H	10	G	1	ft*100 (x,y)	-327.68 : 327.67	Zone boundary
0BH	10	G	1	ft*100 (x,y)	-327.68 : 327.67	Zone boundary
0AH	10	G	1	ft*100 (x,y)	-327.68 : 327.67	Zone boundary
12H	4	N	1	deg	-32768 : 32767	Rear steering angle
11H	10	N	4	deg	-32768 : 32767	Front steering angle/tire
0FH	2	N	1	-	1 : 2	No. tractive effort zones
0DH	10	N	4	% x 10	-3276.8 : 3276.7	Full wheel lockup (-braking, + traction)
0EH	2	N	1	-	1 : 2	No. friction zones
09H	10	N	4	*100	-327.68 : 327.67	Coefficient of friction/tire
08H	4	N	1	sec/in * 10 ⁵	-.32768 : .32767	Velocity correction factor(negative)
07H	10	N	4	lb/deg * 100	-327.68 : 327.67	Cornering stiffness/tire

NOTES:

1. "G" indicates graphic-type input; "N" indicates numeric-type input.
2. Coordinate systems are given as indicated in FIGURE 3.1-1.
3. Ranges shown may not be valid for analysis modules.
4. All numbers are given in either one or two bytes. For two byte numbers, the least significant byte is transmitted first followed by the most significant byte.

is entered by the user. This provides the user with instantaneous feedback as to what information was entered and whether or not it was entered correctly.

The delete file command allows the user to delete files from mass storage if the user wishes to get rid of old files or make room for new ones. This command deletes not only the data file from mass storage but also all output files associated with that data file.

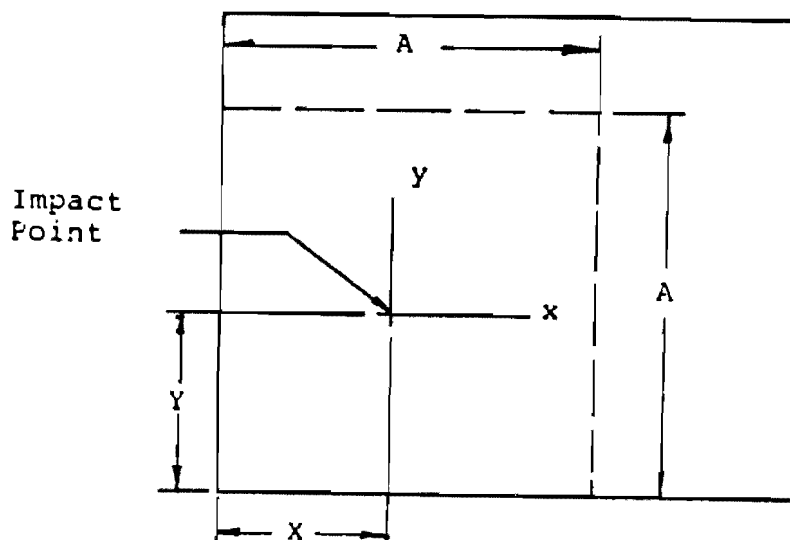
An index of all of the files on mass storage is kept in a separate file. This file can be read by the user through the display file library command. This gives a listing of the file numbers, the status of the data file and the status of any output files associated with the data file.

Redundancies are included in those data file management commands which result in the loss of information. When a new version of a data file is written over an old version with the save command or a file is deleted with a delete command, those commands have to be given twice, consecutively, in order to take effect.

Control and Execution of Analysis Modules.

The various analysis modules can be executed with a specified set of data through the appropriate graphic input device commands.

To execute the MASS trajectory algorithm, TRAJECT, the data file is first selected with the old file



- A - Image Area Dimension (inches)
- x,y - Impact Point Relative Coordinates (feet)
- X,Y - Tablet Relative Coordinates

Figure 5-2. Graphic Input Device Coordinate System

command. Execution of TRAJECT is initiated by the execute pre-crash or the execute post-crash command to generate output for the pre-impact or post-impact sliding phases of the accident, respectively. The output file is created by TRAJECT having the same file number as the data file. The execution of the mass impact algorithm, CRASH follows the execution of TRAJECT except that execution is initiated with the execute crash command and CRASH always reads the post-crash area of the data file for input data.

Graphic Output Device

The graphic output device or Graphics Display Unit (GDU) consists of a Radio Shack TPS-80 Color Computer

(TM) modified with different firmware and special hardware to assist in the task of vehicle accident reconstruction.

The basic TRS-80 Color Computer (TM) consists of a MC 6809E micro-processor unit, up to 64K dynamic RAM, Basic interpreter in firmware, video display unit and RF modular, and other assorted hardware assembled in a compact, self-contained unit including power supply and keyboard. The video display unit referred to can operate in either alphanumeric or several graphics modes of various colors or resolutions. The video display itself can be any color or black and white television set that corresponds to the NTSC standards (U. S. standard). The GDU consists of a basic unit up-graded with the necessary programming in EPROM.

The software in EPROM enables the GDU to operate in either of two modes; as system console or CRT terminal mode or as a graphics display mode. As the system console or terminal, the user can use the GDU to input data as required to "bring the system up" and also for the physical parameters input to the various analysis programs and to supplement the graphics input tablet. With the GDU used to input alphanumeric data, the user can perform actions that cause the graphics mode to be modified. Commands can be issued while graphical data is being displayed to freeze the moving screen, go to a magnification mode of 1X, 2X or 4X or return to an abort condition in the basic command monitor mode.

The graphical data will consist of a single color mode of 256 pixels wide by 192 pixels high. The data will consist of a non-moving background super-imposed on to a foreground of the moving cars for a complete realistic display of an accident reconstruction. The GDU serves to scale "raw data" from the host computer suitable for the graphical display.

Output File Management

Display of the output files generated by TRAJECT or CRASH is initiated through the various display device commands. A list of these commands is given in Table 5-3 and Table 5-4.

Display of TRAJECT output is begun by selecting the appropriate file with either the old file command or the select file command from the graphic display device. The output can be displayed through either the display post-crash output, the display pre-crash output or the display enter output command. Error messages will be displayed if any of the necessary output files does not exist. The user can also choose to display the output file in either alphanumeric or graphic format by giving the set alphanumeric or set graphic mode commands.

In alphanumeric mode, the display device shows various vehicle trajectory data at each integration time step. This data includes the linear and angular velocity, and linear and angular acceleration for each vehicle.

TABLE 5-3
GRAPHIC DISPLAY DEVICE COMMANDS

Command Bytes	ASCII Character	Comment
13H	DC3	Freeze display of output
11H	DC1	Resume display of output
03H	ETX	Terminate display of output
4FH	"O"	Set impact point fixed mode
57H, 31H	"V", "1"	Set vehicle display fixed mode
57H, 32H	"V", "2"	Same for vehicle no. 2
41H	"A"	Set alphanumeric display mode
47H	"G"	Set graphic display mode
58H, 31H	"X", "1"	Set graphic magnification
58H, 32H	"X", "2"	
58H, 34H	"X", "4"	
02H	STX	Begin special command

TABLE 5-4
SPECIAL COMMAND SEQUENCES

Command Bytes	ASCII Character	Interrupt Status	Comment
50H, 4FH	"P", "O"	yes	Display post-crash output
50H, 52H	"P", "R"	yes	Display pre-crash output
45H	"E"	yes	Display combined output
4CH	"L"	yes	Display file library
46H	"F", "nnn"	no	Select output file
43H	"C"	no	Display crash output
44H	"D"	yes	Display data file
ODH	CR	no	Execute special command
18H	CAN	no	Cancel current special command line

Note - Interrupt status indicates whether or not special command execution can be interrupted by display commands.

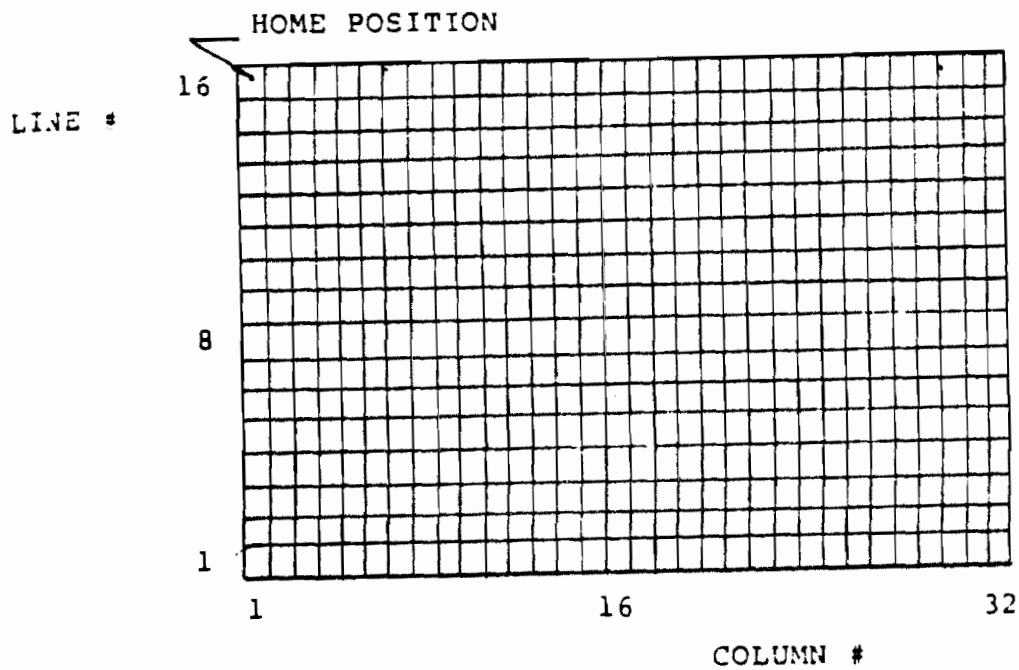


Figure 5-3
Graphic Display Device Coordinate System

In graphic mode, the display device shows the location of the vehicles, the impact point and the background graphics representing curb lines and other boundaries. Several different modes of graphic display include impact point fixed display mode, vehicle fixed display mode and display magnification mode.

In impact point display mode, the user has a bird's eye view of the accident scene. This mode shows the vehicles coming together at the impact point, colliding and separating from each other after the impact. This mode is useful for viewing the results of the collision during the iterative process of forming a reconstruction of the accident.

In vehicle fixed display mode, one of the vehicles is held fixed in the center of the screen and the other vehicle is shown as it comes in to collide with the fixed vehicle. This mode is useful for demonstrating the reconstructed accident from the driver's point of view.

Display magnifications of one, two and four times are available for both impact point fixed and vehicle fixed display modes. Magnification modes are included in the display to improve the resolution in those accident geometries where the scale tends to obscure the fine details such as the orientation of the vehicles.

Display of TRAJECT output can also be controlled by certain graphic display commands. Since the output is displayed sequentially at discrete times, it is necessary to freeze the display at certain times or to change display modes during the output. The display can be frozen with the freeze display command and it can be resumed again with the resume display command. Display modes can also be changed at any time during the display by the appropriate command. Display can be terminated at any time by the terminate display command.

Display of CRASH output is available in alphanumeric format only. Since no numerical integration is involved with CRASH, all output data is displayed on the display screen at once. This output includes pre-impact velocities and directions, impulse moment arms, the force

impulse, speed changes and the coefficient of restitution. Display of this output is accomplished upon the display CRASH output command. Appropriate error messages are printed if the CRASH output file is missing or has not yet been generated.

As an example of how the computer system is used to perform a reconstruction, the following detailed example is presented.

Reconstruction Example

This section describes the steps involved in reconstructing a particular Travis County fatal collision using the various facilities of MASS. The example accident used is the same one presented by Olson [3] and later by Kroeger [5].

Description of Accident.

The accident described in this section involved a fatal broadside collision between two vehicles. Vehicle number one, a 1965 four-door Chevrolet Bel Air, was east-bound when it struck vehicle number two, a 1977 two-door Ford Granada, which was heading north. The scene of the accident is shown in Fig. (5-4).

The Chevrolet struck the Ford broadside and slid to a halt as shown in Fig. (5-4). The Chevrolet suffered severe front end damage with the right front wheels locked and fixed at steering angles of -20 degrees and 5

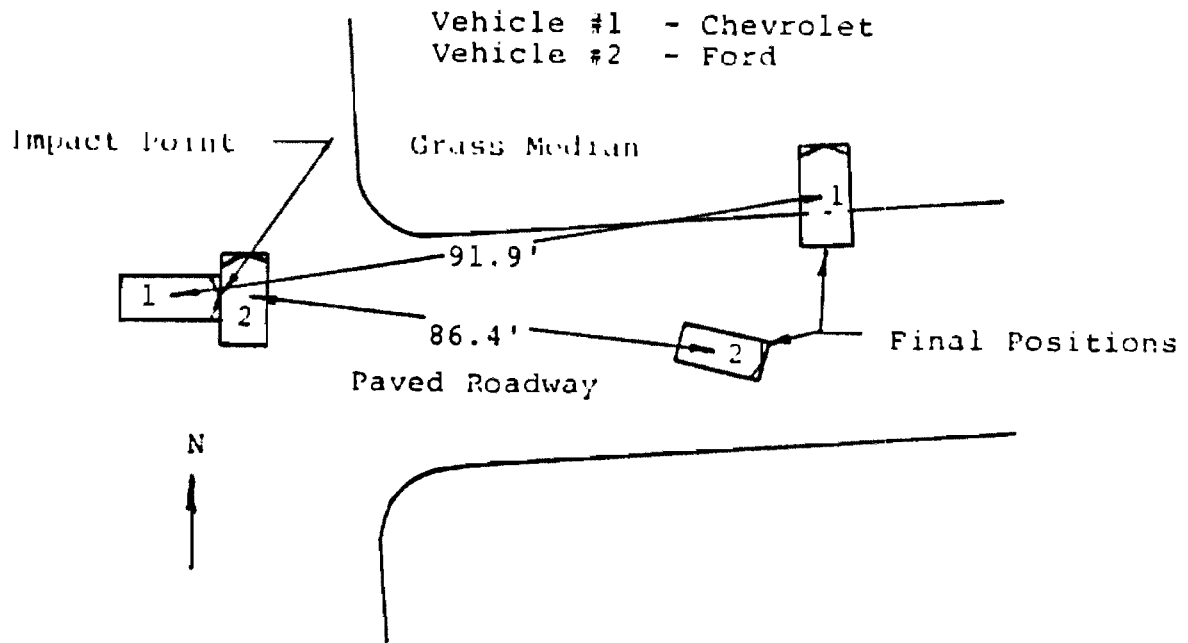


Figure 5-4. Broadside Collision [3]

degrees, respectively. The rear wheels suffered no apparent damage. The Chevrolet slid entirely on the asphalt road surface after colliding with the Ford.

The Ford, which was struck by the Chevrolet, suffered no damage to the alignment of either the front or the rear wheels. The front wheels were assumed to have a steering angle of zero and all wheels were initially assumed to be free to roll. After striking the Ford, the Chevrolet slid partly on the asphalt road surface and partly on the grass median beside the road.

Collection of the Data.

The first step in reconstructing an accident using MASS is the collection of the data. In general, this data came from an on-site investigation, scale drawings, police reports and various handbooks and tables. The final form of this data should be a scale drawing of the accident scene, and a list of various accident parameters.

Scale Drawing.

The scale drawing of the accident should fit entirely on the 20" by 17" graphic surface area of the digitizing tablet. The difference in the width to height ratio of the tablet with that of the graphic display device presents a problem with the display of the data. Since the proposed graphic display is only half as high as it is wide, it has been decided to truncate the upper portion of the tablet graphic surface area when displaying on the graphic output device. If the user wishes to display the accident scene entirely, the drawing should fit entirely in the lower half of the selected image area of the graphic input device.

The scale drawing of the accident should include the following items:

1. The impact point of the accident should be clearly marked on the drawing. All vehicle positions will be calculated relative to this

point.

2. The initial position of the center of gravity of each vehicle should be marked on the drawing. This point will almost always fall in the middle of the automobile. It will not be necessary to draw the outlines of the vehicle as this information is not graphically input.
3. The initial orientations and the initial velocity directions of each of the vehicles should be drawn as a short 1-1/2" line segment extending from the vehicle c.g. in the proper direction. The initial orientation corresponds to the direction the vehicle is facing. The initial velocity direction is the direction the vehicle is moving immediately after the collision. This direction will almost always be on a line connecting the initial position of the vehicle at impact and the final position of the vehicle after coming to rest.
4. The final position of the center of gravity of each vehicle should be marked in the same manner as the initial position. This information is only used for display purposes and is not used in the analysis routines so is therefore optional for running the routines.

5. The final direction of each vehicle is indicated in the same way as the initial direction.
6. The zone boundary for each vehicle is indicated by a line segment. This line divides the boundary between two zones of different steering input, tractive effort (braking) or road friction. At present, only one zone boundary of any type is allowed for each vehicle. Future versions of TRAJECT may allow the user to specify more than one zone boundary for each vehicle and also to specify different boundaries for the steering, tractive and friction zones.
7. Any background graphics that the user wants to display along with the output should also be indicated on the drawing as a series of curved lines. These lines could indicate road boundaries, curb lines, drives, road center lines or anything that is fixed with respect to the accident scene.

The completed drawing for the broadside collision is shown in Fig. (5-5).

Vehicle and Zone Properties.

Vehicle and zone properties are usually obtained from various handbooks and tables. The properties are in-

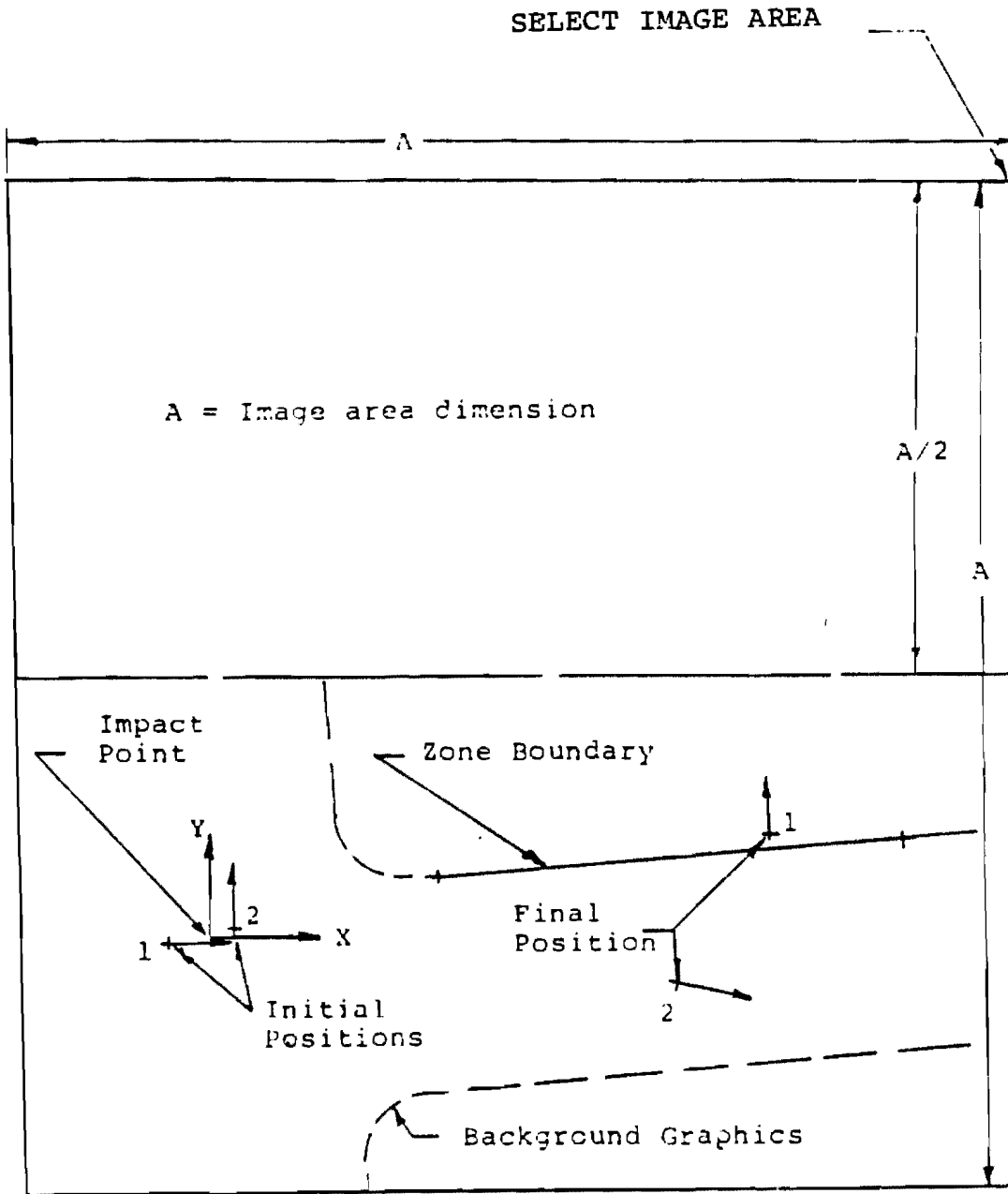


Figure 5-5
Scale Drawing of Broadside Collision

put to MASS as numeric data rather than graphic data and therefore should be compiled in tables rather than in diagrams. In the example for the broadside collision, this procedure is followed.

Values for vehicle geometry data can be obtained from sources like reference [28]. Several geometry parameters are given relative to the vehicle's center of gravity. This location is not usually given in the tables but can usually be assumed to lie roughly in the middle of the vehicle. A conversion factor of $386.4(\text{in-lbm})/(\text{lbf-sec}^2)$ can be used to convert the automobile weight in lbf to MASS consistent units of $\text{lbf-sec}^2/\text{in}$. The parameters for vehicle geometry for the broadside collision are shown in Table 5-5.

TABLE 5-5
BROADSIDE ACCIDENT VEHICLE PARAMETERS

Parameter	Vehicle 1 Chevrolet	Vehicle 2 Ford
CG to front axle (in)	58.1	53.8
CG to rear axle	60.7	56.1
Tread width (in)	60.0	60.0
Vehicle mass ($\text{lb}\cdot\text{sec}^2/\text{in}$)	9.96	9.64
CG to front bumper (in)	97.3	91.2
CG to rear bumper (in)	115.9	106.5
Vehicle width (in)	79.6	74.0
Right front steering angle (deg)	-20	5
Left front steering angle (deg)	0	0
Rear axle steering angle (deg)	0	0

Note: Steering angles are measured as positive counter-clockwise

Cornering stiffness parameters are slightly more difficult to determine. These values are dependent on tire construction, inflation pressure and the weight supported by the tire. The following procedure was used by Olson in reference [3] to determine the tire cornering stiffness parameters for the broadside collision:

1. The cornering stiffness at normal inflation pressure and 1200 lbf normal load for each tire was obtained from Table A-1 in reference [3].

Chevrolet:

Taking average cornering stiffness for
G 78-14 bias and G 78-14 belted bias tires:

$$CS = (138 + 117)/2 = 127.5 \text{ lbf/deg}$$

Ford:

For F 78-15 tires:

$$CS = 114 \text{ lbf/deg}$$

2. The correction for a normal load other than 1200 lbf is found by determining the percentage change in a graph of cornering stiffness vs. normal force for the particular tire construction. The normal load on the tire can be estimated at one fourth the total weight of the vehicle.

Chevrolet:

$$\text{Normal load} = 9.96 * 386.4 / 4 = 962 \text{ lbf}$$

From figure A-5 in [3] for G 78-15 tires:

$$\text{@ 1200 lbf} \quad \text{CS} = 167 \text{ lbf/deg}$$

$$\text{@ 962 lbf} \quad \text{CS} = 155 \text{ lbf/deg}$$

Ford:

$$\text{Normal load} = 9.64 * 386.4 / 4 = 931 \text{ lbf}$$

From Figure A-10 in [3] for F 78 bias belted tires:

$$\text{@ 1200 lbf} \quad \text{CS} = 165 \text{ lbf/deg}$$

$$\text{@ 931 lbf} \quad \text{CS} = 154 \text{ lbf/deg}$$

3. The actual cornering stiffness is then determined by applying the correction found in step 2 to the values for CS found in step 1.

Chevrolet:

$$\text{CS} = .928 * 127.5 \text{ lbf/deg} = 118.33 \text{ lbf/deg}$$

Ford:

$$\text{CS} = .931 * 144 \text{ lbf/deg} = 134.0 \text{ lbf/deg}$$

Tractive effort inputs should be determined next. These values will be given as a percentage of full wheel lock-up with negative values corresponding to braking and positive values indicating positive traction or spinning. These values are given in Table 5-6. From the scene evidence, it was determined that the front wheels of the

Chevrolet were locked into place. All other wheels are initially assumed free to roll.

TABLE 5-6
VEHICLE TRACTIVE EFFORT INPUTS

Tire	Chevrolet	Ford
Right Front	-100.0	0.0
Left Front	-100.0	0.0
Right Rear	0.0	0.0
Left Rear	0.0	0.0

Since simulation results are highly sensitive to the road friction parameters, these values should always be determined from on-site measurements. For this example, the road friction will be determined from table B-1 in reference [3]. The velocity correction factor is a way of incorporating the change in road friction due to velocity. These factors range from -0.0003 sec/in to -0.0005 sec/in [3] with somewhat lower values for wet roads. The friction parameters for the broadside collision are given in Table 5-7.

The final property to be determined is the separation vehicle velocity immediately after the impact. This value can be estimated from the following equation:

$$V_I = \sqrt{2\mu gh + V_F^2} \quad (5-1)$$

TABLE 5-7
ROAD FRICTION PARAMETERS

	Asphalt Road	Grass Median
Coefficient of friction	0.75	0.45
Velocity correction	-.0002	-.0002

Chevrolet:

$$u = 0.75$$

$$d = 86.4 \text{ ft}$$

$$v = \sqrt{2 u g d} = \sqrt{2 (0.75) (86.4 \text{ ft}) (32.3 \text{ ft/sec}^2)}$$

$$v = 64.6 \text{ ft/sec} = 44.0 \text{ mph}$$

Ford:

u is weighted between the road coefficient of friction (0.75), and the median c.o.f. (0.45) by the distance of sliding on each surface (2/3 on road and 1/3 on median)

$$u = 2(0.75)/3 + 0.45/3 = 0.65$$

$$d = 92 \text{ ft}$$

$$v = \sqrt{2 u g d} = \sqrt{2(0.65)(92 \text{ ft})(32.2 \text{ ft sec}^2)}$$

$$v = 62 \text{ ft/sec} = 42.3 \text{ mph}$$

Input of Data to Mass.

The next step involved in reconstructing an accident using MASS involves the input of data. These steps are listed below:

1. The power for the digitizer, micro-computer and graphic display device should be turned on.
2. The scale drawing discussed previously should be taped onto the surface of the tablet.
3. The system should be initialized with the proper command. If MASS is properly initialized, a banner message will be printed at the graphic display device which describes the name and version of the various modules of MASS.
4. The new file command should be given at the graphic input device. The first step in doing this is to select the new file option with the stylus. A short "beep" will sound if this selection is made correctly. The next step is to input the new file number. This is done by selecting the digits of the file number from left to right with the stylus in the numeric entry area of the tablet. After the number is completely entered, the enter number command should be selected with the stylus to complete the command. If a mistake is made during the entry of the number, the clear number command can be used to start over. If a long "beep" sounds during the process, a mistake has been made

- and the procedure should be started over.
5. The data mode select command is given next. This is done in the same way by selecting the post-crash mode option with the stylus. This completes the input for this command. At this point, the display device will show a portion of the data file. All data entered at this point will be immediately confirmed through the display device.
 6. The define image area command is given next by first selecting the define image area option and then by selecting the upper right hand corner of a square on the tablet surface that would completely contain the scale drawing.
 7. The scale of the drawing is input next by first selecting the scale option and then by entering the scale through the numeric input in the same manner as previously discussed.
 8. The number of vehicles in the reconstruction is entered in a similar manner. Two vehicles were involved in the broadside collision.
 9. In a similar manner, the initial time, final time and integration time step should be entered. These numbers will be entered as integers scaled by a factor of 1000. This

avoids the need for the use of a decimal point in the numeric entry area. The integration step size can be chosen to be about 0.01 sec. If this step is too large for the particular accident, the resulting simulation will be inaccurate.

10. The background graphics are entered next by first selecting the proper option and then selecting a series of points along a curve which defines the particular graphic boundary. This sequence is terminated by the terminate background graphics input command. A long "buzz" will normally sound when this command is terminated. The user should avoid selecting an excessive number of points defining the background graphics.

The next major step in the input of data involves the input of vehicle parameters for each vehicle. These steps are listed below:

1. The impact point is first selected by selecting the appropriate option and then the actual impact point as it is shown on the drawing.
2. The next step is to select the vehicle number for subsequent data input. Vehicle no. 1 will be selected in this example.

3. Vehicle geometry parameters will be input as shown in Table 5-5. Each of these numbers are entered numerically with a scale factor of 10 except for vehicle mass which has a scale factor of 100.
4. The tire cornering stiffnesses are input next. The option is selected and the cornering stiffnesses are entered for the RF, LF, RR and LR tires respectively with a scale factor of 100. Note that this command has four numeric parameters while previous commands had only one.
5. The rear axle steering angle is entered by selecting the proper option and entering the angle numerically.

The zone data for vehicle no. 1 is entered as follows:

1. First, the zone number is selected with the zone number command. Zone no. 1 will always correspond to the zone containing the impact point.
2. Second, the number of steering zones is selected. Since there is only one steering input for vehicle no. 1, the number entered here will be one.
3. Next, the front wheel steering inputs are entered. This is done by selecting the

front steering option and then numerically entering the front steering angles for the RF and LF tires. The graphic input device actually expects four parameters for this command so two additional numerical entries must be made to complete the command. Since the information for these entries is not used by MASS, these entries are arbitrary. The numbers entered for the example are -20, 0, 0 and 0.

4. The number of tractive zones is input to MASS. For the example, there is only one different tractive effort for vehicle no. 1.
5. The tractive effort inputs are entered with the tractive effort command. These inputs are expressed as percent of full wheel lock-up with a scale factor of 10 for the RF, LF, RR and LR tires, respectively. Since the front wheels of vehicle no. 1 were locked, the inputs entered are -1000, -1000, 0 and 0. Note that to enter a negative number, the "-" option replaces the "enter" option.
6. Next, the number of friction zones is input. There is only one friction zone associated with vehicle no. 1.
7. The road friction coefficients are entered with a scale factor of 100 for the RF, LF,

RR and LR tires. For vehicle no. 1, these entries are 75, 75, 75 and 75.

8. The velocity correction factor is entered with a scale factor of 100000. The number entered in this case is -20.

This completes the input of vehicle no. 1 parameters.

Vehicle no. 2 parameters are input in a similar manner with the following exceptions:

1. There are two friction zones associated with vehicle no. 2. Zone no. 1 friction input is made in the same manner as described for vehicle no. 1 except that the number of friction zones is set to 2 for vehicle no. 2.
2. A zone boundary is defined by first selecting the define zone boundary option and then by selecting two points along a line dividing the two zones of friction.
3. Next, zone 2 is selected with the appropriate command.
4. The road friction coefficients are entered for vehicle no. 2, zone no. 2. These values are 45, 45, 45 and 45.
5. The velocity correction factor is entered next in the same manner as described for vehicle no. 1.

Initial conditions for both vehicles are entered next. These are the conditions of the vehicle at the

start of the post-crash sliding phase immediately after the impact. The steps involved are listed below:

1. Vehicle no. 1 input is started by selecting vehicle no. 1 mode.
2. The initial position of vehicle no. 1 is input by first selecting the initial position and then selecting the c.g. of vehicle no. 1 as it is shown on the scale drawing.
3. The initial directions and the initial velocity directions are input next. Recall that on the scale drawing, these directions are indicated by short line segments extending from the vehicle c.g. to the proper direction. These directions are input by first selecting the appropriate option and then by selecting two points on this line segment. The first point is selected on the c.g. and the second is selected on the line about 1" away from the c.g.
4. The initial linear velocity is input by selecting the proper option and then by entering the velocity in miles per hour with a scale factor of 10. The number entered in this case for vehicle no. 1 is 440.
5. The initial angular velocity is entered in a similar nature. Since there is no simple method of estimating the initial angular

velocity, this value will have to be selected by intuition. The input in this case was set to -100.

6. Finally, the final position and direction for vehicle no. 1 is input. These are input in the same manner as the initial position and orientation as described in steps 2 and 3.

Steps 1 through 6 are repeated for vehicle no. 2 to complete the initial condition input.

At this point, the data has been completely entered into the file. The steps involved in executing TRAJECT with this data are listed below:

1. The data file should be saved with the save file command. This is done by selecting the save file option and then by entering the file number under which the file is to be saved. This step is extremely important. If the file is not saved before the analysis module is executed, the information in the file will be lost.
2. The next step is to execute TRAJECT. This is done by selecting the execute post-crash option. The system will now load the analysis module into memory, execute it and reload the device controller module into memory. At this point, the user simply waits

for the display to show the banner screen which signals the completion of the execution module.

Display of Post-Crash Output.

Since the graphic output device has not been totally implemented at the time of the writing of this report, it was necessary to design a simulator for this device. The simulator involved a software interpreter which drove a TEKTRONX 4006-1 graphic terminal. This simulator interpreted a limited set of the graphic commands and performed the necessary manipulations to display this information on the 4006 terminal. The graphic device input commands were input directly from the terminal by the device controller. The key sequences corresponding to the commands are given in Table 5-8.

To display the post-crash output file that was generated previously, the following steps are performed:

1. The data file should be selected with either the graphic input device "old file" command or the graphic display device select file command. The old file command is given by selecting the old file option and then by entering the file number. The select file command is given at the keyboard by entering control-B, "F", the file number and return.
2. Post-crash output can be displayed by enter-

TABLE 5-8
SIMULATOR COMMAND KEY SEQUENCES

Command Byte	Key Sequence	Command
13H	control-S	Freeze display
11H	control-Q	Resume display
03H	control-C	Terminate display
41H	"A"	Alphanumeric mode
47H	"G"	Graphic mode
02H	control-B	Begin special command

- Notes:
1. The sequence, control-x, is accomplished by holding down the "control" key while striking the "x" key.
 2. Special commands are given according to their corresponding ASCII codes.

ing the display post-crash output command at the keyboard. For the simulated system, this corresponds to pressing the keys control-B, "P", "O" and return. At this point, the display of the post-crash output file begins.

3. Several keys can be pressed to control the display of the output file. The display can be frozen with the control-S key and can be restarted with the control-Q key. The display mode can be switched between alphanumeric and graphic mode by pressing the "A" key to set alphanumeric mode and by pressing the "G" key to set graphic mode. The control-C key will terminate the display.

Any of these keys can be pressed in any sequence.

The user will see the trajectory of the two vehicles as they slide from the impact position to their final resting positions. The user will also observe that this resting position does not correspond with the actual final resting position of the vehicle. The user will now have to modify the data file, execute TRAJECT and recheck the new solution. This procedure will be repeated until the calculated final positions of the vehicles are approximately equal to the actual final positions of the vehicles. These iterations should be accomplished in the following manner:

1. A single parameter for each vehicle should be changed with the proper graphic input device command. In general, only one parameter should be changed for each iteration. According to Olson [3], the initial velocities should be iterated upon first.
2. The next step is to save the modified file with the save file command.
3. The final step is to execute the analysis module and examine the resulting output.

For the example, it was apparent that iteration on the velocities alone would not achieve an adequate reconstruction. By changing the tractive efforts on the rear wheels of vehicle no. 2 to -100%, a reconstruction

found that approximately matched the actual accident conditions. The results of the reconstruction are shown in Table 5-9.

TABLE 5-9
BROADSIDE ACCIDENT POST-CRASH RECONSTRUCTION [3]

	Vehicle 1	Vehicle 2
Initial velocity (mph)	30.0	40.0
Initial angular velocity (deg/sec)	-11.0	25.0

Impact Analysis.

The results of the post-crash analysis are the velocities that the vehicles had as they bounced off of each other after impact. The objective of impact analysis is to determine the velocities the vehicles must have had immediately before impact.

Impact analysis can be made as soon as post-crash analysis has been completed. No additional input is required to execute the analysis module. The steps to carry out this analysis are as follows:

1. The data file to be analyzed is first selected with the old file command.
2. The analysis module, CRASH, is executed by selecting the execute crash option.
3. After the banner screen is printed at the display device signaling the completion of the analysis, the output can be read by

pressing the keys control-B, "C" and return. The output is displayed in alphanumeric format. These results are shown in Table 5-10.

TABLE 5-10
BROADSIDE ACCIDENT IMPACT ANALYSIS [3]

	Vehicle 1	Vehicle 2
Impact velocity (mph)	68.2	4.78
Impact direction (deg)	90.0	182.0
Impulse moment arm (in)	-1.23	2.34
Force impulse (lb-sec)		6721.4
Coefficient of restitution		0.158

The results given in Table 5-10 are the final results as far as this particular reconstruction is concerned. A pre-impact speed of 68.2 m.p.h. for the Chevrolet suggests some fault on the part of the driver especially when viewed in terms of the very low (5 m.p.h.), pre-impact speed for the Ford. It should be noted from the coefficient of restitution that this collision does qualify as a fairly plastic collision.

Olson [3] also reconstructed this collision using SMAC. With SMAC, Olson obtained pre-impact velocities of 68.8 m.p.h. for the Chevrolet and 9.0 m.p.h. for the Ford. Comparing these values with those obtained using MASS, one can see that these results are in close agreement.

SMAC has been verified with actual collision data. Olson [3] stated that SMAC gives initial velocities that are within +5% of the measured velocities. It should be noted that sufficiently accurate data were required to achieve this accuracy and that uncertainties in the data, in particular in the coefficient of friction, will drastically affect the accuracy of SMAC, as well as MASS.

Pre-Crash Analysis.

Pre-crash analysis is only necessary when there is evidence of braking before the impact. If this is not the case, the final results are those determined from the impact analysis. This was the case for the broadside accident.

For an accident with pre-impact skidding, the following steps can be used to complete the reconstruction.

1. The data file is selected with the old file command.
2. The data mode is set for pre-crash data with the select pre-crash input option.
3. The data is input in the same manner as was described earlier.
4. After the file has been saved, the pre-crash analysis can be performed by selecting the execute pre-crash option.
5. The output can be displayed by pressing the keys control-B, "P", "R" and return. In

this case, the object of the iteration is to achieve a match between the final position and the impact position of the vehicle and the final velocity and the velocity obtained in the impact analysis. Another difference between the pre-crash and post-crash analysis is that the final velocity is not zero for the pre-crash case. This forces the user to include the final integration time as an iteration parameter.

Miscellaneous Information.

Several additional items should be explained regarding the use of MASS which have not been explained in the preceding sections.

The graphic input device transmits the coordinates of the initial and final positions of the vehicles relative to the impact point and in units of feet with a scale factor of 100. For this block to be correctly formatted, the graphic input device has to know the image area, scale and impact point beforehand. With this in mind, the user should always enter these parameters before entering vehicle positions.

A display library index command is provided to list all data and output files saved in permanent storage. This command can be given from either the graphic input device or the graphic display device.

Using the graphic input device command, the user first selects the display file library file option and then enters a single numeric parameter which is not currently used by the system. The index of the files will be displayed in groups of three, each showing the file number and the status of each file. To display the next three files of the index, the user selects any command at the graphic input device except for the terminate execution command which terminates the display of the library index.

Using the graphic display device, the user can display the library file index by pressing the control-B, "L" and return keys. The display is then carried out in the same way as for the graphic input device command. The display is continued by pressing any key except for the control-C key which terminates the display.

A graphic display device command is provided which displays the contents of a data file. This command is entered by pressing control-B, "D" and return. The data file is displayed by pages at the display device. To display the next page of the file, any key can be pressed except for the control-C key which terminates the display of the data file.

CHAPTER VI

MEASUREMENT OF ROAD/TIRE FRICTION CHARACTERISTICS

As mentioned in several of the preceding chapters, the trajectory analysis routines are quite sensitive to the value of the coefficient of friction, μ , between the tire and road. Inaccuracies in the specification of μ represent the most serious recurring source of error in the analysis algorithm. Without an accurate and consistent method of measuring μ , much of the care taken in other areas of this project would be negated. Therefore, work was begun in this important area and this chapter will be dedicated to discussing the theoretical considerations necessary to understand the problem of measuring μ , as well as the hardware/software system developed to accomplish this task.

General Considerations.

The nature of all forces controlling the vehicle's motion are a function of the coefficient of friction except during short periods when the vehicle is impacting another vehicle or object. Determining the exact characteristics of μ is, therefore, essential if accuracy of vehicle dynamics is going to be achieved.

In a sample of 1000 accident cases studied during the Multidisciplinary Accident Investigation Program

(MDAI), nearly twenty percent of all cases involved braking, nine percent involved steering, and nearly six percent involved both braking and steering. In addition, nearly sixty-six percent involved no evasive action at all [3]. Therefore, approximately seventy-four percent of the accidents where evasive actions were taken involved braking.

When locked wheel skidding has occurred, the measured length of the skid marks, the coefficient of friction, and the estimated velocity at the time of impact can be used to determine the velocity of a vehicle prior to the skid. An accurate measurement of μ must be made at the accident site if the above velocity estimate is to be precise. Therefore, the methods used in obtaining μ must be precise and repeatable.

In the past however, μ has been one of the least credible factors. The equipment used to gather the data at the accident site has generally been quite unsophisticated. In some cases, only a vehicle and a measuring tape were used [4]. In this type of test, the procedure requires the investigator to drive his vehicle at a documented speed (usually 30 miles per hour) and skid to a stop. The investigator then measures the length of the skid marks with a measuring tape and calculates the coefficient of friction by using the following equation:

$$\mu = (V)^2 / (2gs) \quad (6-1)$$

where

μ is the average coefficient of friction (dimensionless),

V is the velocity of the vehicle prior to the skid (feet per second),

s is the length of the skid (feet), and

g is the gravitational acceleration (feet per second squared).

This is easily converted to the following approximation for ease and convenience:

$$\mu \approx (v)^2 / (30s) \quad (6-2)$$

where

v is the velocity of the vehicle prior to the skid (miles per hour)

s is the length of the skid (feet), and

$$30 \approx 2(32.2 \text{ ft/sec}) / (1.466666 \text{ ft/sec/MPH})^2.$$

There are, however, several inaccuracies built into the above equations and, therefore, into the procedure. The vehicle's velocity prior to the skid is difficult to obtain with the requisite accuracy. If it is not accurate, the error is increased by the squaring factor. The distance is also difficult to obtain because the actual skid marks may not begin until the vehicle has skidded for several feet. Even then, the beginning of the skid marks are sometimes hard to pinpoint. It should be noted also that this procedure yields a single value coefficient (i.e. μ_{ave}) that contains no information concerning the nature of μ with respect to time, distance, or velocity.

Equation (6-1) was developed from the work-energy theorem. The assumption is made that all the vehicle's kinetic energy is transformed by the forces acting at the tire-road interface with most being converted to heat and dissipated into the tire or at the road interface. The kinetic energy, E of the vehicle moving at velocity, V is:

$$E = m(V)^2/2 \quad (6-3)$$

where

m is the vehicle mass.

The work, W performed by the road on the skidding tires is:

$$W = Fs \quad (6-4)$$

where

F is the force applied by the road to the tires,
and

s is the distance of the skid.

The work required to stop a moving vehicle is equal to the initial kinetic energy or:

$$Fs = m(V)^2/2 \quad (6-5)$$

The only force applied to a skidding vehicle is through the tires and hence a function of the coefficient of friction. This equates to:

$$F = \mu N \quad (6-6)$$

where

N is the normal component of force acting on the

tires, and

μ is the dynamic coefficient of friction.

The combined normal force of all the tires is equal to the total weight, w of the vehicle.

With Newton's Second Law of Motion:

$$F = ma \quad (6-7)$$

where

a is the acceleration, and

m is the vehicle mass,

Equation (6-6) becomes:

$$\begin{aligned} F &= \mu w \\ &= \mu mg \end{aligned} \quad (6-8)$$

Combining Equations (6-5) and (6-8) yields:

$$\mu mgs = m(V)^2/2 . \quad (6-9)$$

Rearrangement of Equation (6-9) produces Equation (6-1).

At one time, this method was considered the interim standard for measuring μ [5].

The μ calculated for Equation (6-1) is an average dynamic coefficient of friction between a vehicle's tires and the road surface over a velocity range from the initial velocity down to zero. Since μ is directly proportional to the vehicle's deceleration by a factor of g , Equation (6-1) implies that the deceleration of a vehicle is constant throughout the skid as depicted in Figure 6-1a. With a constant deceleration, the velocity decrease will be linear.

Testing of the phenomena began during the early 1950's and showed that the deceleration of a skidding vehicle is not in fact constant [29]. Typically, the deceleration of a vehicle in a locked-wheel skid acts more like that depicted in Figure 6-2. Braking forces build up from zero to the incipient peak where skidding begins. The deceleration drops off slightly and slowly increases again as the skid continues.

In addition to those noted above, there are other inaccuracies built into Equation (6-1) also. This equation assumes that all the kinetic energy dissipated during a skid is done through the tire-road surface interface. During the actual skid this is true, but there is a short period of time, approximately 0.12 seconds [30,31], where the brakes are applied and the wheels are not locked. This brake build-up time, in addition to the fact that the initial skid marks may not actually start for several feet after brake lock-up, causes the calculated μ , from Equation (6-1) to actually be higher than the true μ . This discrepancy is very undesirable because it severely limits the accuracy of the analytical accident reconstruction.

The coefficient of friction, μ , is a function of many variables which affect the tire-road surface interface. These variables include, but are not limited to:

1. Speed [29, 30, 31, 32, 33, 34, 35, 36, 37
38];

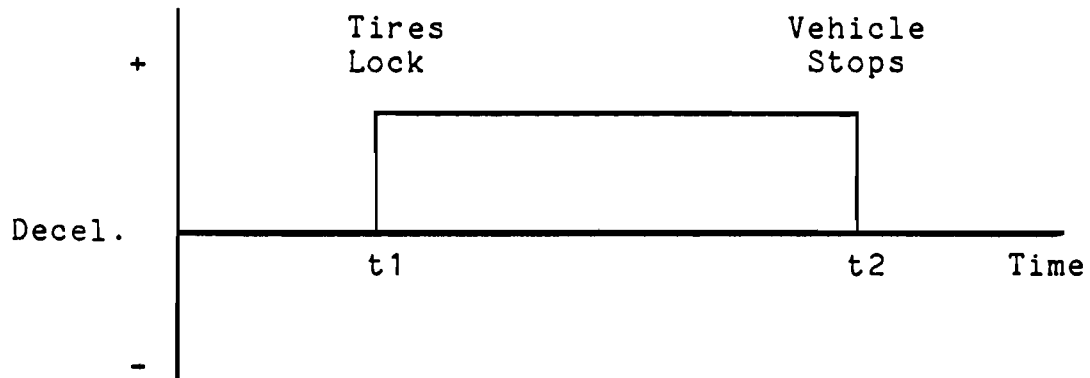


Figure 6-1a Constant Deceleration as a Function of Time

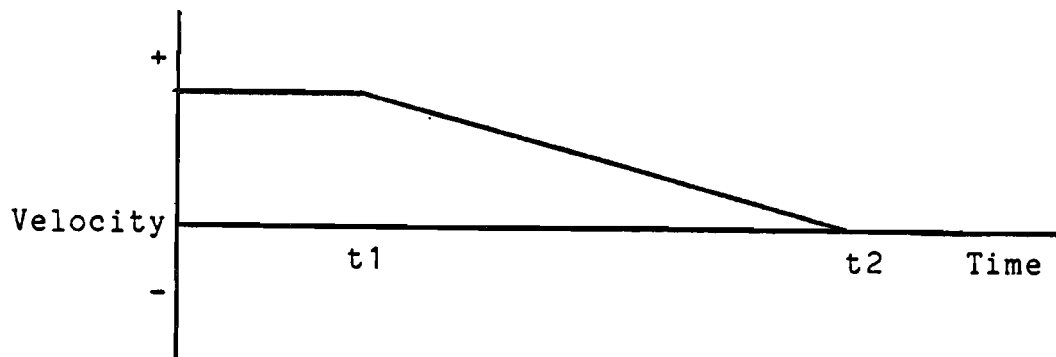


Figure 6-1b Velocity Curve Resulting from Constant Deceleration

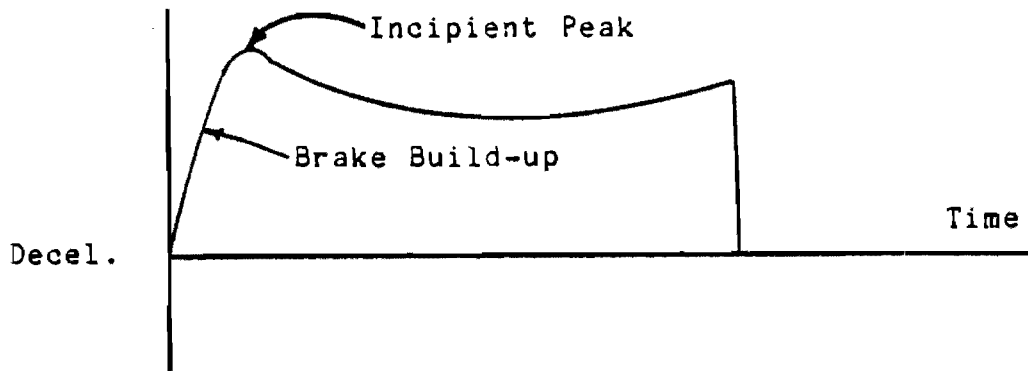


Figure 6-2. Typical Deceleration Curve for an Automobile Skid Test

2. Tire construction and materials
[30,31,32,34,36,37,39,40,41,42];
3. Vehicle suspension and geometry conditions
[30,31,34,43];
4. Vehicle mass [30,31,34,37,39,43];
5. Ambient conditions [30,35,43];
6. Tire temperature [30,35,37,39,43,44,45,46];
7. Tire inflation pressure [37,45];
8. Road surface roughness [30,32,34,36,37,39,42,44,45,47,48];
9. Road contaminants [30,32,39].

These variables for a particular accident or test site can be grouped according to how they affect the test procedure and results. Group "A" variables are "site" specific and are not considered functions of vehicle speed. Group "A" variables include ambient conditions, tire temperature, tire pressure, road surface roughness and road contaminants. This group is set at the time of the accident. Group "B" variables include

the vehicle's mass, the vehicle's suspension and geometric conditions, tire construction, and tire materials. These variables also affect μ but are not site specific. Group "B" may change, however, as the suspension system parts wear. As a result, these variables are also established at the time of the accident. Group "B" variables are considered "vehicle" parameters, whereas Group "A" variables are considered "site" parameters. The Group "C" variable, vehicle speed, is the only one that is directly controlled by the driver and is not part of the vehicle or site. It is, however, the variable which ultimately is to be determined from the skid length measurements and the coefficient of friction.

The goal of this research is to show how the different variables influence the coefficient of friction and then to develop an accurate and consistent method of obtaining an instantaneous μ during a locked-wheel or yaw skid, recording the information and using it to reconstruct the vehicle dynamics.

The Coefficient of Friction.

The physics of the tire-road friction at this point in time is not completely understood. This is primarily a result of the lack of test equipment sophisticated enough to accurately measure and record the data and then to evaluate the data. Numerous methods have been used in the past to measure and record μ but none have

truly been able to accurately represent this phenomenon. This is partly because the total coefficient of friction is influenced by many variables which are impossible to isolate from the whole. The Society of Automobile Engineers (SAE) defines eleven kinematic and geometric variables that completely describe the steady state motion and orientation of the tire to the road [43]. When these variables are added to the list of variables previously discussed, it is easy to see how complex the phenomenon of tire traction really is.

There are four basic elements which contribute to the total coefficient of friction: adhesion, deformation, tearing, and wear [30,36,41,44,45]. Adhesion results from the molecular attraction between the tire and the road surface asperities. It is considered a static property because it is not a function of the relative motion of the pavement and the tire. Adhesion is a property which follows the definition of Coulomb friction in which the frictional force is a function of μ and the normal force, but is not a function of the contact area [49]. During a skid, the temperature increase of the tire-road contact surface results from adhesion.

Also during sliding, the rubber deforms at the macroscopic tire to road surface asperity and tends to wrap around the asperity in a direction opposite the direction of the skid. This deformation contributes to μ because it takes more energy to deform the rubber than is

regained when the rubber returns to the undeformed state. This process is called hysteresis. Modulus is another property of rubber that contributes to the overall coefficient of friction. It is a measure of the hardness of the rubber and reflects the ease in which it deforms. Most automobile tires today use synthetic rubber which has a relatively lower modulus than natural rubber, of which most truck or severe service tires are made. The lower the modulus, the easier the rubber deforms around the asperity resulting in a higher μ but at a sacrifice to the wear characteristics [41]. The deformation of the rubber results in a heat build-up beneath the tire contact surface.

Tearing and wear are both associated with abrasion. These factors are functions of the tensile and shear strengths of the tire material. A higher tensile strength will result in higher abrasive friction, assuming all other variables remain unchanged. The distinction between tearing and wear lies in the fact that wear results in the formation of loose wear particles and therefore, material loss while in tearing the material remains attached.

The four basic factors which affect tire friction are pictorially represented in Fig. 6-3. "Experts" in the tire friction area concur that these four basic factors combine to form the total coefficient of friction but the agreement stops there. There is little agreement

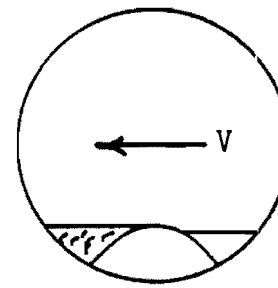
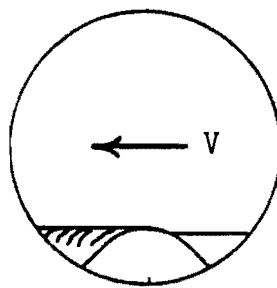
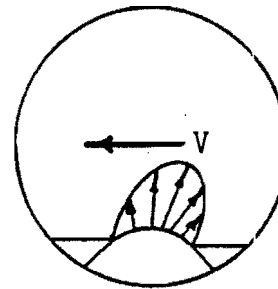
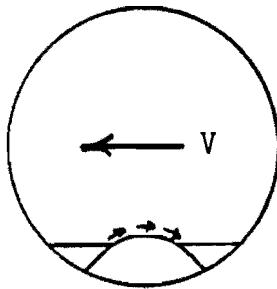
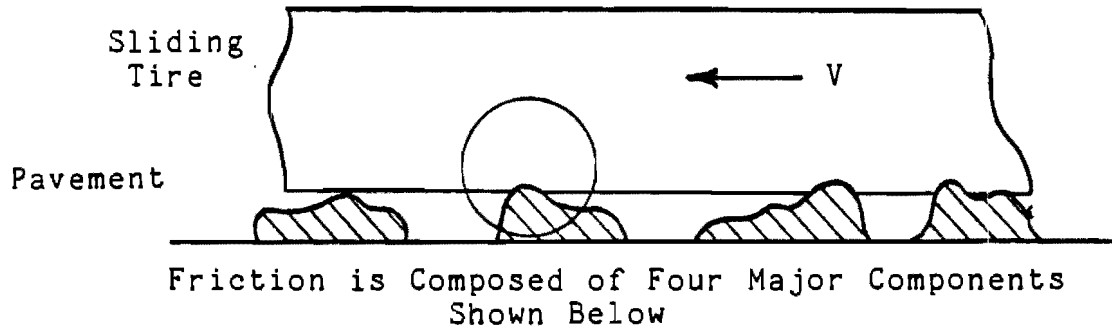


Figure 6-3. The Four Major Components of Tire-Pavement Friction [4]

on how each of the factors contributes to the overall μ or how the physical variables (speed, temperature, road contaminants, etc.) affect the contribution of the four factors. Some "experts" claim that 80 percent of the total μ is caused by adhesion [36], while others claim that friction is an energy-dissipating process and only through hysteresis can energy be dissipated [36,39]. A third view of the tire-road surface friction process is that adhesion is the main component of μ at low speeds while deformation, tearing, and wear occur at high relative velocities [44]. This theory is graphically represented in Fig. 6-4. The curve shows how μ changes as slipping increases from no skidding to 100 percent skidding depending on whether the primary component is adhesion, deformation, tearing, or wear. Curve ABC depicts μ as a function of pure adhesion and curve FDE depicts μ as a function of deformation, tearing, and wear. In this case, μ is a function of vehicle velocity. Neither curves ABC or FDE occur in actual automobile skids but a combination of the two, curve ABGDE, does. The value of μ is limited to the lower value because the lower μ dominates in the friction process. The peak of the ABGDE curve at G never reaches the intersection of ABC and FDE; this is because BGD is considered the transition region between the curves ABC and FDE.

The tire-to-road frictional interaction is complex in itself, but when additional variables such as

speed, temperature, etc. are considered the measurement of μ becomes an exhaustive task. Numerous studies have been made to determine μ using various methods in laboratory and field environments. These studies are at first more confusing than informative to a student studying tire friction, because the results are usually contradictory without close examination. With further study, the differences in test procedures become apparent. The compared goals, data, methods, and results are different in most cases. Therefore, subject tests often can not be effectively compared with others. Some of the disagreements between "experts" in this field result from non-uniform test procedures. For example, Grough [44], states:

Most laboratory measurements of friction of various rubbers or polymer blends have been

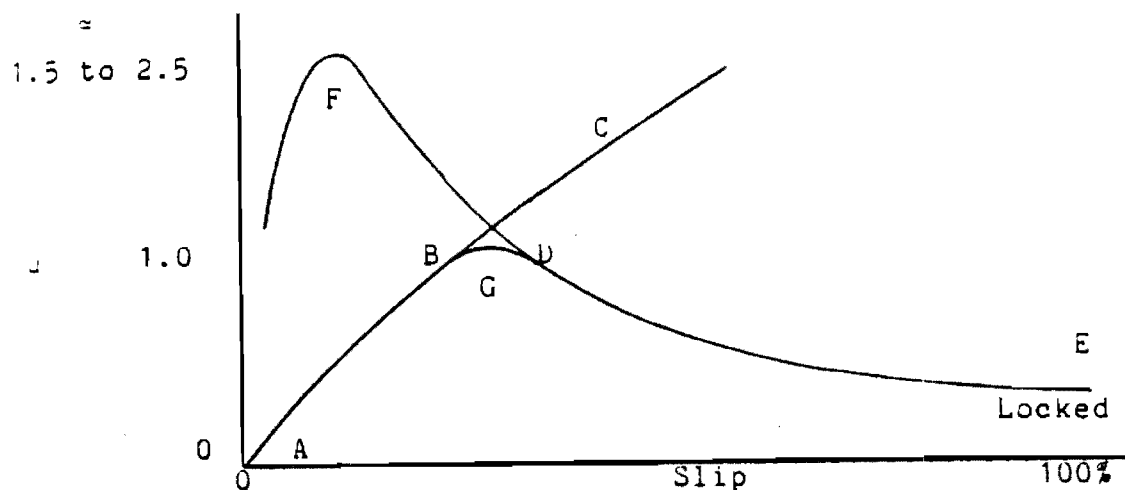


Figure 6-4. Braking Force Due to Adhesion and Skidding Effects as a Function of Tire Slip [44]

made under steady state sliding at low speeds. It is commonly noted that initial values are lower than at final steady state; or put another way, movement between rubber and ground is necessary to achieve maximum friction pertinent to the materials and operating conditions.

While Meyer and Kummer [46] state, "As sliding speed is increased friction decreases, but eventually increases again." These two tests can not be compared without realizing that in reference [44], the sliding speeds were low but not specifically explained; whereas, reference [46] specifically explains that sliding velocities were less than one foot per second. The friction in reference [44] may have involved deformation, tearing, and wear, where reference [46] probably involved mostly adhesion.

There is general agreement, however, in the belief that most of the energy dissipated in a locked-wheel skid is through heat generation and loss of the heat to the road surface and tire. Grosch [5] explains in detail the relationship between different test conditions and the amount of heat build-up in rubber and compared them with standard empirical equations. The relationships between temperature and heat transfer for a skidding vehicle partially explains why laboratory and field friction tests rarely produce similar values of μ .

With the complexities of the frictional components not being completely understood, determination of the "correct" method to measure μ is difficult if not impossible, but it is reasonable to assume that duplication of as many of the variables as possible is the "safest" way to accomplish the task.

Measurement Techniques.

There have been numerous methods employed to measure the coefficient of friction [7,29-48,50,51] but there has been little correlation of the results from one test procedure to another. Some of the most popular methods used in the past are:

1. Specialized laboratory tests;
2. Analytical methods;
3. Pulled trailer skid force methods;
4. Pulled trailer slip angle methods;
5. Automobile length of skid tests;
6. Accelerometers in automobiles;
7. Fifth-wheel automobile skid tests;
8. Automobile dynamometer tests;
9. Specially instrumented automobile and automobile test models; and,
10. Photographic test procedures.

The reasons for performing these tests are as varied as the different procedures themselves. The most prevalent reason has been to compare the coefficient of

friction from one road surface to another and to compare μ on the same road surface under different atmospheric conditions. Very little has been done in determining μ for the purposes of automobile accident reconstruction. Each of the above methods were evaluated prior to deciding the best method for determining μ for this application.

Specialized laboratory tests display the broadest range of μ . The types of tests that have been devised are numerous [31,35,36,43,44] . While the laboratory environment provides the best control of variables which are uncontrollable in a field test, the laboratory does not have the inputs from the test site which are important in the accident reconstruction area. Laboratory tests have measured μ as high as 3 for rubber materials similar to those used in automobile tires [35] , but a μ this high at a test site is extremely unrealistic. For these reasons, laboratory tests have been ruled out as a method for measuring μ for this research.

Analytical methods [35,39,43,44,47] , by themselves, suffer within the context of this research because they have no way to accurately account for many "real world" variables which are prime considerations in accident reconstruction.

The pulled trailer skid test method is one of the most popular techniques for measuring the coefficient of friction on various road surfaces [31,34,48]. The procedure utilizes a vehicle to pull a trailer which has one

or more tires locked. The force required to pull the trailer is measured at the trailer tongue by a load cell. This force is proportional to the coefficient of friction by a factor of the tire loading. Many variations to the basic trailer method have been devised. These variations include different ways to load and lock the trailer's tire(s), various sensing devices, and general construction of the trailer. Some trailers are also equipped to measure the "incipient force" (friction force just prior to lock-up). During testing, the trailers are usually pulled at a constant speed. The tow vehicle can also be equipped with a water storage tank and a wetting system for making tests on wet pavement.

Pulled trailer slip angle force testers are very similar to the trailer skid force testers except that the trailer's tire(s) are positioned such that the longitudinal axis of the tire-wheel assembly is at an angle (called the slip angle) to the direction of the trailer motion. Fig. 6-5 pictorially describes the slip angle. Most trailers are designed such that the slip angle can be changed.

The advantages of the trailer methods are that specialized test equipment can be incorporated into the trailers and that the trailers can be towed at a constant speed. Therefore, testing can be performed without significantly disrupting traffic flow. The disadvantages of the trailers are that they are large, expensive, usually

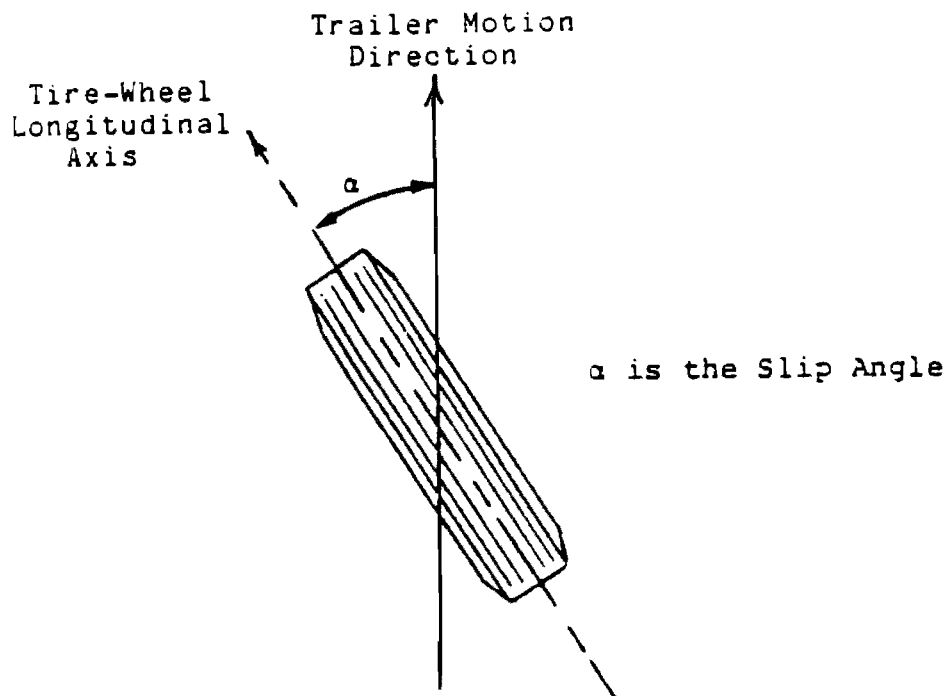


Figure 6-5. Slip Angle

require a specialized tow vehicle, and have dynamic characteristics different from the automobile. Additionally, correlation of data between trailer testing methods has been poor [34]. Due partly to the fact that the skid trailer does not reproduce many of the variables in the vehicle skid, this method has also been ruled out.

The automobile length of skid test method [32, 29, 31, 33, 34, 42] was described earlier. This method involves skidding an automobile from a known velocity to a stop and measuring the skid length. The initial speed (V) and the skid length (s) are used in the equation:

$$\mu = v^2/2gs$$

to find the average coefficient of friction (μ). The advantages of this type of test are that it requires very little equipment, it is simple to perform, measure and calculate the results, and, most importantly, it can closely approximate the actual skid variables, especially if a similar vehicle and tires are used. The disadvantages arise from the inaccuracies of observing the initial speed, determining the initial skid location, and from the fact that the calculated μ is only an average value for speeds from the initial velocity to zero. Very little additional information is available from the length of skid test method. This method is also ruled out for the purpose of motor vehicle accident reconstruction in this research, although it is the basic method for obtaining μ for this purpose.

Instrumenting an automobile with an accelerometer for measuring deceleration during skid tests [29,31 32,33] has all the advantages of the length-of-skid tests and also gives the instantaneous μ over the skid duration. Therefore, an accurate measurement of the skid length and initial velocity are no longer required. Instantaneous values of velocity and distance can also be obtained by successive integrations of the acceleration versus time data. With the accelerometer calibrated in g.'s, the acceleration is equal to μ . As described previously, the classical definition of friction force is:

$$F = \mu N \quad (6-6)$$

where

F is the friction force;

μ is the coefficient of dynamic friction; and,

N is the normal force between the two subject objects.

Additionally, from Newton's Second Law, a force (F) is equal to a mass (m) under acceleration (a):

$$F = ma \quad (6-7)$$

When the vehicle under the influence of a 1 g. gravitational attraction, the normal force is:

$$\begin{aligned} N &= m(lg) \\ &= w \end{aligned} \quad (6-10)$$

where w is the total weight of the vehicle. Combining Equations (6-6), (6-7) and (6-10) yields:

$$\mu w = ma$$

or,

$$\mu = a/g \quad (6-11)$$

where μ is dimensionless. The disadvantages of the automobile length-of-skid test method using an accelerometer are that it is more costly than automobile length-of-skid tests and that it requires a knowledge of the instrumentation.

Fifth-wheel input to automobile skid tests [31] can make additional information available. The exact skid length can be measured at the time the skid is occurring and it can be used to verify the data from the double in-

tegration of the accelerometer data. The disadvantages of a fifth-wheel are mainly the added cost, the required operator knowledge, and the additional equipment. Another disadvantage to the fifth-wheel device is the difficulty in attaching it to the test vehicle. The fifth-wheel should be used cautiously without an accelerometer, however, because of the difficulty in the numerical differentiation of the data to obtain the velocity and acceleration information.

Automobile dynamometers are often used to measure and compare tractive forces of various tires [43] , but are of little use for accident reconstruction data acquisition at a test site.

Specially instrumented automobiles [31,51] can be used to gather almost any kind of data desired about the physical phenomenon occurring in an automobile during skids. Photographic analysis can also be incorporated into this category. More data can be made available for the analytical reconstruction of an accident using these two techniques, but cost prohibits them from being used beyond the extent of an accelerometer in the test vehicle.

Earlier, three categories of variables that affect μ were described. They were Category "A" (site), Category "B" (vehicle), and Category "C" (vehicle controlled) variables. From the previous discussion of tire traction, it becomes understandable how many of the physical interactions which take place at the tire-road inter-

face remain mysteries to us, especially when the above variables are included. To insure accurate reproduction of the skid which took place prior to a collision, it is necessary to duplicate as closely as possible the variables which were present at the time of the skid. Category "A" variables are duplicated by performing a controlled skid test as soon as possible after the accident in question (or at least before the weather conditions change). Category "B" variables differences are reproduced as closely as possible by using a similar, if not identical, vehicle with similar or like tires as the one(s) involved in the collision. Since all vehicles have mechanical characteristics which vary from one vehicle to another, it is important to understand some of the variables that affect stopping distance and the maximum error that can result from them.

Although by no means complete, the published literature of previous testing indicates the following factors which affect the tire-road friction and measurement testing:

1. The dynamic characteristics and geometric parameters of different vehicles influence tire-road skidding behavior [29,30,32,34];
2. Tire design characteristics (structural and material) affect skid performance [30,32,34 35,36,37,40,41,42,43,44];

3. Driver input to vehicle affects stopping distance with all other variables remaining constant [29,30,32,37];
4. Load on a tire and tire inflation pressure have a slight influence on skid performance [30,34,37,39,40,43];
5. Vehicle speed affects skid performance [31,32,33,34,35,37];
6. The maximum variation of μ as a result of the automobile variables is approximately 10 percent. This value can be significantly reduced by choosing a test vehicle of similar construction with similar tires to the accident vehicle [34].

The last variable, speed, is unknown and is the variable which is to be determined by performing the analysis of μ . Performing a skid test in a similar vehicle with similar tires as soon as possible after the accident can duplicate the unknown variables and provide $\mu(t)$ consistent with performing an accurate analysis of vehicle dynamics.

The published results of previous tests indicate that road surface characteristics have the single greatest effect on variations in the measured coefficient of friction for automobile skid tests [29]. For this reason, as well as equipment size, ease of operation, cost, repeatability, reliability, and adaptability, a portable acceler-

ometer transducer was chosen as the most suitable for the purpose of automobile skid tests.

An accelerometer for this exact purpose was designed and built by Mr. Scott Reid [7]. The accelerometer consists of a small, vertically oriented cantilever beam with a mass attached to the free end and a strain gage bridge mounted near the fixed end. The simplicity, small size and mass, low cost, and reliability were key considerations for deciding to continue with this type of accelerometer.

The accelerometer, however, is of no use by itself. There must be a method of recording the instantaneous values of acceleration over the entire skid duration so that the data can be integrated to acquire the velocity and distance versus time data.

There are numerous ways in which this recording and analysis can be accomplished. For example:

1. Manual observation and recording;
2. High speed photographic methods;
3. Hard copy real time plotting;
4. Recording oscilloscope and photographic techniques;
5. Real time magnetic tape recording of transducer output; and,
6. Computerized data acquisition, storage, and transfer.

Manual observations were eliminated from consideration because of the speed at which the acceleration changes during the skid process. It would be humanly impossible to record all the necessary data.

High speed photographic recording of the accelerometer output would be an accurate and permanent record of the skid process especially if a timing device were included in the photographs. The difficulty lies in the analysis of the data once it is obtained. Manual graphing or digitization and integration would be required which is, at best, tedious and time consuming. The expense involved for equipment and film and the inherent inaccuracies of manual integration prohibit this method from being used in this work.

Hard copy real time plotting, real time magnetic tape recording and the recording oscilloscope and photographic techniques are also accurate ways of recording the output from the accelerometer but as in the photographic method, manual integration of the data would be necessary. Numerical integration techniques by computer could be used in these methods but the data must first be digitized. The inherent inaccuracies of these methods also prohibit them from being used in this work.

Computerized data acquisition, storage, and transfer methods can be adapted for this purpose. The ability of a micro-processor to make thousands of samples of data per second from numerous sources and to store the

data in a retrievable memory makes this system ideal for the purpose of automobile accident reconstruction. This system also has the capability of transferring the data in memory to a more permanent type of storage device, like a magnetic recording tape. Once the data is permanently stored on the tape, the computer and memory are free to record the data from another skid test. The recording tape can transfer the same data into another computer at a laboratory for analysis and evaluation. All this can be accomplished without human interpretation of or interaction with the data. There are some drawbacks to this method, however. The complexities of micro-computers requires a knowledge of micro-computer programming to make the system work, but once the system works correctly, it can be operated by anyone with a basic understanding of computers. The added cost is also a drawback but the accuracies gained by this method far outweigh the extra cost. There also must be computer equipment available to perform the analysis of the data once it is collected, but this is true in all of the above methods if any accuracy is to be expected at all. For the above reasons, a micro-computer data acquisition, storage, and transfer system was selected as the best method for the purpose of motor vehicle accident reconstruction.

To verify the results of the numerical integration of the accelerometer data, a fifth-wheel tachometer is also added to the total system. The micro-computer can

then store the elapsed distance as a function of time from the instant an external interrupt is triggered.

Accelerometer

The accelerometer designed by Reid [7] is a vertically oriented cantilever beam with a small mass mounted at the free end and a temperature compensated strain gage bridge mounted approximately three-quarters of an inch from the fixed end. Constructed of standard spring steel stock 0.020 inches thick, it is three inches long by one-half inch wide with a 0.028 pound mass at the free end. With the beam oriented horizontally, the mass will cause a deflection of 0.025 inches under the influence of a one-g gravitational field. To insure that the spring steel would not be over-stressed, the maximum stress at the fixed end was calculated at 2523 pounds per square inch, well within the maximum stress for spring steel of 58,000 pounds per square inch.

The undamped natural frequency was also calculated to determine if any undesired resonances would be excited during testing. The calculated frequency, 19.8 cycles per second, is very close to the natural frequency of the automobile suspension (10 to 15 cycles/sec) and decreasing the mass to increase the natural frequency would cause an undesirably low deflection and a smaller strain gage output. To reduce the chances that the automobile frequencies will cause the undesired vibrations in the

beam, a damper system was used to modify the beam dynamic response.

The damper consists of a friction lever arm connected to the mass by a link. By varying the tension on the spring which presses the lever arm between two washers, the amount of damping can be adjusted. A Hewlett-Packard Model 5423A Structural Dynamics Analyzer was used to analyze the beam, mass and damper shown in Fig. 6-6. The first resonant frequency for the undamped system (damper, link, and lever arm removed), was a 19.4 cycles/sec, which is very close to the predicted frequency. For the undamped system, the damping ratio (percent of critical damping) is 1.9 percent, and the time constant (time for the system to damp motion to $1/e$ times its original displacement) is 0.428 seconds. Fig. 6-7 shows the response of the undamped system and Fig. 6-8 shows the system's response with varying amounts of damping. The plot in Fig. 6-8 with the lowest peak is representative of the damper setting that allowed the best output from the completed system in actual skid tests. As the amount of damping increases by tightening the damper pivot nut, the damping ratio is increased and the time constant is decreased. Table 6-1 lists the resonant frequency, damping ratio, and time constant for the undamped system (from Fig. 6-7) and for the three settings of the damper system (from Fig. 6-8). Although the first natural frequency can be damped so that unwanted oscillations do not confound

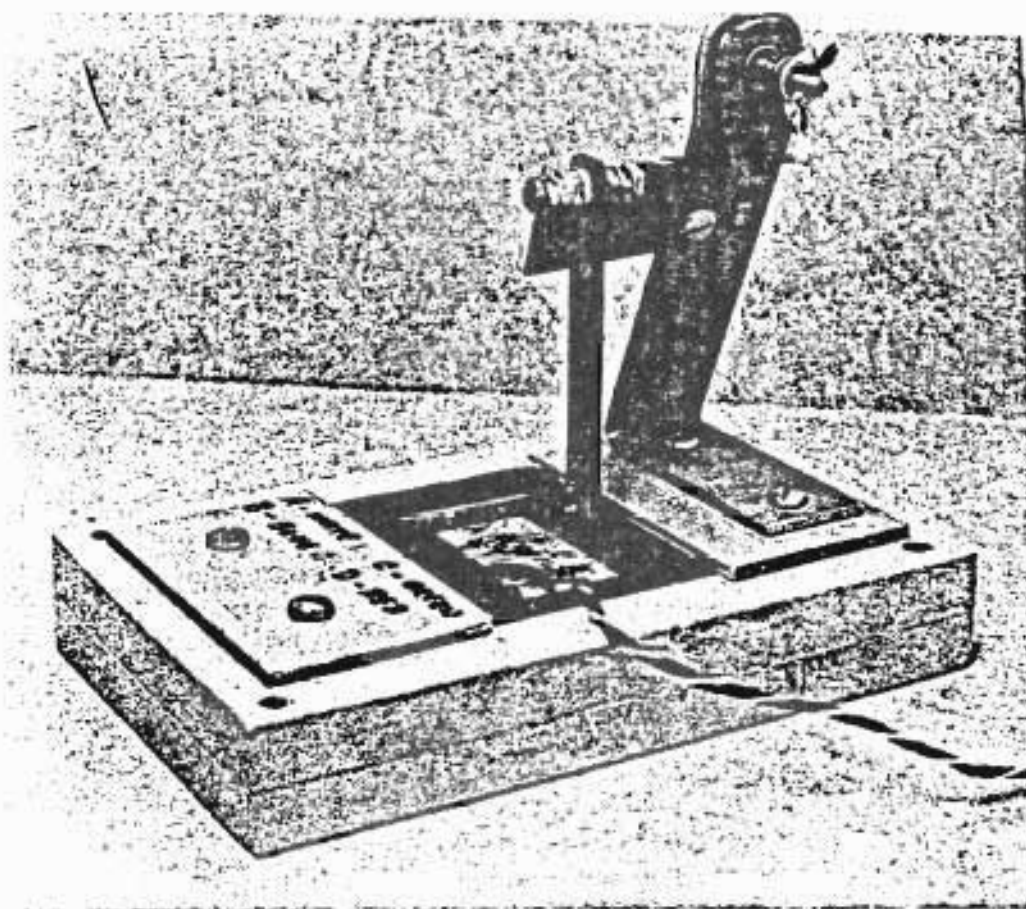


Figure 6-6. Spring, Mass, Damper, Limiter Arm and Strain Gage Accelerometer

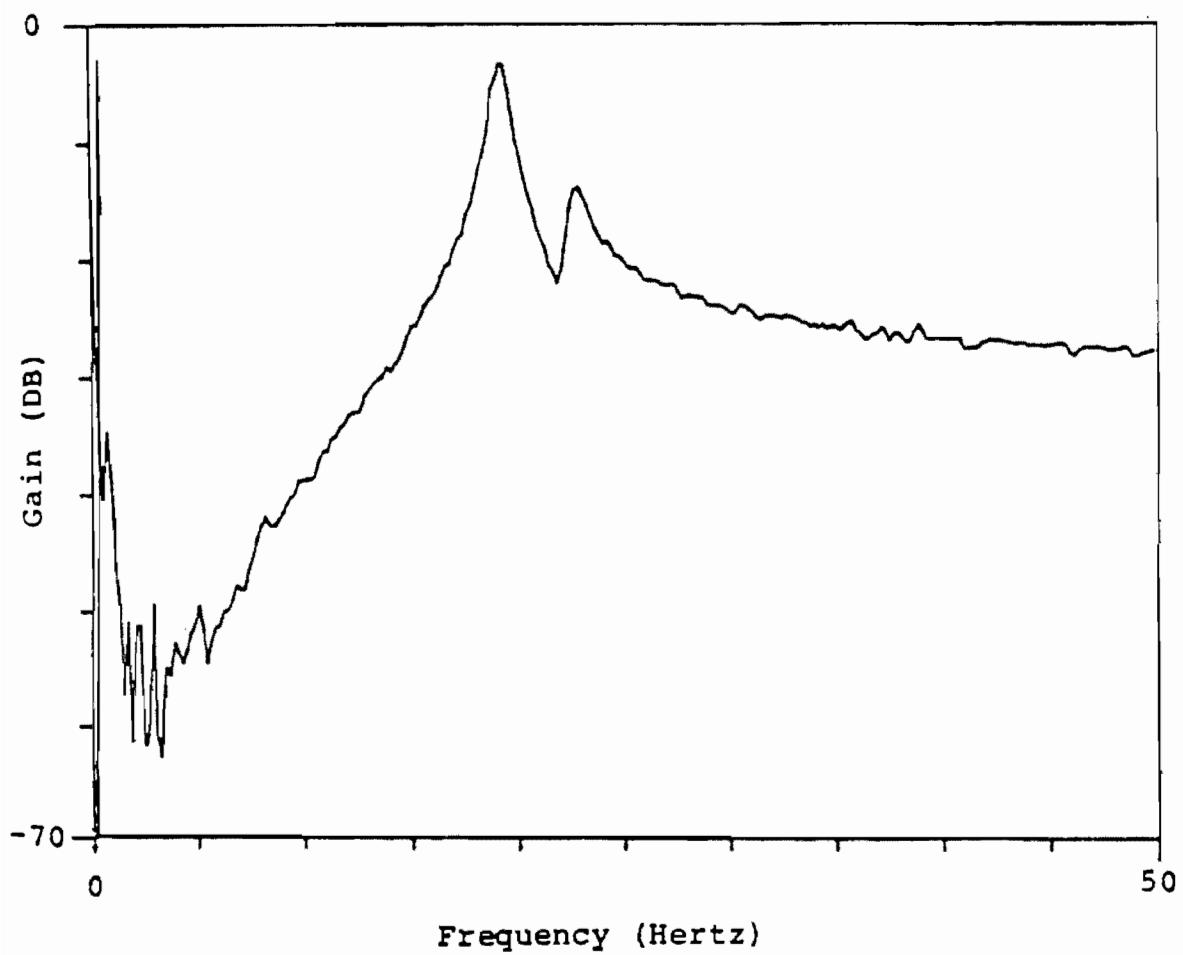


Figure 6-7. Transfer Function of the Undamped Accelerometer Showing the First Resonant Frequency [7]

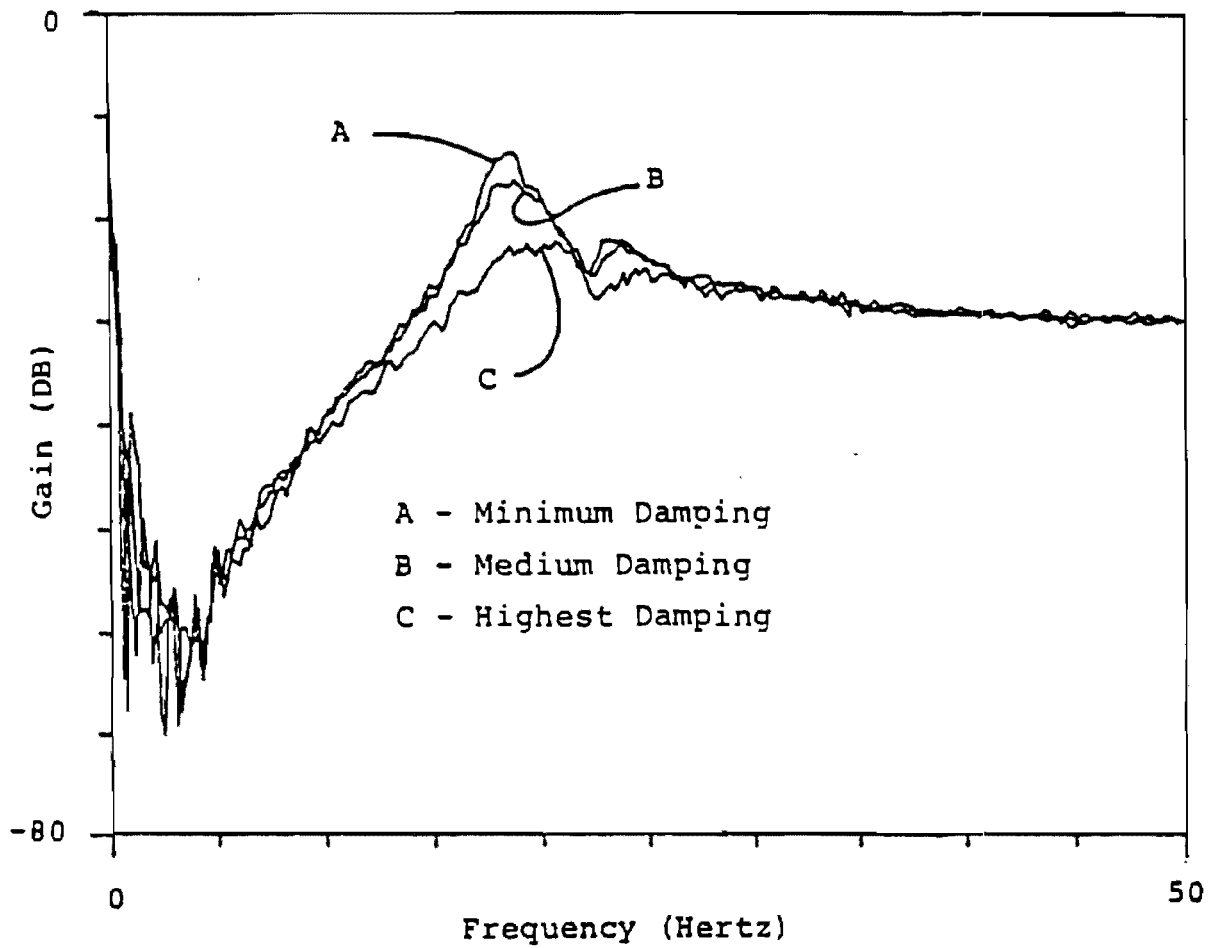


Figure 6-8. Transfer Function of Lightly Damped Accelerometer Showing First Resonant Frequency [7]

TABLE 6-1
 FIRST RESONANT FREQUENCY, DAMPING RATIO AND
 TIME CONSTANT FOR UNDAMPED AND LIGHTLY DAMPED
 SYSTEM

	FREQUENCY (Hertz)	DAMPING RATIO (Percent)	TIME CONSTANT (Seconds)
Undamped	19.14	1.9	0.428
Minimum Damping (A)*	18.39	5.5	0.156
Medium Damping (B)*	18.51	7.6	0.113
Highest Damping (C)*	19.27	13.5	0.061

*A, B, and C refer to Fig. 6-8

the test data during tests, no usable information with frequencies near or above 19 cycles/sec can be obtained from the accelerometer.

The limiter arm, also shown in Fig. 6-6, was installed to prevent the beam from being over-stressed during testing and handling.

The cantilever beam spring-mass-damper system was combined with strain gages to become the accelerometer. Four matched, foil-type strain gages were attached to the beam and were connected to act as a temperature compensated wheatstone bridge. Micro-Measurements type EA-06-125BT-120 strain gages were used, each with a nominal resistance of 120 ohms. An electrical circuit was designed and incorporated onto the main computer board to provide the strain gage bridge with an input voltage and

to amplify the output by a factor of 1000. The strain gage bridge is not perfectly balanced so the output from the strain gages, after amplification, is a constant of approximately 0.2 volts (beam undeflected). With an amplification factor of this magnitude, it proved difficult to find four strain gages which were perfectly matched. When the beam is deflected by the mass under one-g, the strain gages produce an amplified output of approximately four volts.

The amplified strain gage output is fed into an 8 bit analog-to-digital (A/D) converter which was an input voltage range from zero to five volts. The A/D converter converts the analog voltage to a digital code which is proportional to the analog voltage on a decical scale of 0 to 255 or a hexidecimal scale from 0 to FF. During the Calibration and Execution phases of operation, the output of the A/D converter is sampled by the micro-processor.

Micro-computer.

The micro-computer, designed and built by Mr. Grover Edmiston, consists of the following main components:

1. An 8085 based micro-processor manufactured by Intel Corp.;
2. 2 each No. 2516 Texas Instruments 2 K Erasable Programmable Read Only Memory (EPROM) units;

3. 4 each 1 K No. MK4118A-4 Mostek Random Access Memory (RAM) units;
4. A hexadecimal keypad, a 6 digit hexadecimal display panel, and an Intel Corp. No. 8279 Programmable Keyboard/Display Interface module;
5. An Intel Corp. No. 8253 Programmable Interval Timer;
6. An Analog Devices No. AD 7574 8 bit Analog-to Digital Converter; and,
7. An Analog Devices No. AD 521KD Instrumentation Amplifier.

Figure 6-9 is a block diagram of the computer board which shows the interconnection of the components and the connection to the accelerometer and the fifth-wheel. Figure 6-10 shows the actual accelerometer and micro-computer unit.

The micro-processor is programmed to perform various operations which are written in 8085 assembly language [52] and stored in the EPROM. It automatically begins processing the instructions contained in the EPROM starting at memory location 0000 when the power is turned on or when the reset button is pressed. The exact programming procedures used in assembly language are of an extensive and detailed nature and therefore, beyond the scope of description in this report.

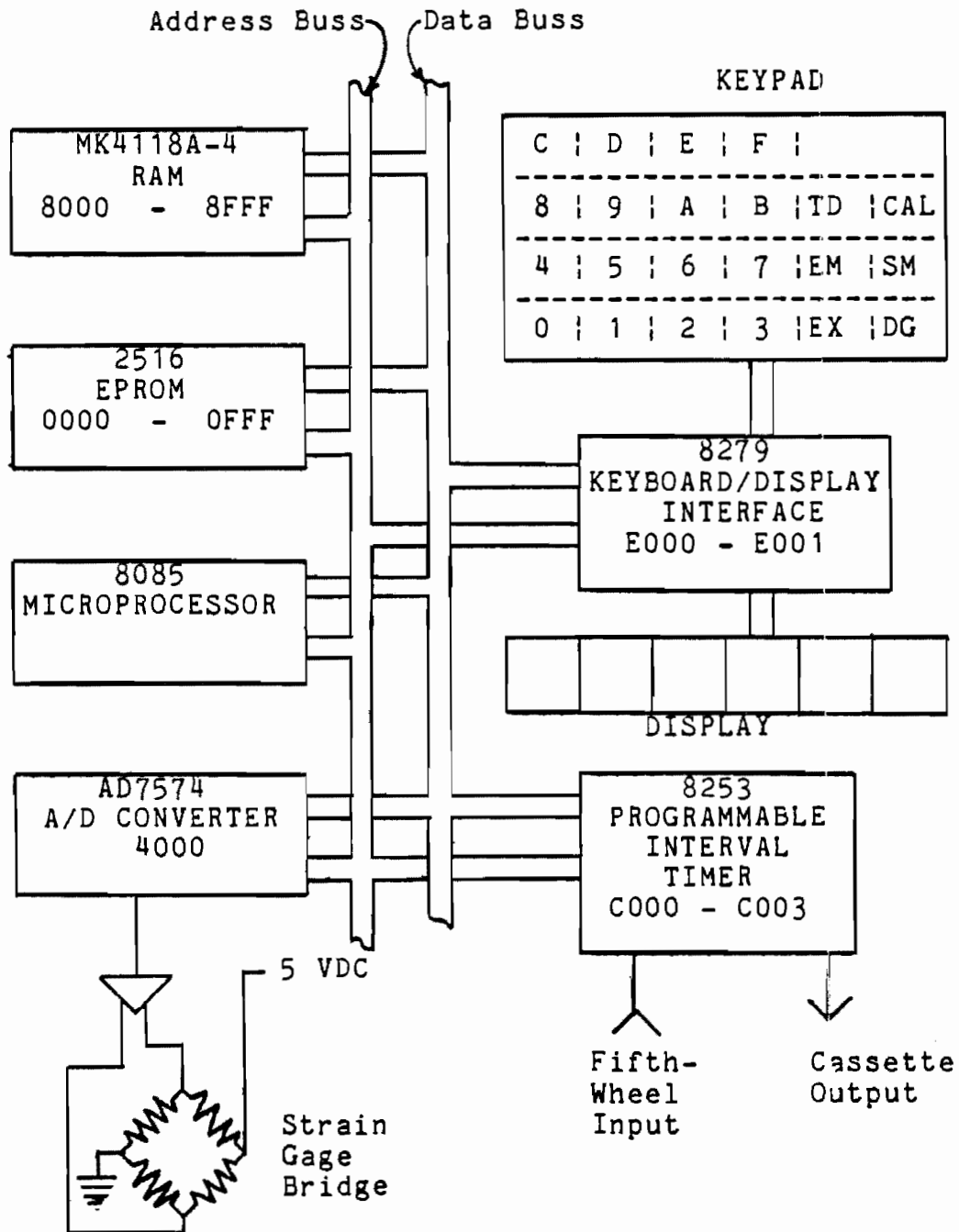


Figure 6-9. Block Diagram of Computer Board and Accelerometer and Fifth-Wheel Interconnection

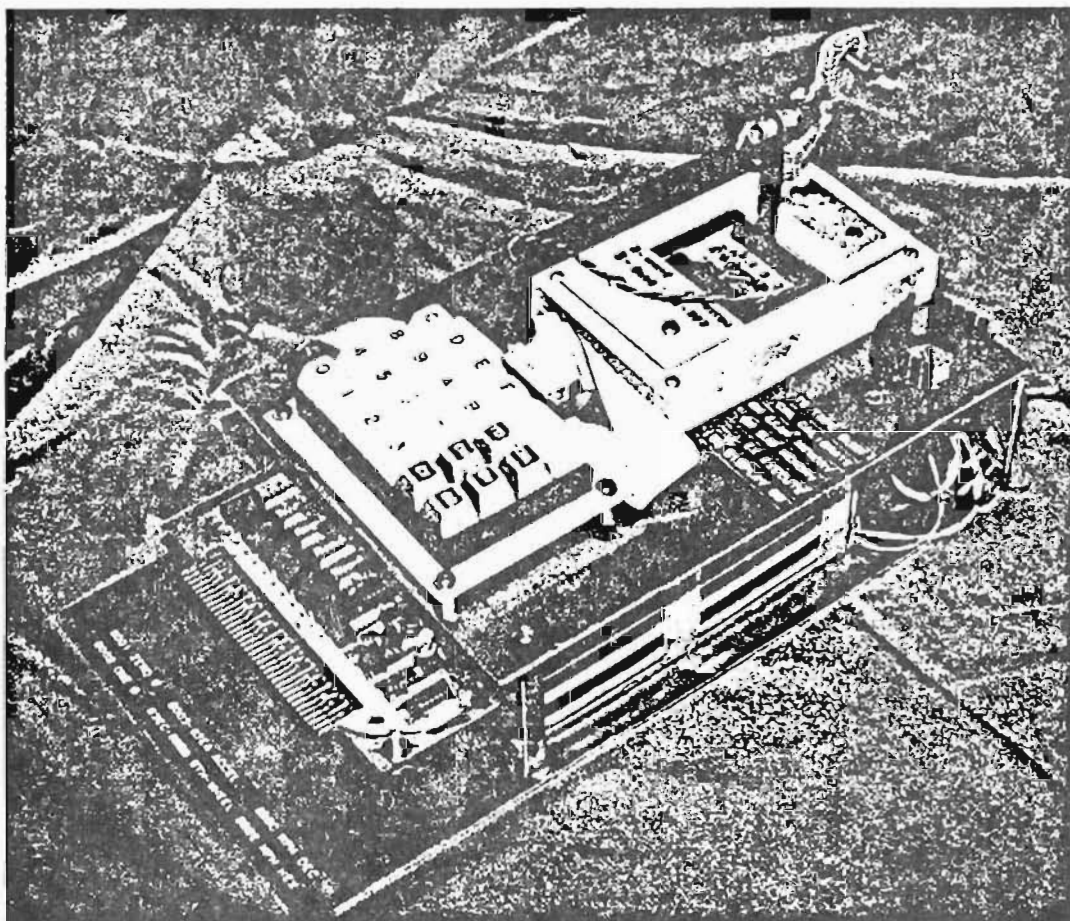


Figure 6-10. Accelerometer and Micro-Computer Unit

The Intel 8085 micro-processor was used in this application because of the speed at which it can operate. It is driven by a 6.144 megahertz clock in this system. The 6.144 MHz signal is internally divided by two to clock the actual execution processes within the micro-processor. The different executable instructions require varying numbers of clock cycles depending upon the complexity of the instructions. On the average, instructions take approximately 10 clock cycles to be executed. With a 3.072 MHz clock, the micro-processor completes approximately 300,000 instructions per second, making it ideal for the high speed data acquisition which is required for this application.

The main functions of the micro-processor in this application are as follows:

1. To program and communicate with the 8279 Keyboard/Display Interface module;
2. To program and communicate with the 8253 Programmable Interval Timer;
3. To sample the data from the A/D converter;
and,
4. To store the data in the RAM.

The function of the EPROM is to provide non-volatile storage for the executable code. The information stored in the EPROM is not lost when the power is turned off so the micro-processor will always operate when the power is turned on.

The Random Access Memory (RAM) consists of 4 K of 8 bit words. Its primary purpose is to store the data from the accelerometer A/D converter, and the fifth-wheel count provided by the Programmable Interval Timer (PIT). The contents of the RAM can be read by the micro-processor or written over by it. Since the RAM is volatile, its contents must be stored on tape before the power is turned off or before another test is run.

The hexadecimal keypad, hexadecimal display panel, and the Keyboard/Display Interface module provide the operator with a means of controlling the operation of and communication with the micro-processor.

The keypad has 22 keys which perform the following functions:

1. 0 - F hexadecimal number keys;
2. TD Taped Dump;
3. CAL Calibrate;
4. EM Examine Memory;
5. SM Substitute Memory;
6. EX Execute; and,
7. DG Display G's.

The keyboard/display system allows the operator to examine the contents of any memory location and to deposit into any RAM location data that he or she desires. Upon pressing the hardware reset button on the computer board, the display will automatically show memory location 8000 in the left four digits and its contents in the right

two digits. The contents of 8000 are automatically set at FB (hex) by the reset routine to mark the beginning of data. This flag will be used during the tape read operation. If the EM key is pressed, the address is automatically incremented by one and the contents of that location are automatically displayed. Any memory location can be accessed by entering the address using the 0 - F keys (most significant digits first) and its contents will be displayed. If the operator wishes to enter his or her own data into RAM, he or she can enter the address as above, press the SM key, and then enter the data. The data will then be in RAM at that location.

The Programmable Interval Timer (PIT) has three individually programmable 16 bit counters, each of which can operate independently and in various modes depending on the requirements of the main program and the application. Programming the PIT is accomplished through addresses C000 through C003. Addresses C000 through C002 are used to pass data between the micro-processor and counters 0, 0, and 2 and C003 is used to pass programming information to the PIT.

The PIT in this application has two primary functions. First, it produces the required frequencies used in the Tape Dump routine for converting the bit values in the data words to Kansas City Standard data transmission format. Second, it acts as a counter for keeping track of the number of pulses produced by the fifth-wheel de-

vice for conversion to distance and miles per hour.

The AD7574 8 bit Analog-to-Digital Converter and the AD521KD Instrumentation Amplifier combine to amplify the signal from the strain gage bridge on the accelerometer and to convert the amplified output in a digital code. The amplifier raises the output voltage from the accelerometer from 0 to 5 millivolts to 0 to 5 volts, an amplification factor of 1000. The A/D converter then converts the 0 to 5 volts to an 8 bit binary code which is read by the micro-processor during the Execute routine and during the Calibrate routine. The binary code is converted to hexadecimal code for display on the 6 digit display panel. The range of the A/D converter is from 00 to FF (hex).

Computer Mode Operations.

The first executable routine which the micro-processor must perform is the Reset routine. The primary function of the Reset routine is to initialize all the peripheral devices so communication with them will be possible. The Keyboard/Display Interface module must be programmed to receive data from the keypad and micro-processor and to transmit data to the display panel. Communication with the Keyboard/Display Interface is accomplished through memory locations E000 (data) and E001 (command) which are addressable by the micro-processor. The Reset routine also initializes the PIT to set the modes and

counts of the three individual counters within the PIT. Certain key memory locations are also initialized to specific values during the Reset routine. Figure 6-11 is a memory map of the memory used in this micro-computer. Memory locations in Figure 6-12 (RAM Memory Map) highlighted by an asterisk (*) are those which are initialized by the Reset routine. After the Reset routine has been completed, the micro-processor is ready to accept instructions and to perform the operations required by the operator.

Calibration.

During a locked-wheel skid, the vehicle is decelerating at some time varying rate. This rate of deceleration is determined by the coefficient of friction and by the gravitational field acting on the vehicle creating a normal force on the tires. This relationship allows the accelerometer to be calibrated prior to the tests using gravity as a reference without knowing the effects of any of the unknown parameters discussed earlier.

The strain gage bridge produces a small output when the beam is deflected. When amplified and coded by the A/D converter, the undeflected reading is called the zero-g output. The one-g accelerometer reading can also be obtained simply by orienting the beam horizontally. This will cause a one-g output from the A/D converter. During an actual skid test, the data from the accelerometer

0000	\	EPROM
--		Operating
0FFF	/	System
1000	\	
--		Not Used
3FFF	/	
4000		A/D Converter
4001	\	
--		Not Used
7FFF	/	
8000	\	
--		RAM
8FFF	/	
9000	\	
--		Not Used
BFFF	/	
C000	\	
--		PIT
C003	/	
C004	\	
--		Not Used
DFFF	/	
E000	\	
--		Keyboard Display Interface
E001	/	
E002	\	
--		Not Used
FFFF	/	

Figure 6-11. Memory Map

8000* (FB)	Data Beginning Flag
8001	Zero G Location
8002	One G Location
8003	\
--	Accelerometer Data (1000)
83EA	/
83EB* (FF)	Data Division Flag
83EC	\
--	Fifth-Wheel Data (2000)
8BBB	/
8BBC	MPH (decimal)
8BBD (00)	
8BBE	MPH (hex)
8BBF (00)	
8BC0* (FF)	Data End Flag
8BC1* (FF)	Data End Flag
8BC2	\
--	Not Used
8FD7	/
8FD8* (03)	Display G's Start LSB
8FD9* (80)	Display G's Start MSB
8FDA	Not Used
8FDB	Not Used
8FDC* (00)	Tape Start LSB
8FDD* (80)	Tape Start MSB
8FDE* (C2)	Tape Stop LSB
8FDF* (8B)	Tape Stop MSB
8FE0	\
--	Stack
8FFF	/

Figure 6-12. RAM Memory Map

will be proportional to one-g by a factor of μ . The coefficient of friction at any point in time can be calculated using the following equation

$$\mu = (\text{DATA} - \text{Zero g}) / (\text{One g} - \text{Zero g})$$

The calibration procedure involves two steps. The first step is to vertically orient the accelerometer in the vehicle and press the CAL button. Second, rotate the beam toward the front of the vehicle until the beam passes through horizontal. The computer will sample the accelerometer through the A/D converter every 5 milliseconds for a period of 10 seconds. The zero-g reading is stored at location 8001 immediately after the CAL button is pressed and the maximum value obtained during the 10 second sampling period will be stored at location 8002 in RAM and is the one-g value.

Execution.

The Execution operation is the data acquisition phase of the system. Upon pressing the EX (Execute) button, the computer begins to process data from the PIT (Programmable Interval Timer) to calculate the velocity of the vehicle in miles per hour. One of the counters in the PIT is clocked by the output from the fifth-wheel. Every second the counter is reset to zero and, for a one second duration, the counter counts the number of clock pulses. The number of pulses per second is proportional to the velocity in miles per hour by a factor f , calculated as

follows:

$$f = (9.75" * 2 * 3.1415926) / 12 * 36 * 1.466667) \\ = 1/10.3426$$

where

9.75 is the radius of the fifth-wheel tachometer;

2 * 3.1415926 is the conversion of radius to circumference;

12 is the conversion from inches to feet;

36 is the number of clock pulses per revolution;

and,

1.466667 is the conversion from ft/sec to MPH.

The speed is continuously displayed and is updated every second. Upon pressing the brake pedal, the speed, in miles per hour, is stored in memory and the data acquisition phase of the execution operation begins.

During the data acquisition phase of the execution operation, the accelerometer and fifth-wheel are sampled at incremental periods of time with the RAM size limiting the number of samples that can be taken during a skid test. One sample of the accelerometer takes one 8 bit memory location while one sample of the fifth-wheel requires two 8 bit memory locations because the counters in the PIT are 16 bit counters. As a result, three memory locations are required for each sample. There are 4096 RAM locations; therefore, the maximum number of samples is limited to approximately 1350 leaving 46 locations for computer use storage referred to as Stack. The horizontal

resolution of the digital plotter used to plot the data is one one-thousandth of the total width, making more than 1000 sample points unnecessary. For these reasons, a sample number of 1000 was chosen.

A "worst case" skid example was required to calculate the interval between the sample points. Using a "worst case" of μ of 0.5 and a speed of 60 miles per hour, the time to stop a skidding vehicle was calculated at 3.7 seconds. To be safe, a time duration of 5 seconds was chosen. This puts the interval between samples of 5 milliseconds. This time interval is maintained by dividing the micro-processor clock down to a 5 milli-second interval by knowing how many steps are required to perform each instruction in the program between samples and adding in a delay loop to make the difference.

The combined sampling of the accelerometer and the fifth-wheel make up the data to be evaluated by a computer at the laboratory site.

Tape Dump.

The Tape Dump routine is a program which transmits the data contained in RAM onto a cassette tape for permanent storage. The data will then be read into another micro-computer in the laboratory for analysis.

The micro-computer steps through the data stored in RAM and examines each bit in the data word one at a time. The micro-processor then programs the PIT to

transmit 8 cycles of a 2400 Hz signal if the bit is a 1, or, 4 cycles of a 1200 Hz signal if the bit is a 0. To create the correct frequency, the PIT divides the 3.072 MHz clock by the appropriate number. This format for data coding and transmitting is called the Kansas City Standard format. The output of the counter is then fed into a cassette recorder's auxiliary input jack for recording. Using this method, the entire RAM contents can be stored on tape in approximately two minutes.

Display G's.

The Display G's routine is a program which will display every tenth accelerometer sample with respect to the zero and one-g calibration values. This allows the operator in the field the ability to examine the skid characteristics immediately after the skid test is completed. The values displayed are in percent of one g and are approximately equal to the coefficient of friction at that point. Each tenth data point is displayed for approximately one second requiring one and one half minutes to examine the acceleration characteristics.

Fifth Wheel.

The fifth-wheel device is constructed from a 20 inch bicycle tire, a plastic wheel, an aluminum frame, and a small electrical circuit. Attached around the edge of the wheel are 36 evenly spaced magnets. An electrical circuit using a Hall Effect switch produces a pulse every

time a magnet passes by the Hall Effect switch which is mounted on the frame adjacent to the magnets. This pulse clocks the counter during the Execution phase. The fifth-wheel attaches to the rear bumper of the test vehicle with a set of mounting bolts and is free to rotate about the horizontal axis of the mount to allow for vertical movement. The fifth-wheel is not required in all operations of the micro-computer system and may be deleted altogether in some cases. Figure 6-13 shows the fifth-wheel attached to an automobile.

System Testing and Data Evaluation.

Field tests of the system were conducted at two locations using two different vehicles. The tests were run with the assistance of the Austin Police Department using an APD patrol car. Prior to the brake actuation, the vehicle speed is displayed by the computer using the output from the fifth-wheel. The displayed velocity was in complete agreement with the speed indicated by the "certified" patrol car speedometer and with external radar during the tests. Observers outside the vehicle watched for the initial tire lock-up and measured the skid length.

The accelerometer was calibrated prior to each skid to obtain the one-g reference by rotating the beam to the horizontal position. The computer's calibration routine automatically stores the highest strain gage output it sees during this phase. The adjustment on the ac-

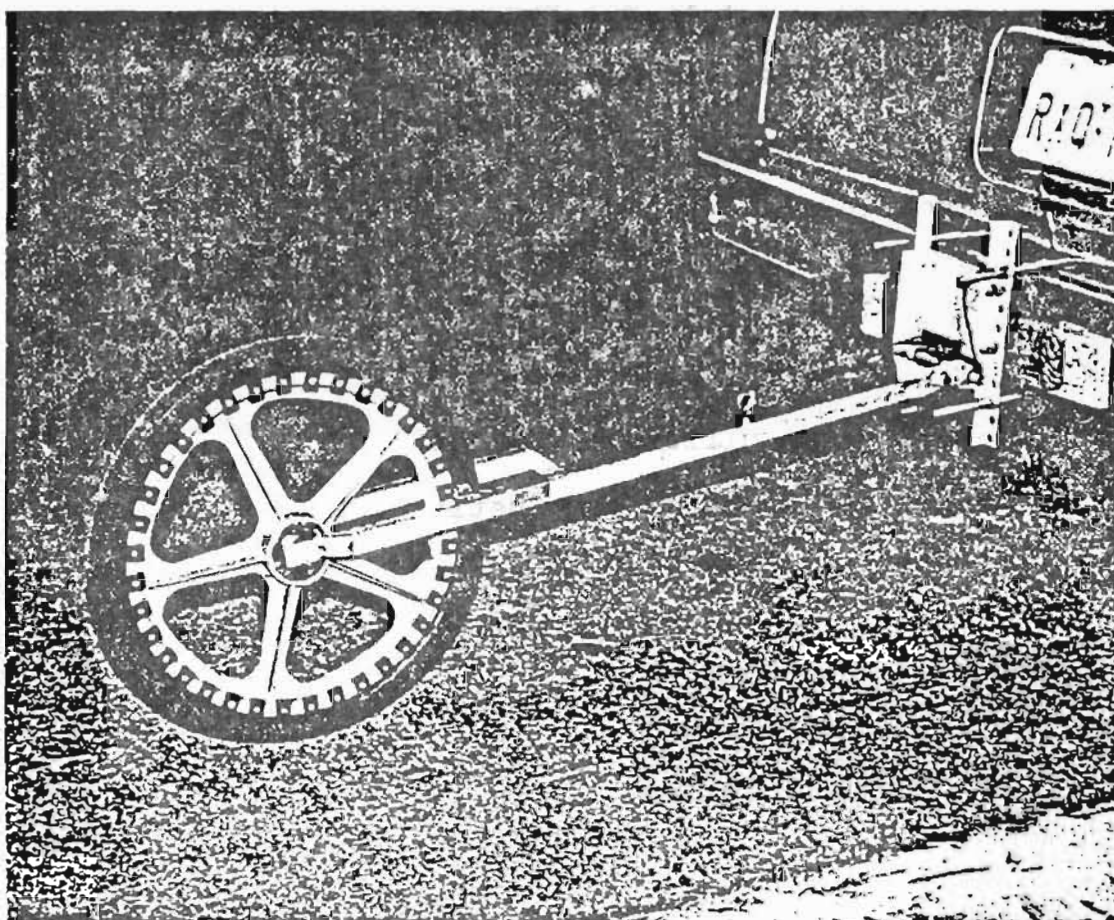


Figure 6-13. Fifth-Wheel

celerometer damper was modified before each test to obtain the damping ratio which would allow for quick response without unwanted oscillations.

The first test was performed on June 17, 1982, at Crossing Place, 0.1 miles north of Riverside Drive in Austin, Texas, with a 1979 Ford LTD patrol car. The road was chosen because it had very little use and, therefore, little deterioration making it a very coarse surface. The temperature was approximately 80 degrees Fahrenheit.

The second series of tests were performed in Austin, Texas, on June 18, 1982, on Guadalupe Drive at the intersection of 24th Street in the northbound lanes. Guadalupe Drive is a main traffic artery for the University area of Austin which is heavily travelled. Therefore, the surface is highly polished and contaminated. The temperature was also approximately 80 degrees Fahrenheit and again, the tests were run using a different Ford LTD.

Testing Procedure.

Before testing began, the micro-computer/accelerometer unit was electrically connected to the vehicle. The cigarette lighter socket was used as a 12 volt power source. Otherwise, any 12 volt DC source and ground connection could have been used. A conductor was also connected from the lightbulb side of the brake light switch to the computer "BRAKE" input. This served as the triggering source for the data acquisition subroutine.

The fifth-wheel was mounted on the rear of the vehicle and the power and signal lines were run to the computer unit. With all the connections made and the vehicle in position, the accelerometer was calibrated. The CAL button was pressed and the accelerometer was rotated to the horizontal position. When this sequence was complete, testing began.

After releasing the brake, the EX button was pressed and the vehicle was accelerated. The velocity at which the test vehicle was travelling was continuously displayed and updated every second by the micro-computer. That same velocity was also stored in a designated memory location for use during the analysis of the data.

At the instant the brake pedal was pushed to initiate the skid, the micro-computer began to sample both the A/D converter (connected to the accelerometer) and the counter (connected to the fifth-wheel) every five milliseconds. One thousand samples were taken for a total duration of five seconds. Each sample from the A/D converter and from the counter was stored in the computer RAM.

At the completion of the skid, the data from the skid, which was now in RAM, was converted into Kansas City Standard format and recorded onto a cassette tape. The TD button on the computer is used to initiate this function.

When the test sequence was completed, the cassette tape with the recorded data was read into the memory of a micro-computer development system. To make

analysis easier to eliminate having to read the cassette each time, the data was transferred onto a flexible disk under a file name which reflects the date and test number. The computer utilized in this work is a 64K Z-80 based system running under the CP/M (Control Program/Micro-computer) operating system.

Test Results.

The results from the second tests will be evaluated and explained in detail and the results of the first test site will be presented, but not explained in the same detail.

Figure 6-14, 6-15 and 6-16 show the actual deceleration vs. time plots for the three tests performed at the second test site. The heading of each plot indicates the date and test number.

All of the data recorded by the computer system is in digital form so that use of a digital filter will smooth the data to the beams equilibrium position. A first-order digital filter, as described in reference [53], was used to filter out the unwanted oscillations in the data. The digital filter used in the analysis filters out all oscillations above a frequency of 10 Hz. The following equation is the digital equivalent of a first-order filter:

$$D(n) = D(n-1) + (T_s/(T_s+T))(X(n) - D(n-1)) \quad (6-12)$$

where

JJ168281
DECELERATION(GS)
VS TIME

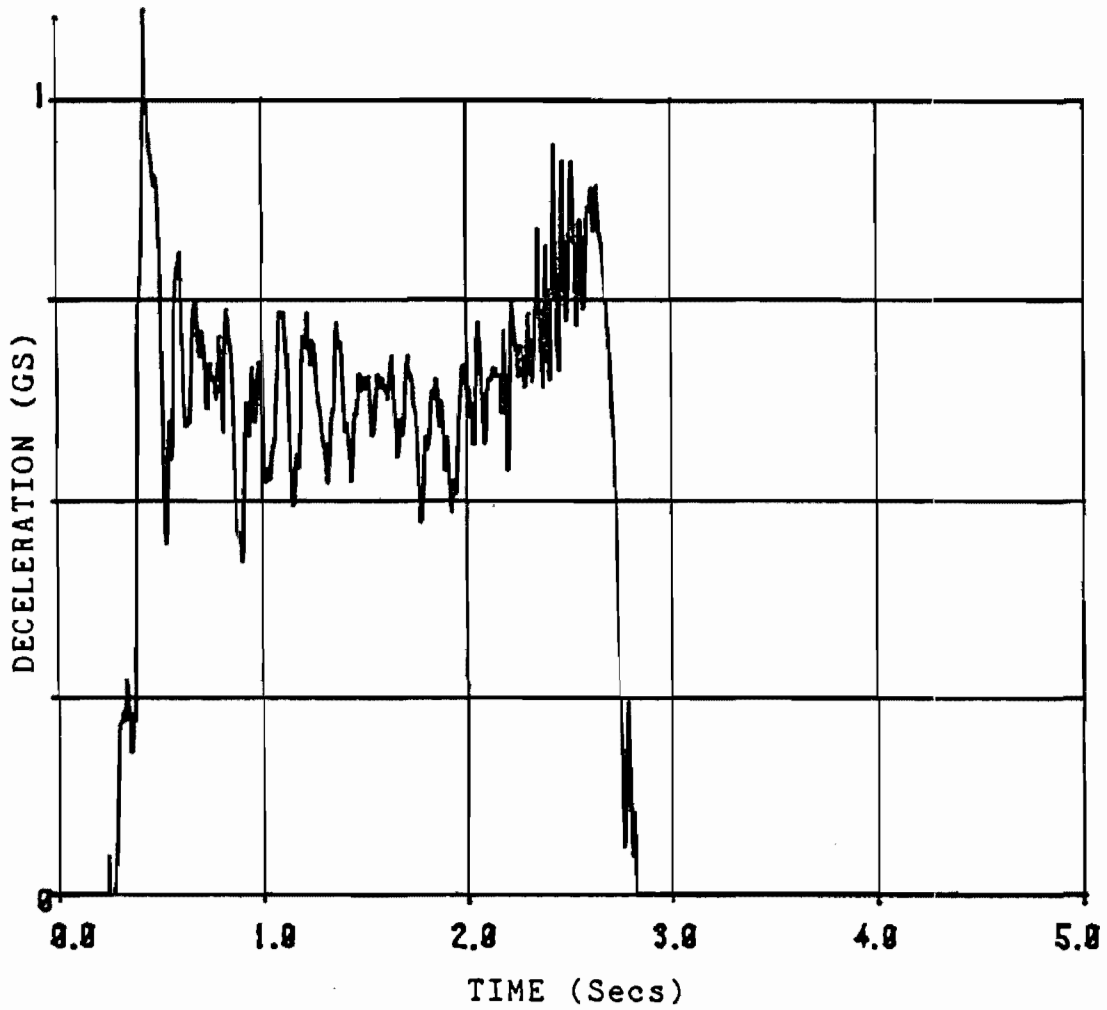


Figure 6-14. Deceleration vs. Time
June 18, 1982 - Test One
Unfiltered

JU186292
DECELERATION(GS)
VS TIME

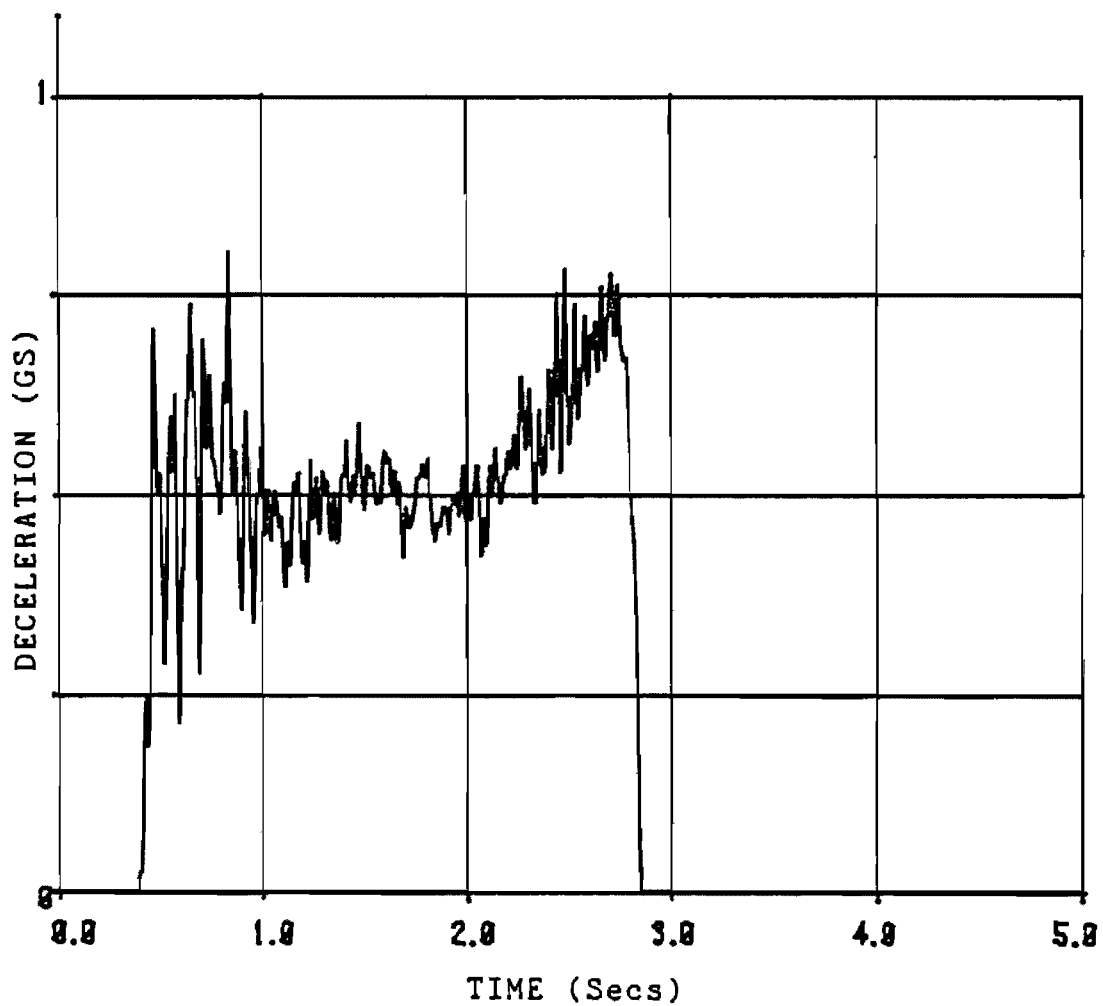


Figure 6-15. Deceleration vs. Time
June 18, 1982 - Test Two
Unfiltered

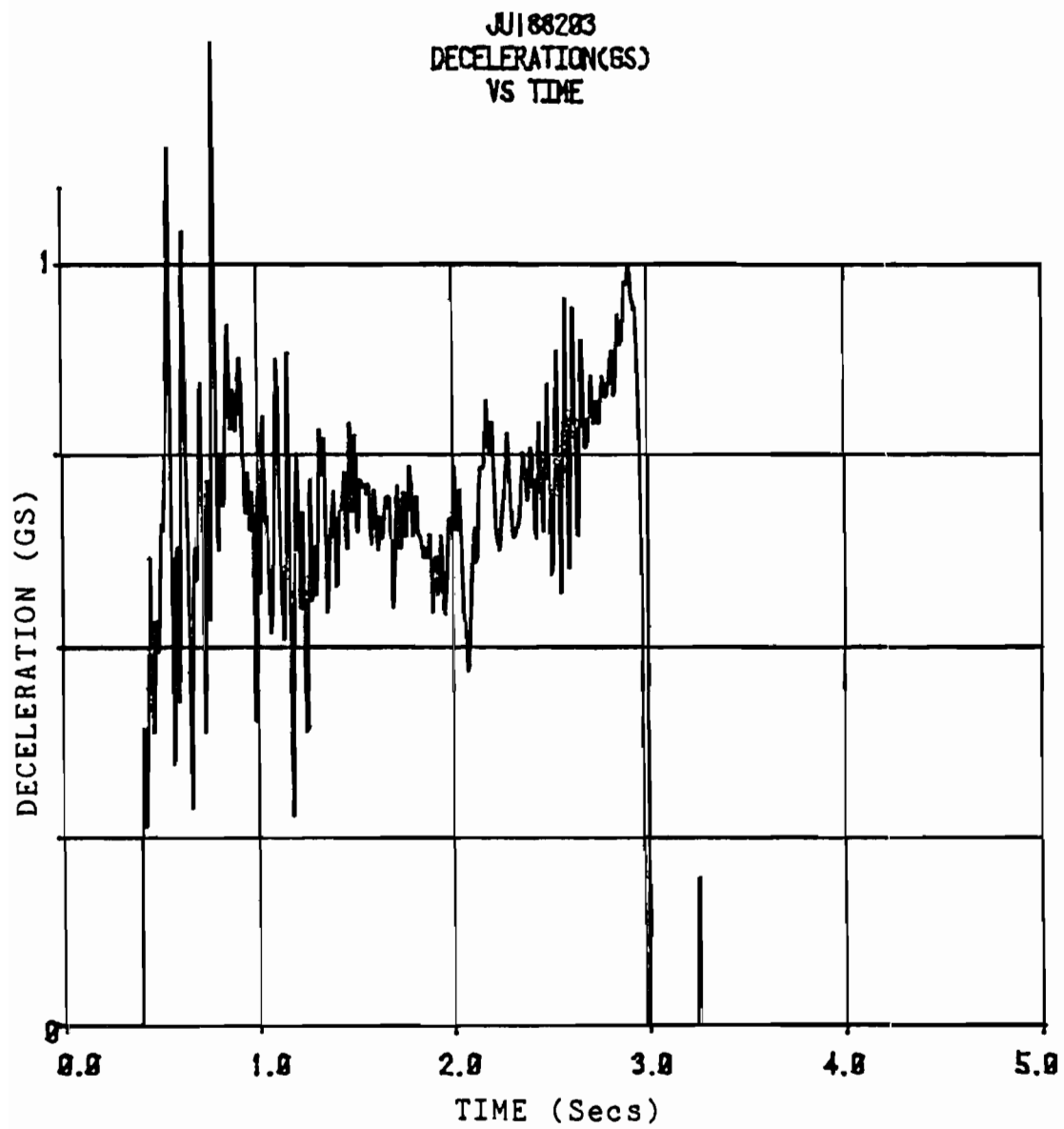


Figure 6-16. Deceleration vs. Time
June 18, 1982 - Test Three
Unfiltered

$D(n)$ and $D(n-1)$ are the filtered values at times n and $n-1$;

$X(n)$ is the unfiltered value at time n ;

T_s is the sample interval (0.005 seconds); and,

T is the period of the cut-off frequency (0.1 secs).

For this case, the cut-off frequency chosen was 10 Hz so the value of $(T_s/(T_s+T))$ is $1/20$ or 0.05.

Figures 6-17, 6-18 and 6-19 represent the deceleration versus time plot employing a digital filter. It can be seen by comparing the equivalent tests that the filtered data represents the equilibrium position of the unfiltered data. To verify that the filtering does not alter the results, an integration with respect to time was performed on the filtered and unfiltered data and the results were in very close agreement, within 0.01 feet per second.

Using sample dynamic principles, the integration of the deceleration versus time yields the change in velocity. Since all testing was done to a complete stop, the initial velocity equals the integral of the deceleration versus time curve.

In the skids at test site two, the initial velocity of the vehicle, as recorded by the fifth-wheel/computer combination, did not agree with the integration of the deceleration versus time curve. Since the velocity, as displayed and recorded by the fifth-wheel/computer unit,

JU165281
DECELERATION(GS)
VS TIME

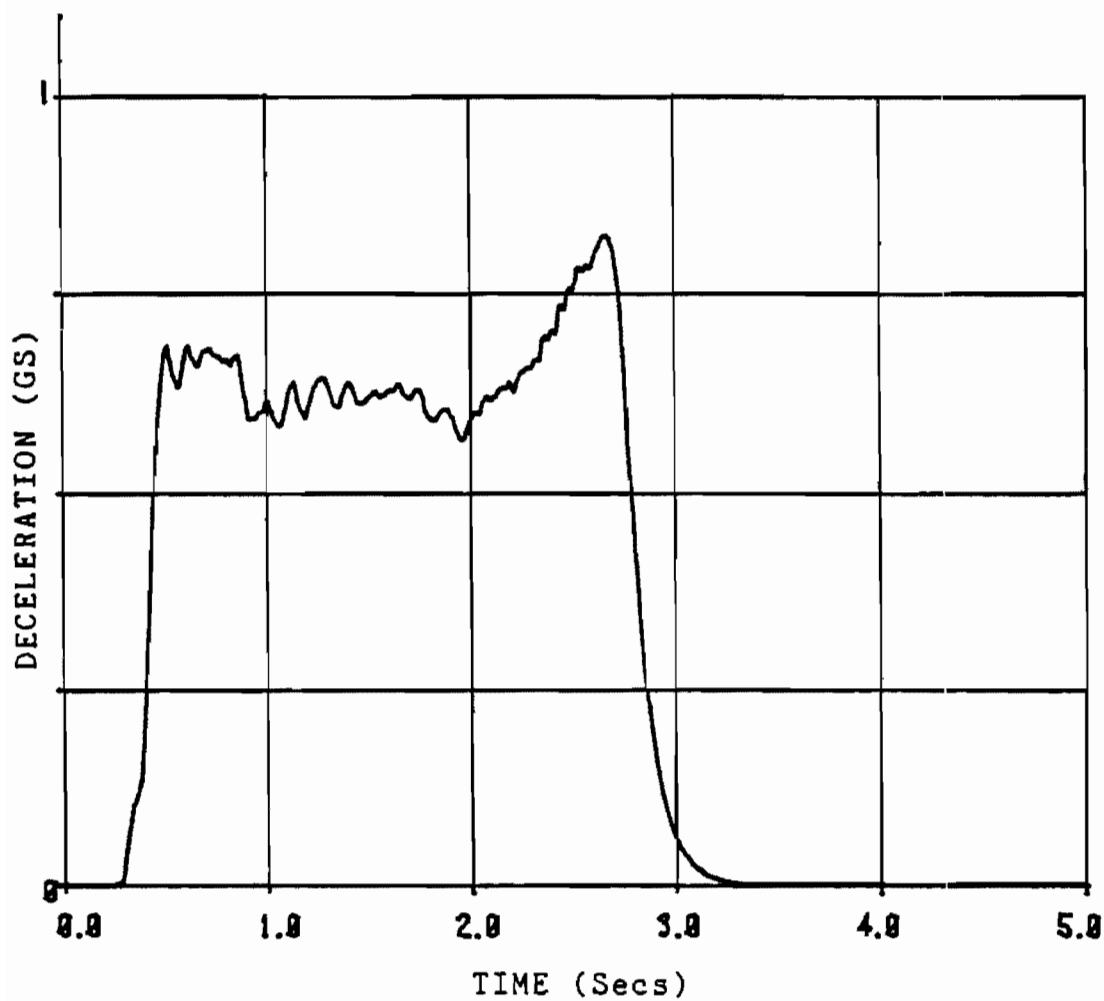


Figure 6-17. Deceleration vs. Time
June 18, 1982 - Test One
Filtered

JJ188282
DECELERATION(GS)
VS TIME

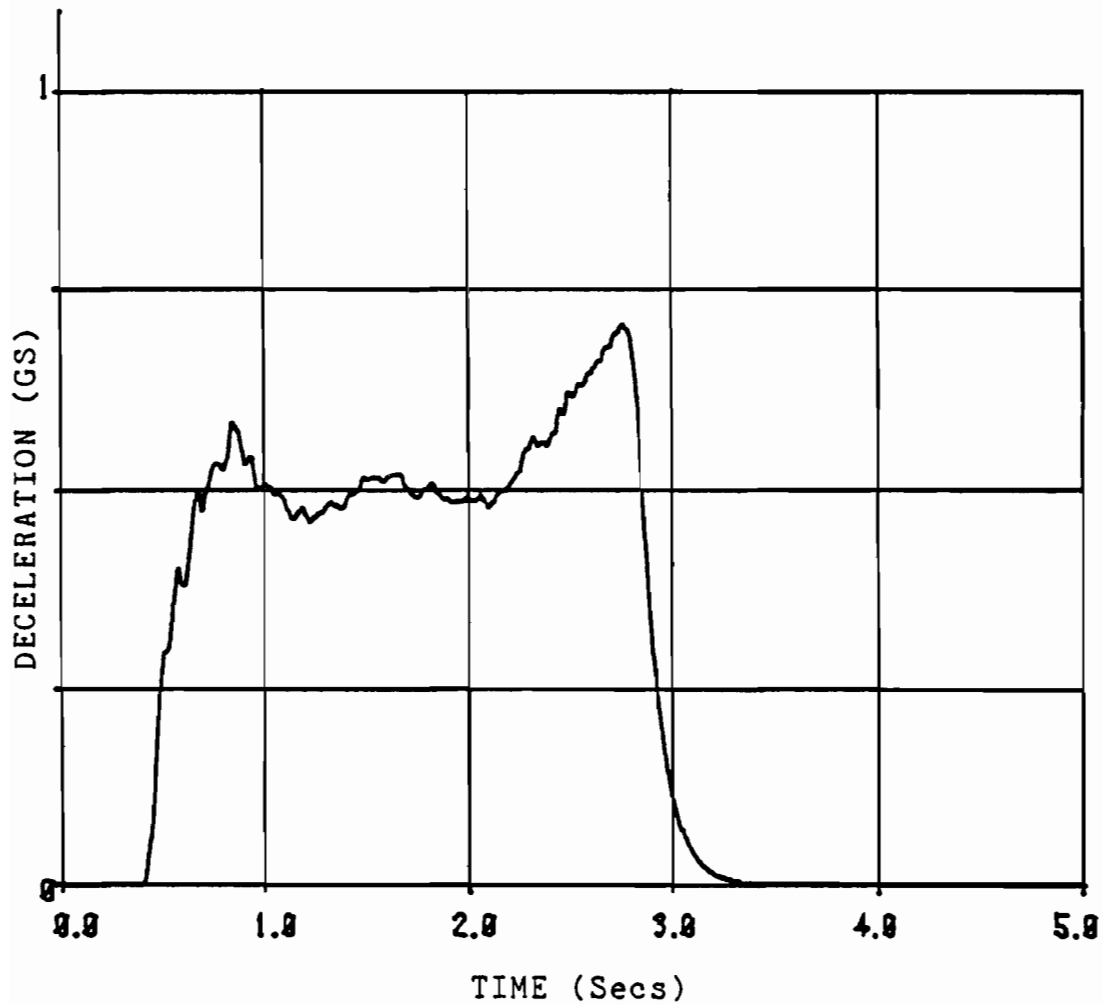


Figure 6-18. Deceleration vs. Time
June 18, 1982 - Test Two
Filtered

JU168283
DECELERATION(GS)
VS TIME

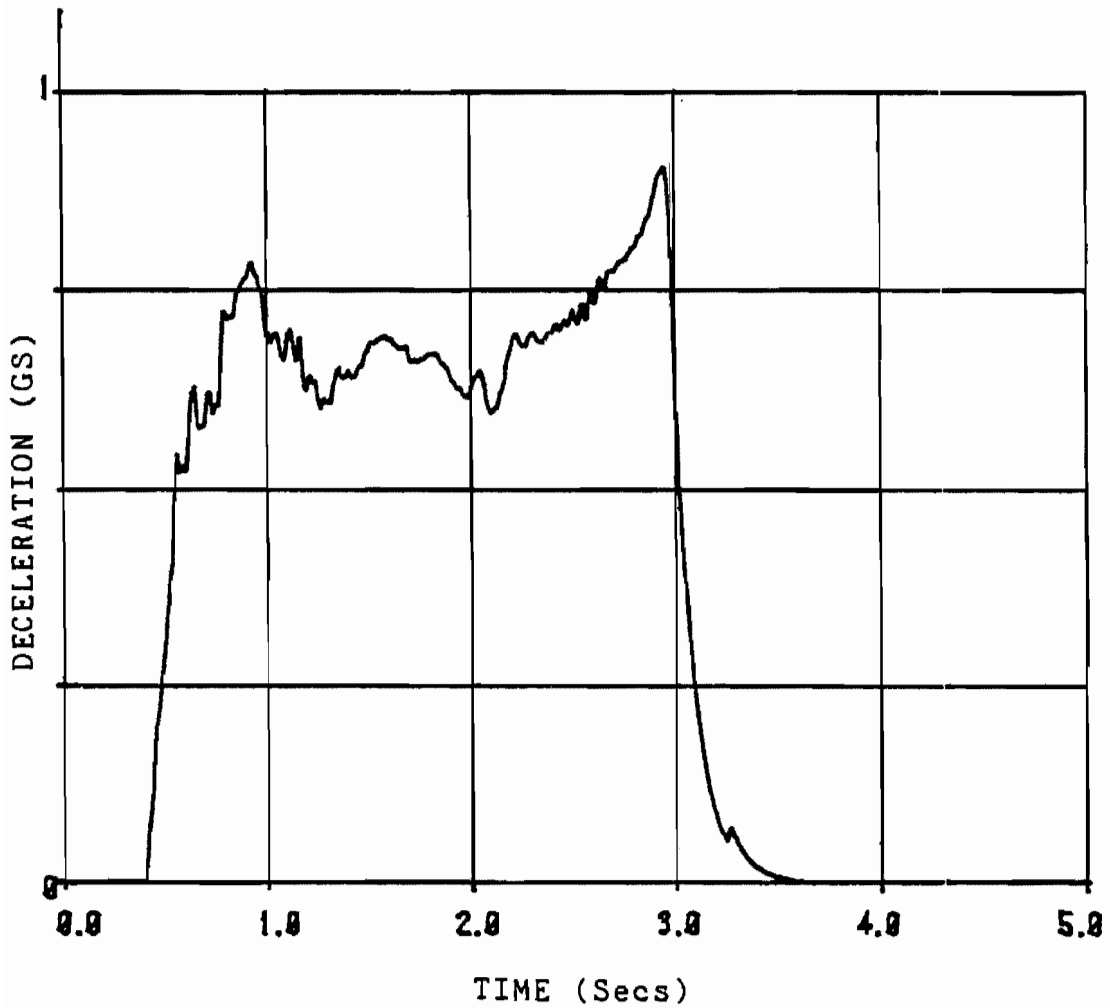


Figure 6-19. Deceleration vs. Time
June 18, 1982 - Test Three
Filtered

was closely calibrated and experimentally verified, it must be assumed that the integration of the deceleration versus time curve is incorrect.

The accelerometer records the relative changes in deceleration over the skid time so the only conclusion that can be reached is that the exact magnitude of the deceleration data is incorrect. During the calibration phase, the beam is moved slowly, so that it has been essentially statically displaced to the horizontal, one-g position. But when the beam is undergoing deflection during a skid, it is under the influence of a dynamic force and is also being driven by frequencies near its natural frequency. It is concluded that the damping system is preventing the beam from deflecting to its equilibrium position while under the influence of the dynamic force of the mass under acceleration. The damper is necessary, however, since it prevents the beam from being driven too far by the vibrations near its natural frequency.

To make the integration of the deceleration versus time data equal to the initial velocity, the one-g calibration value was recomputed. The displayed fifth-wheel velocity is accurate to within +0 to -0.00 miles per hour or the speed indicated by the computer is the minimum velocity it could be sensing. The actual velocity could be as much as the indicated velocity plus 0.99 miles per hour. In other words, the computer rounds down to the

nearest integer velocity. This leads to the fact that there is a range of one-g calibration values which will satisfy the accuracy of the fifth-wheel when the deceleration versus time curve has been integrated. Figures 6-20, 6-21 and 6-22 show the ranges that the deceleration versus time curves can have and still satisfy the accuracy of the indicated initial speed for the three skid tests conducted at site two. The lower deceleration curve reflects the higher one-g calibration value. These curves also reflect the ranges in the coefficient of friction in dimensionless units from 0 to 1.

Table 6-2 shows the results from the three skid tests done at the second site. The original one-g calibration value is shown for each test as well as the range in the one-g calibration values which satisfy the accuracy of the initial velocity when the deceleration versus time curve is integrated. The initial velocities obtained from the integration of the adjusted deceleration versus time curves are also listed.

The initial velocity of the vehicle is verified and recorded by the fifth-wheel/computer combination and that velocity is obtained by adjusting the one-g calibration factor. The velocity versus time curve can thus be obtained by integrating the deceleration versus time curve once to obtain the initial velocity and then reintegrating the deceleration versus time data one incremental time segment at a time and subtracting it from the previous

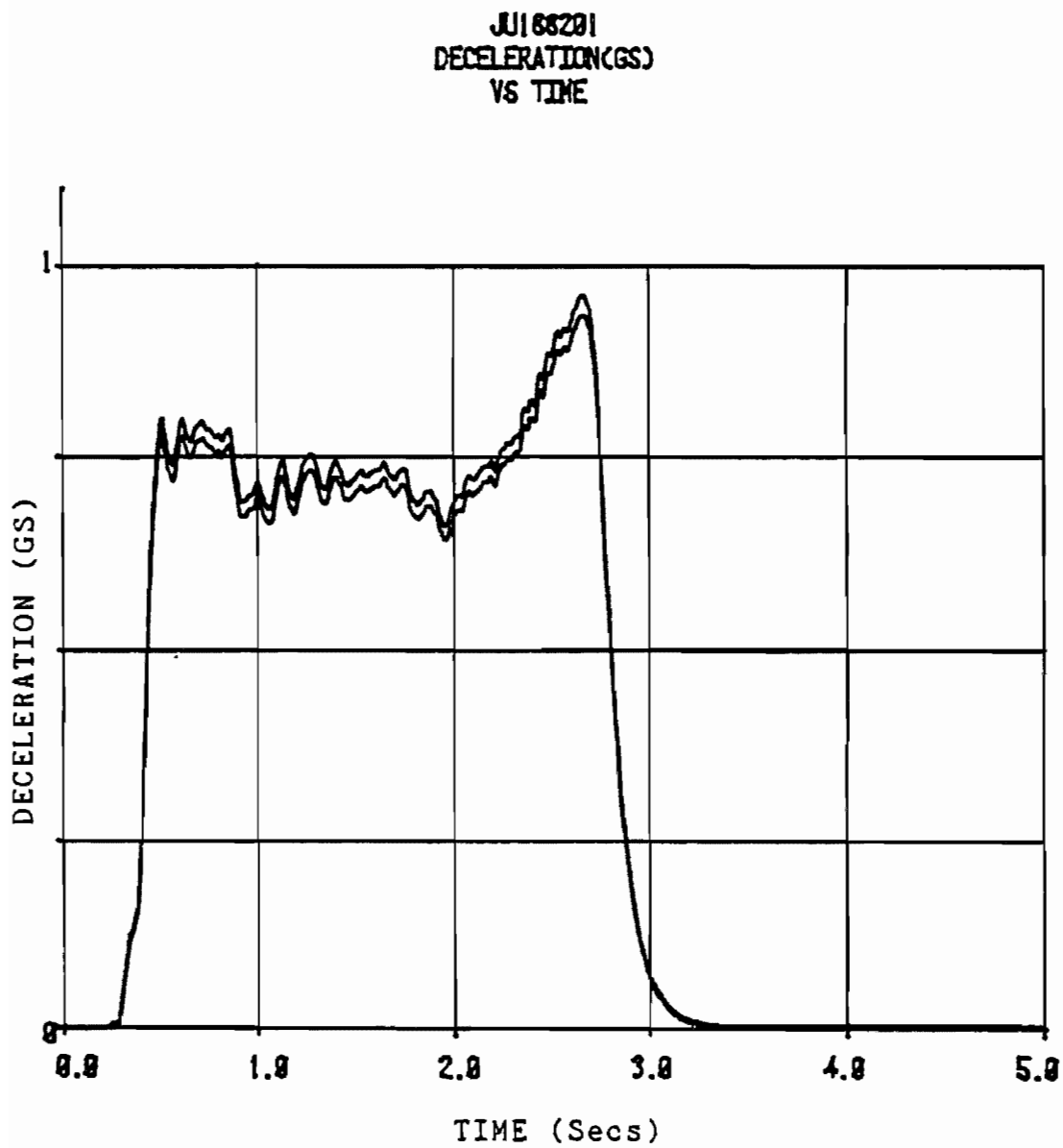


Figure 6-20. Deceleration vs. Time
June 18, 1982 - Test One
Filtered, One G Calibration Range

JU166202
DECELERATION(GS)
VS TIME

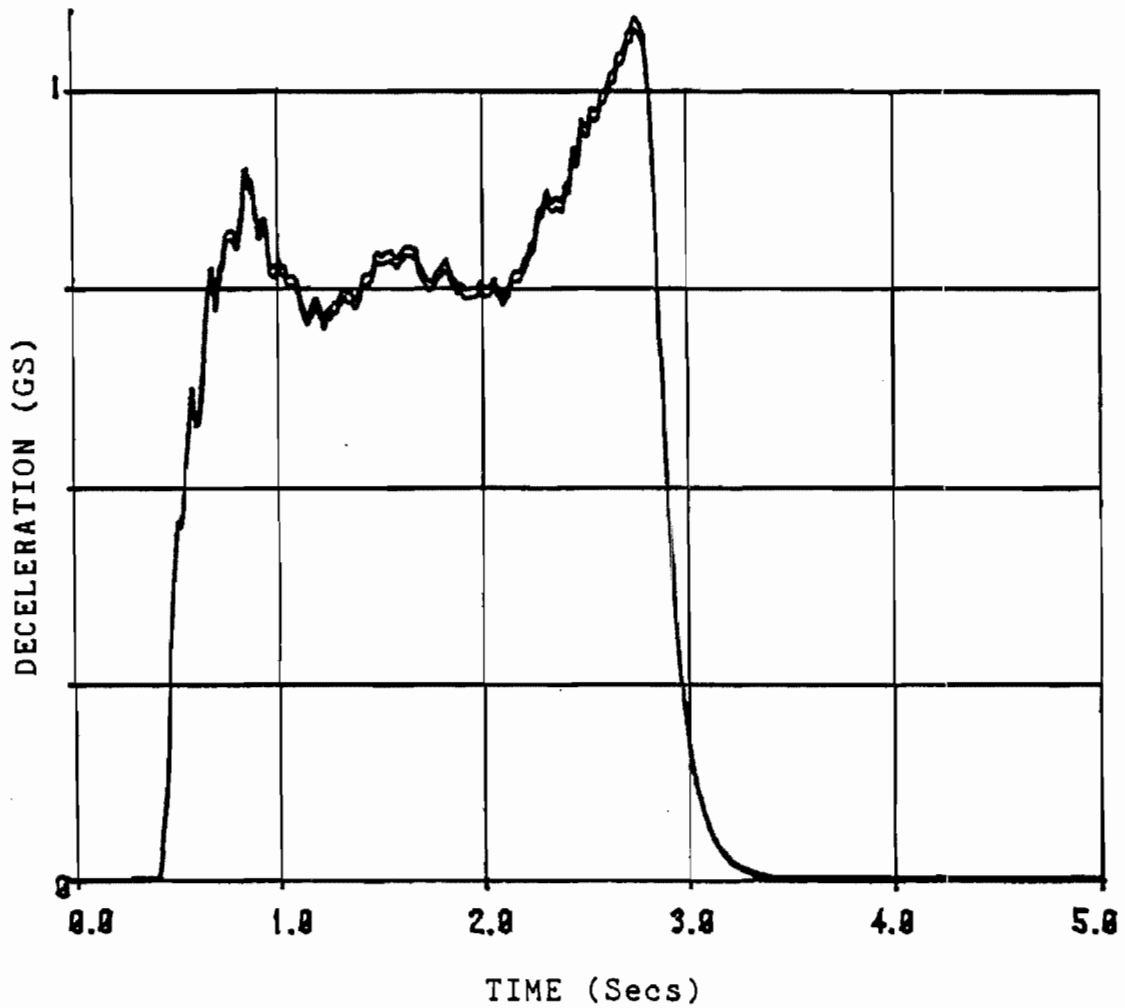


Figure 6-21. Deceleration vs. Time
June 18, 1982 - Test Two
Filtered, One G Calibration Range

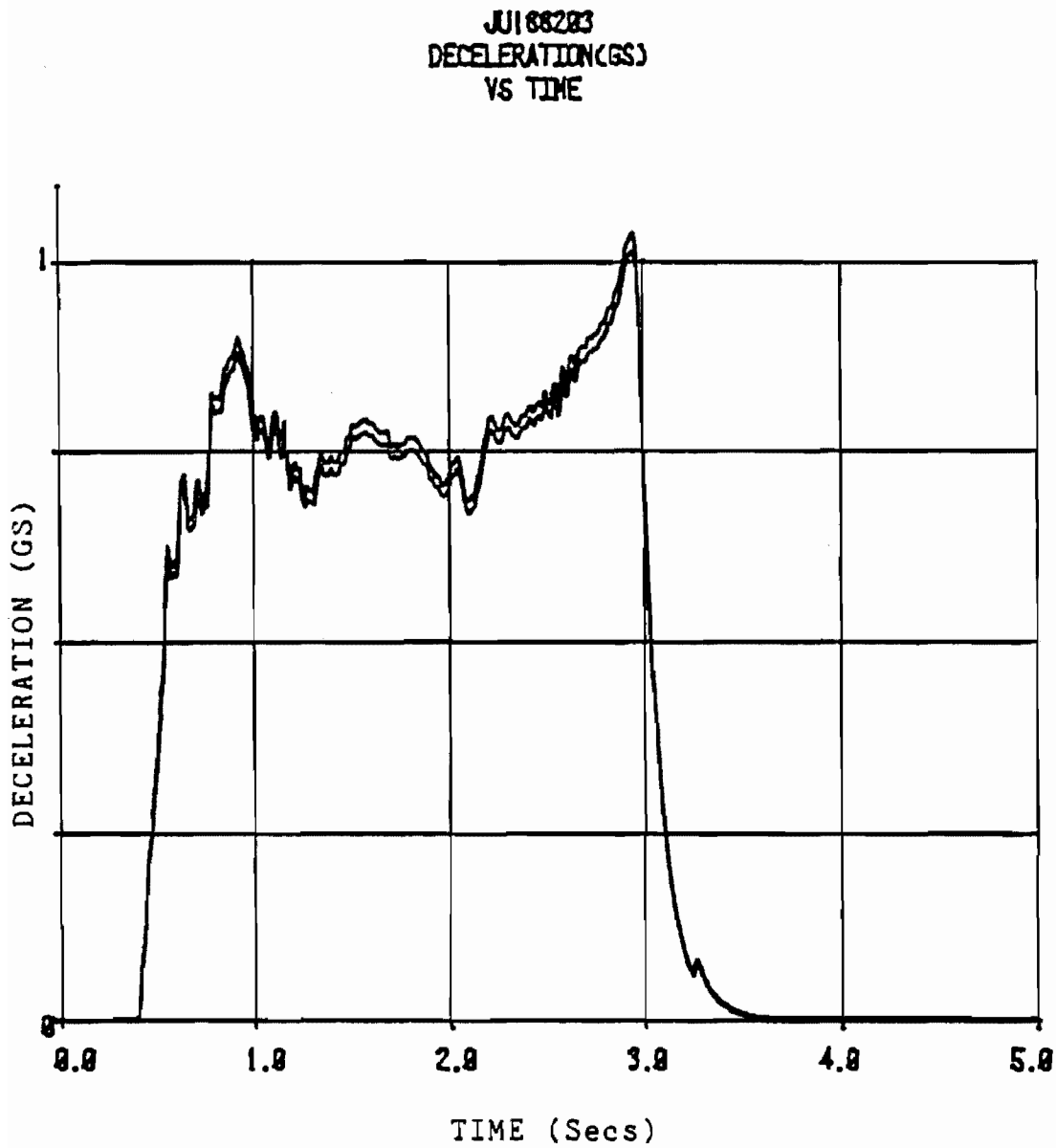


Figure 6-22. Deceleration vs. Time
June 18, 1982 - Test Three
Filtered, One G Calibration Range

TABLE 6-2
RESULTS OF SKID TESTING AT SITE TWO
JUNE 18, 1982

Description	Test Number		
	1	2	3
1. Initial Velocity (5th-wh)	40 MPH	43 MPH	44 MPH
2. Initial Calibration Value	8F	86	79
3. Calibration Range Adjust	7E - 7B	58 - 57	6C - 6A
4. Velocity Range Using Calib. Range	40.21-40.86 MPH	43.29 - 43.75 MPH	44.10-44.89 MPH
5. Fifth-Wheel Distance	81.5 FT	97.41 FT	107.6 FT
6. Skid Length Measurement	70.5 FT	66.5 FT	76 FT
7. Initial Velocity Using 5th-Wheel Energy	36.62-36.91 MPH	38.86 - 39.08 MPH	41.00-41.38 MPH
8. Calculated Distance Using Double Integration Of Decel. Data	97.8 - 99.4 FT	112.8 - 114.1 FT	118.4-121.9 FT

velocity. Figures 6-23, 6-24 and 6-25 represent the velocity versus time curves for the second series of tests using the above procedure.

The velocity versus time curve can then be integrated to obtain the distance versus time curves shown in Figures 6-26, 6-27 and 6-28.

The cross integration of the deceleration versus distance data will yield the total energy of the skid as defined by Equation (6-9), where $g = a$ and a is the non-constant deceleration. Equation (6-9) becomes:

$$m \int a \, ds = m v^2 / 2 \quad (6-13)$$

or

$$v = \left[2 \int a \, ds \right]^{1/2} \quad (6-14)$$

This cross integration was performed with the results in exact agreement with the single integration of the deceleration versus time data. All of the integration carried out in this analysis where time is one of the factors is done numerically using Simpson's method of numerical integration, as defined in Reference [54].

Another distance versus time curve is generated by the sampling of the fifth-wheel counter during the skid process. This fifth-wheel distance versus time curves are shown in Figures 6-29, 6-30 and 6-31 for the three tests at site two.

It is then possible to integrate the deceleration data obtained from the accelerometer with respect to the distance data obtained from the fifth-wheel to get the

JJ166281
VELOCITY (FT/SEC)
VS TIME

FINAL VELOCITY = 8.11 FT/SEC

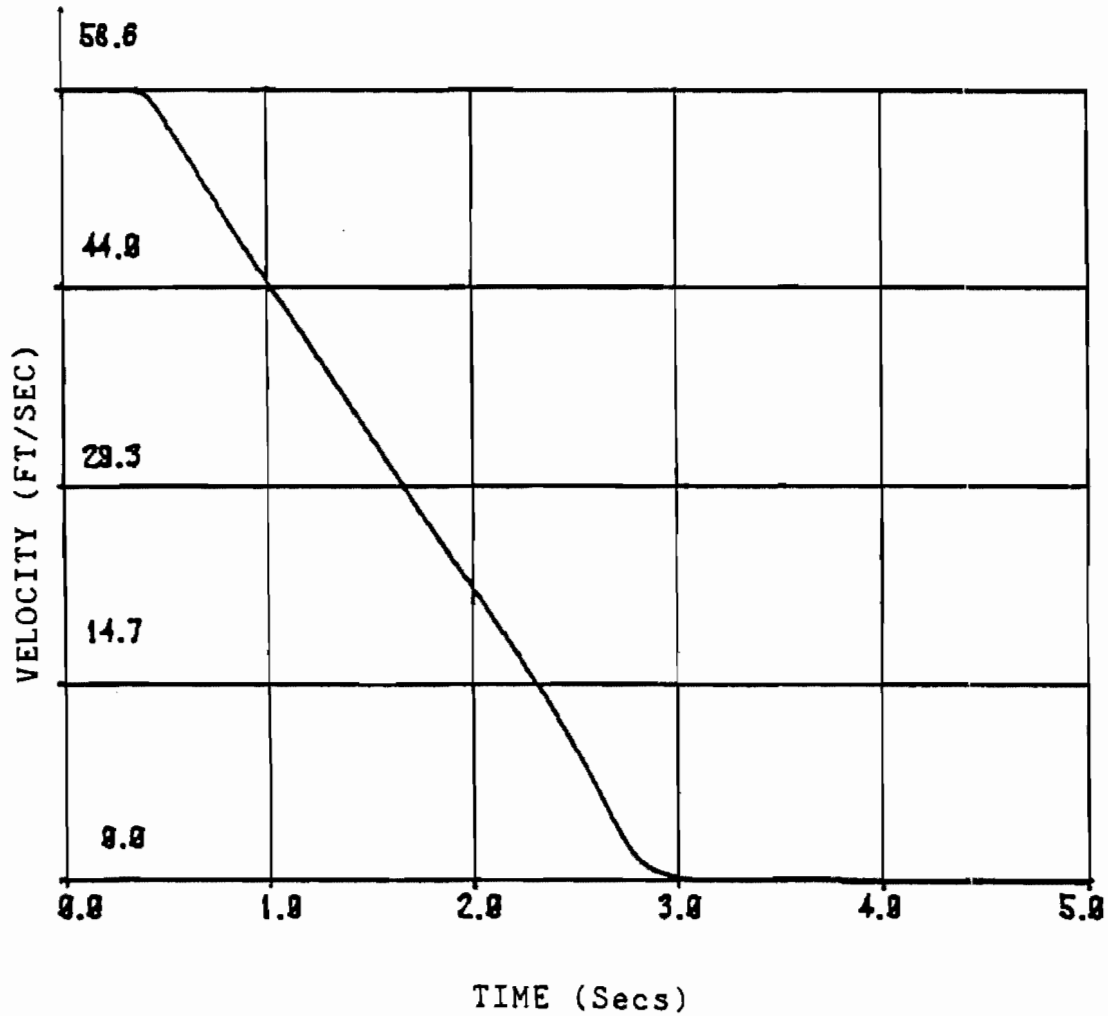


Figure 6-23. Velocity vs. Time
June 18, 1982 - Test One

JJ168282
VELOCITY (FT/SEC)
VS TIME

FINAL VELOCITY = 8.8 FT/SEC

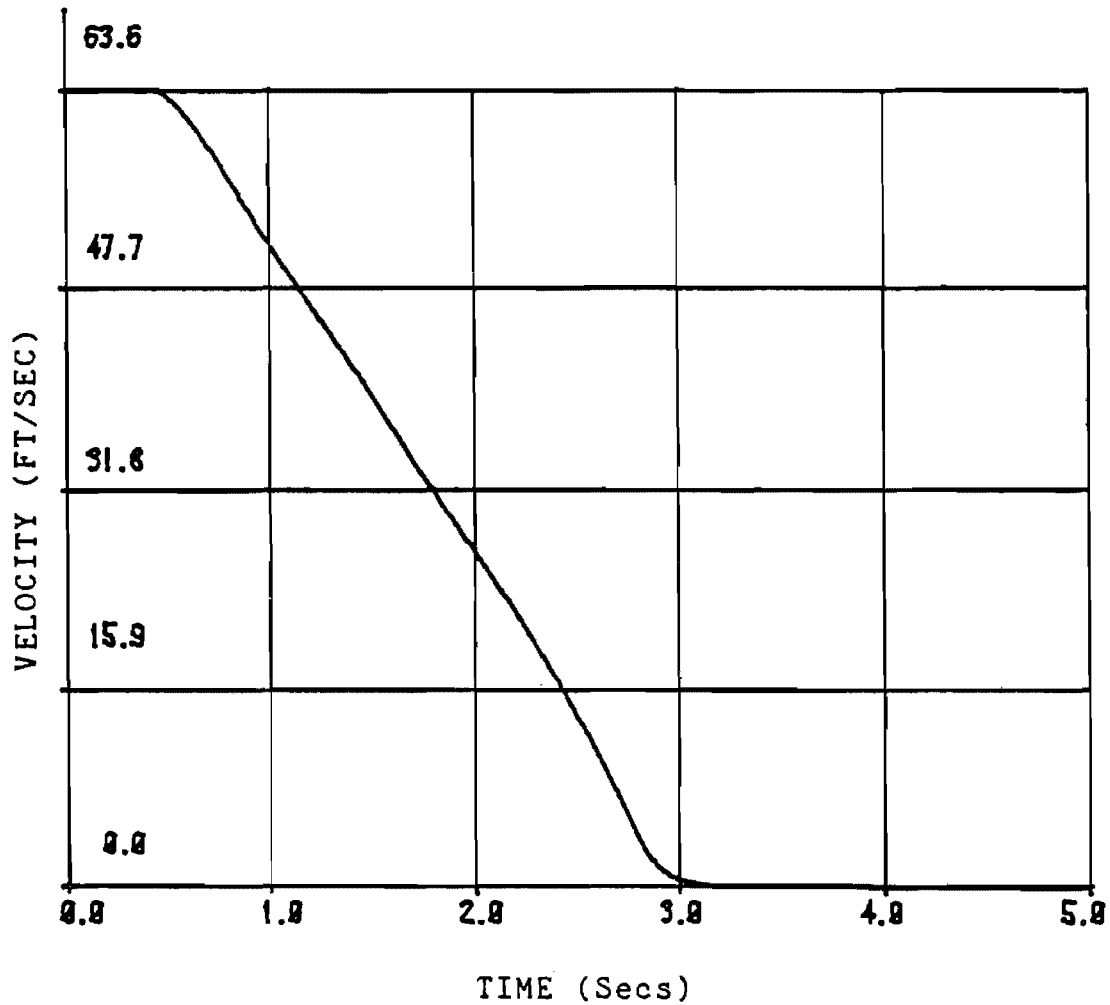


Figure 6-24. Velocity vs. Time
June 18, 1982 - Test Two

JU188203
VELOCITY (FT/SEC)
VS TIME

FINAL VELOCITY = 4.8 FT/SEC

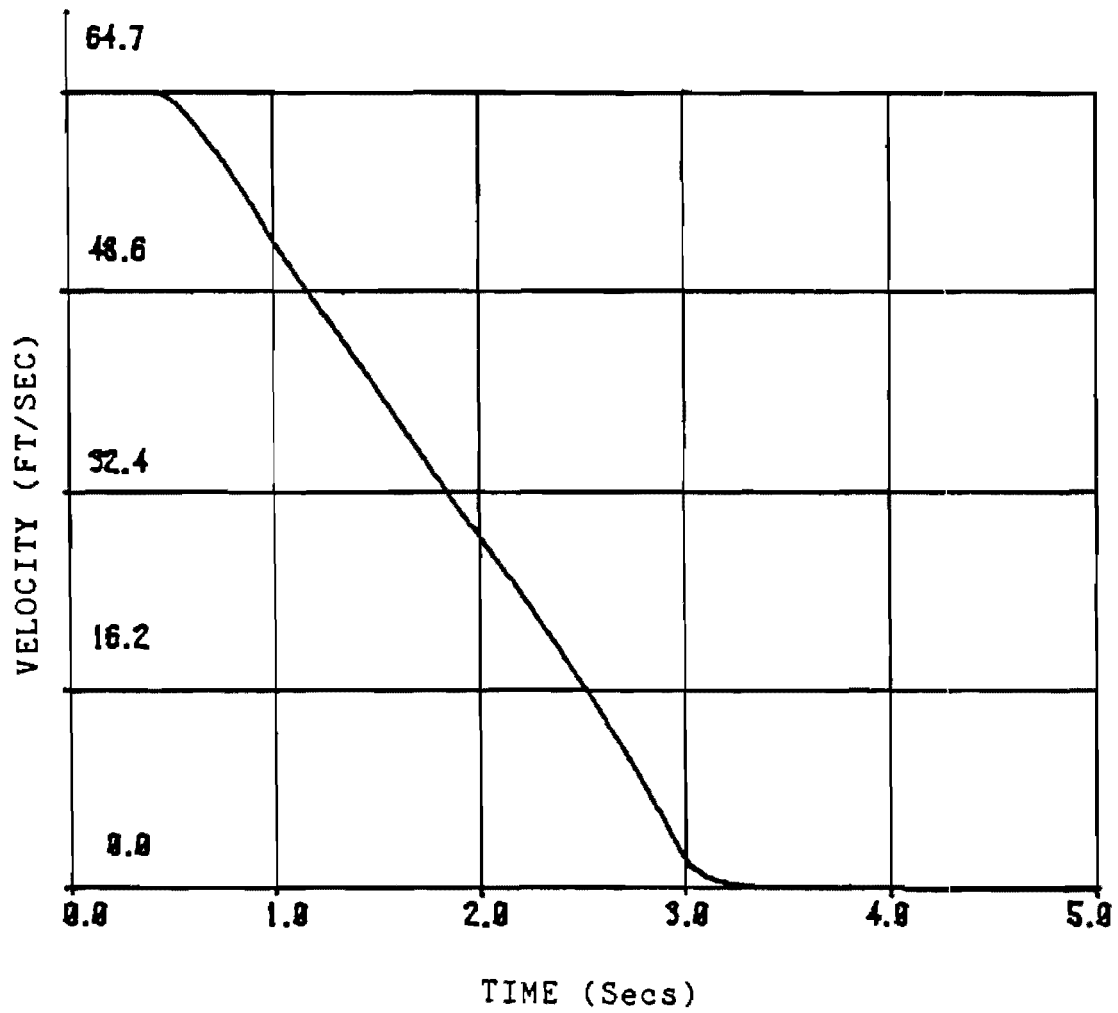


Figure 6-25. Velocity vs. Time
June 18, 1982 - Test Three

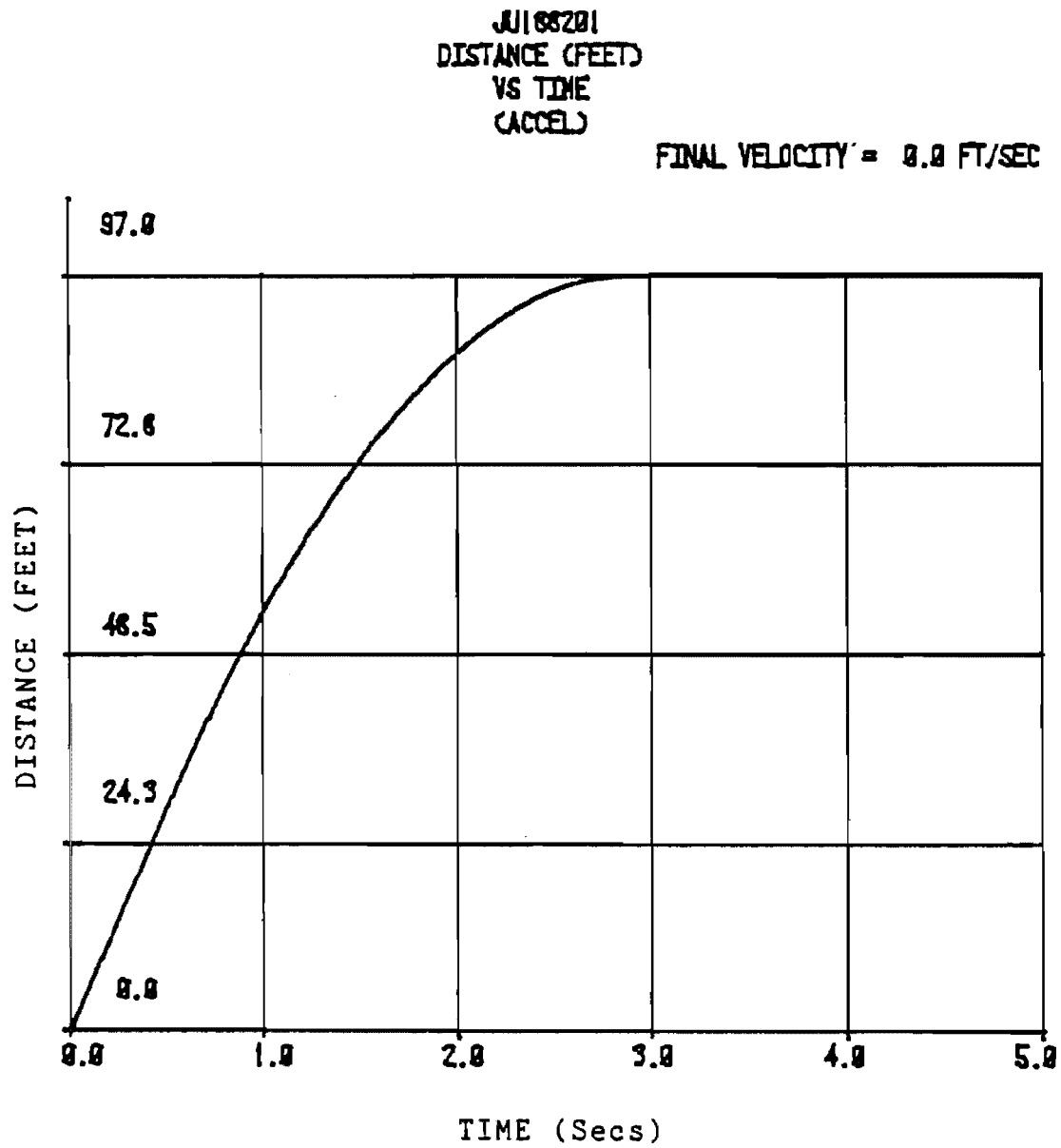


Figure 6-26. Distance vs. Time
June 18, 1982 - Test One

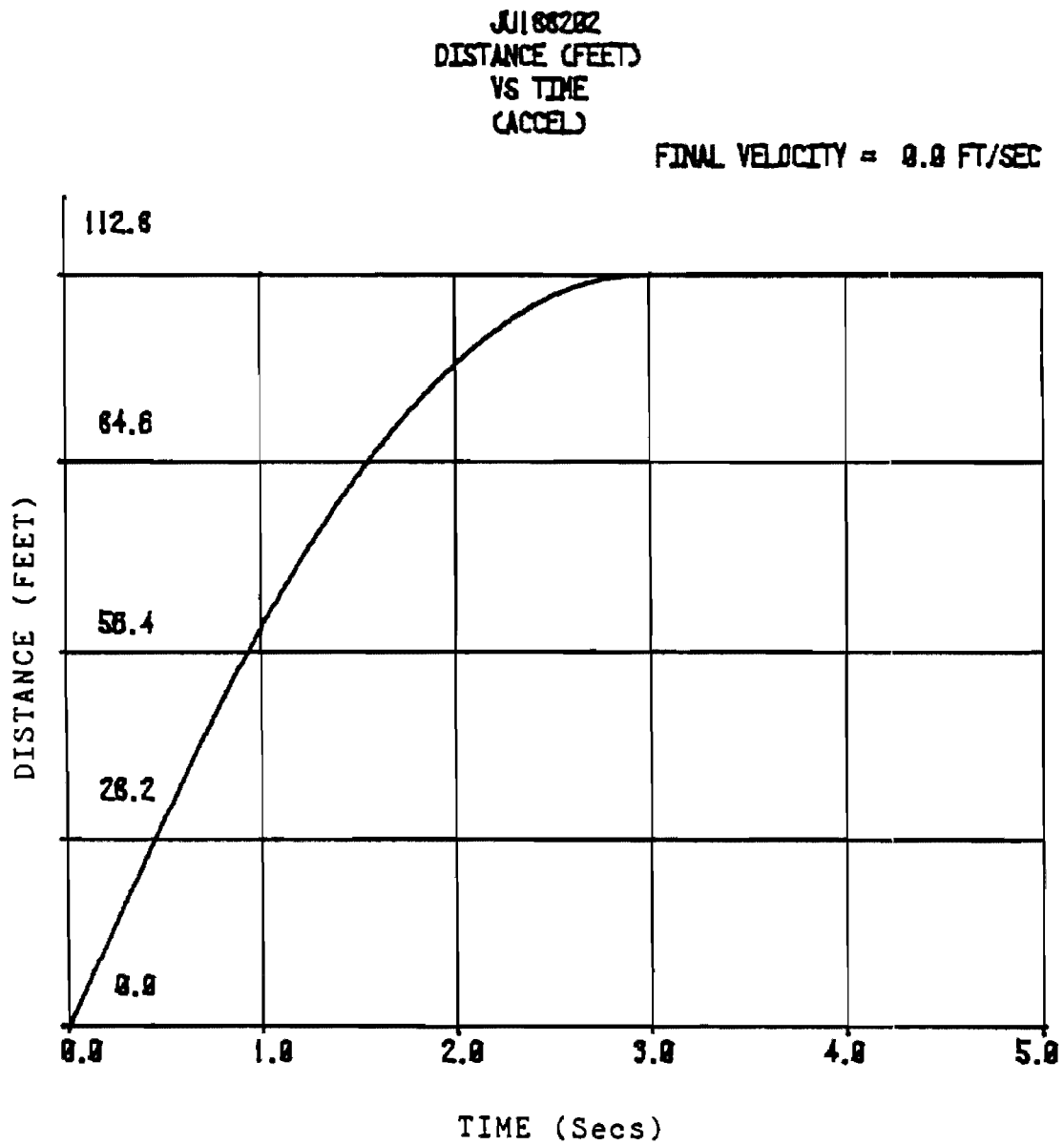


Figure 6-27. Distance vs. Time
June 18, 1982 - Test Two

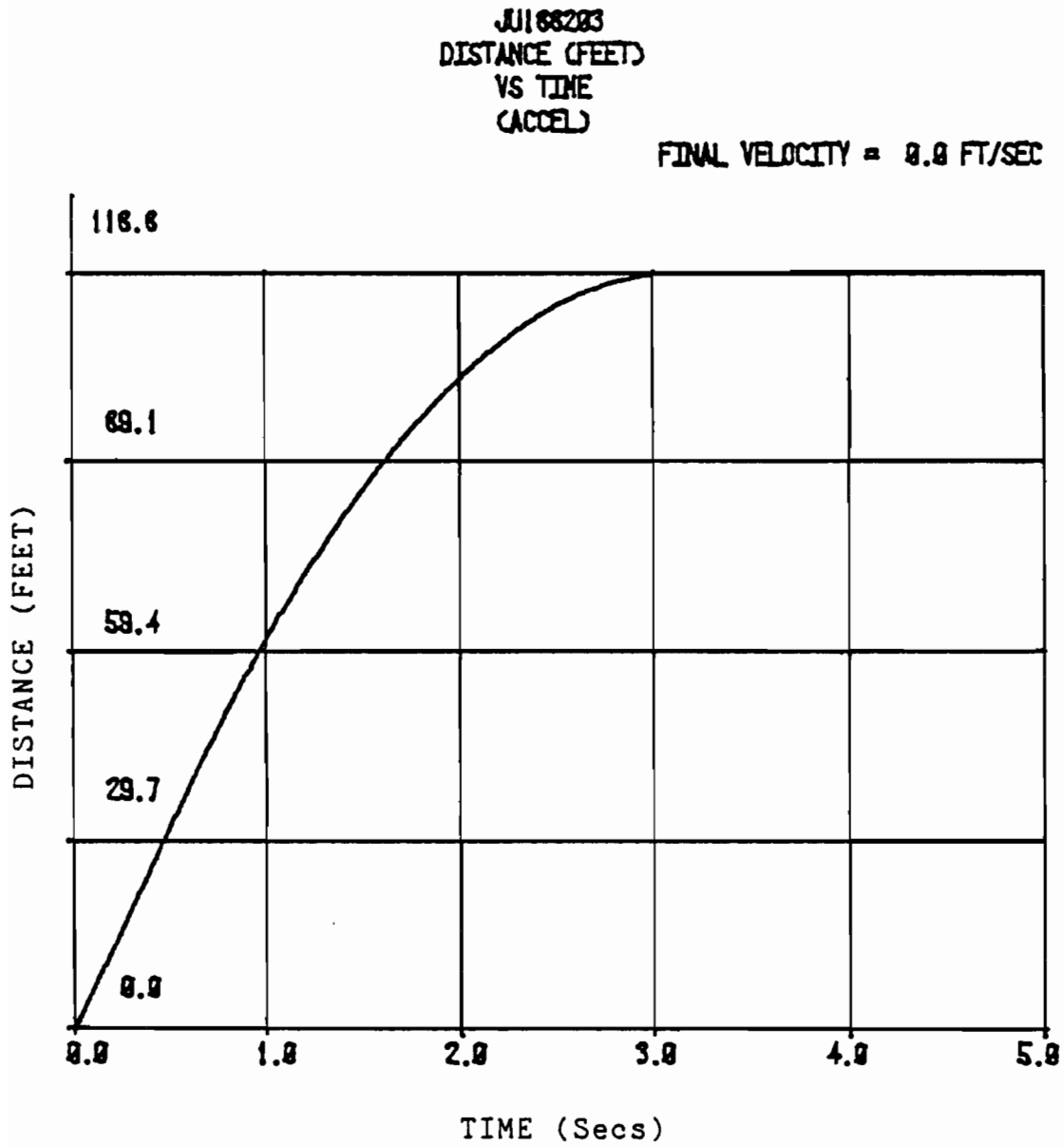


Figure 6-28. Distance vs. Time
June 18, 1982 - Test Three

JU168201
DISTANCE (FEET)
VS TIME
(5TH-WH)

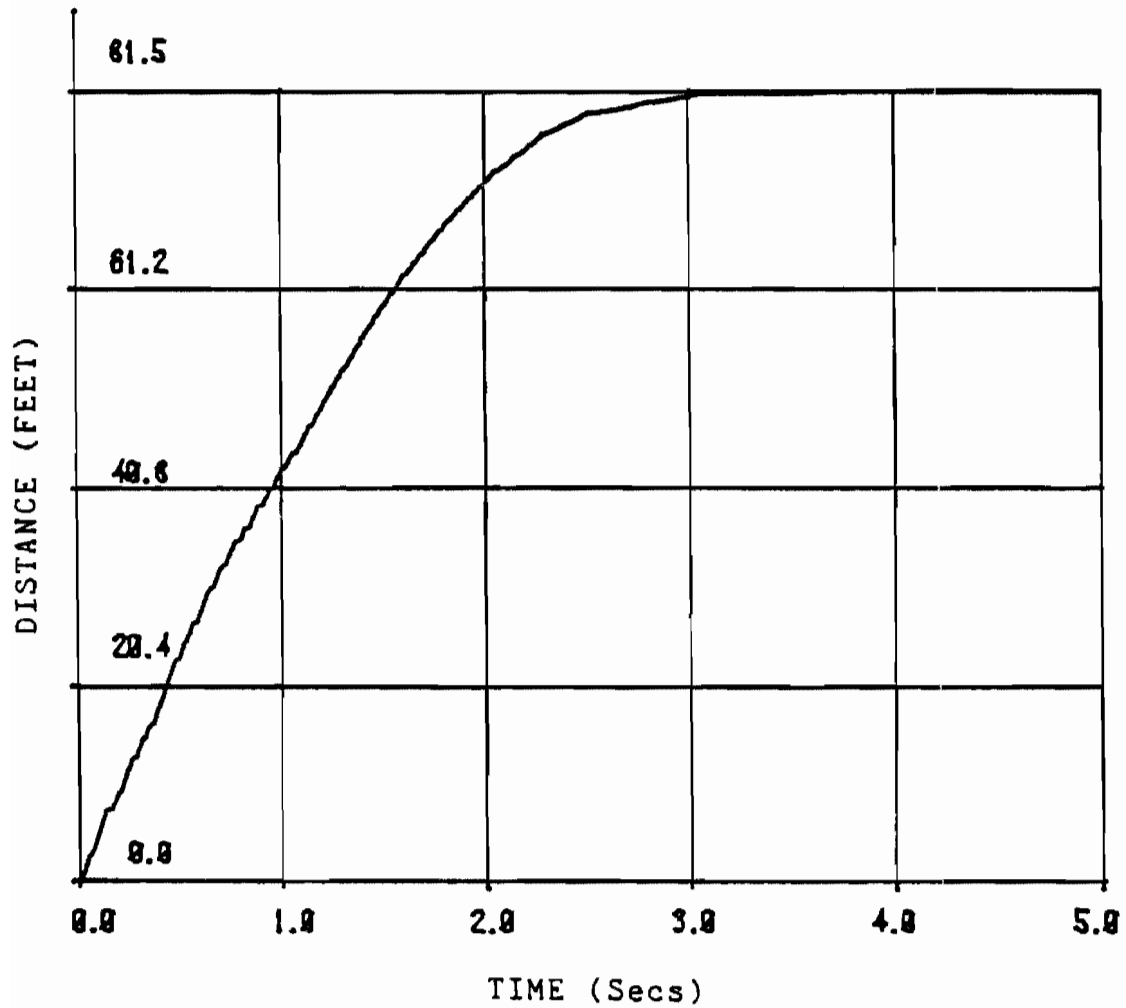


Figure 6-29. Distance vs. Time
June 18, 1982 - Test One
Fifth-Wheel Data

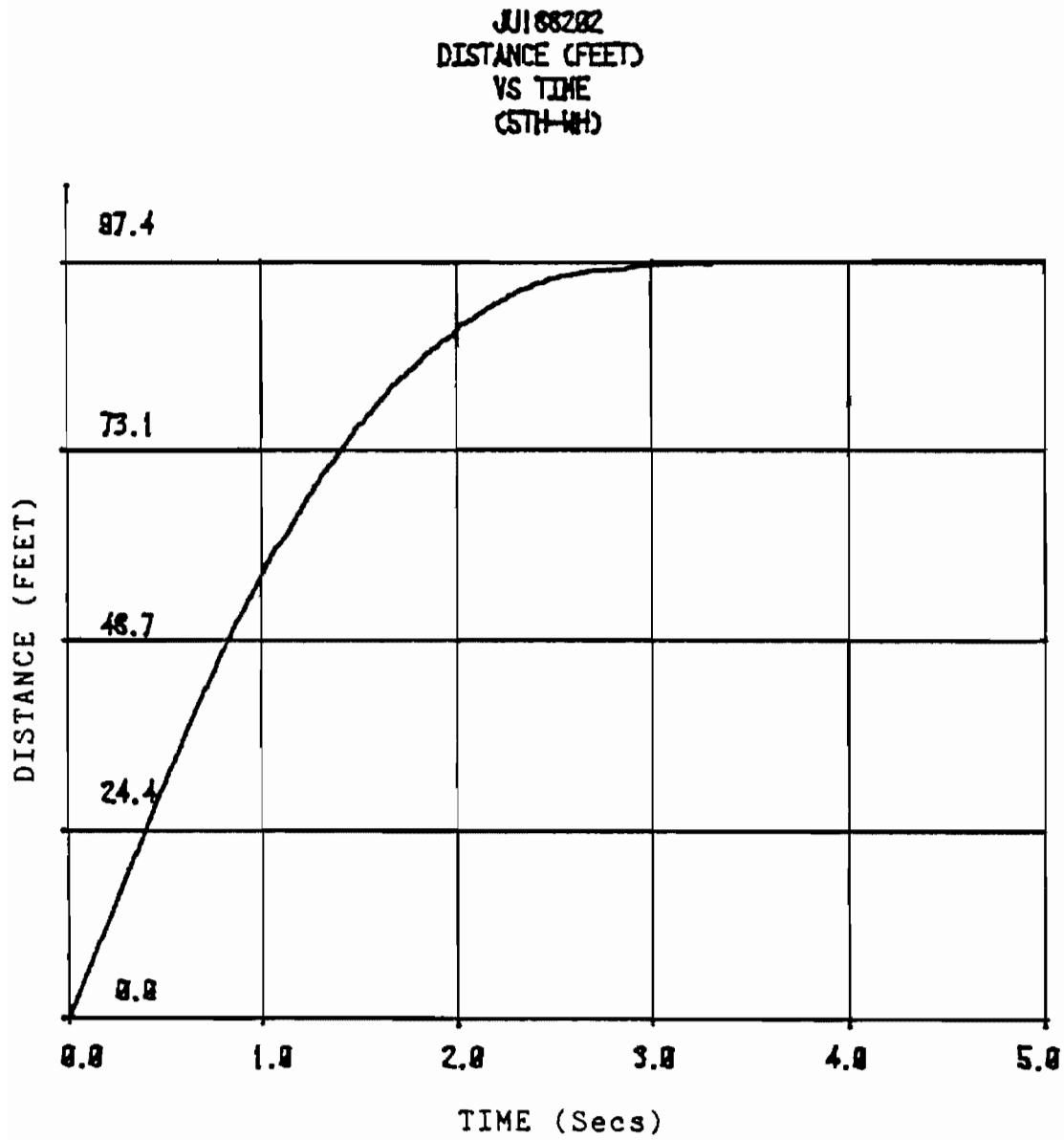


Figure 6-30. Distance vs. Time
June 18, 1982 - Test Two
Fifth-Wheel Data

JU188283
 DISTANCE (FEET)
 VS TIME
 (5TH-WHD)

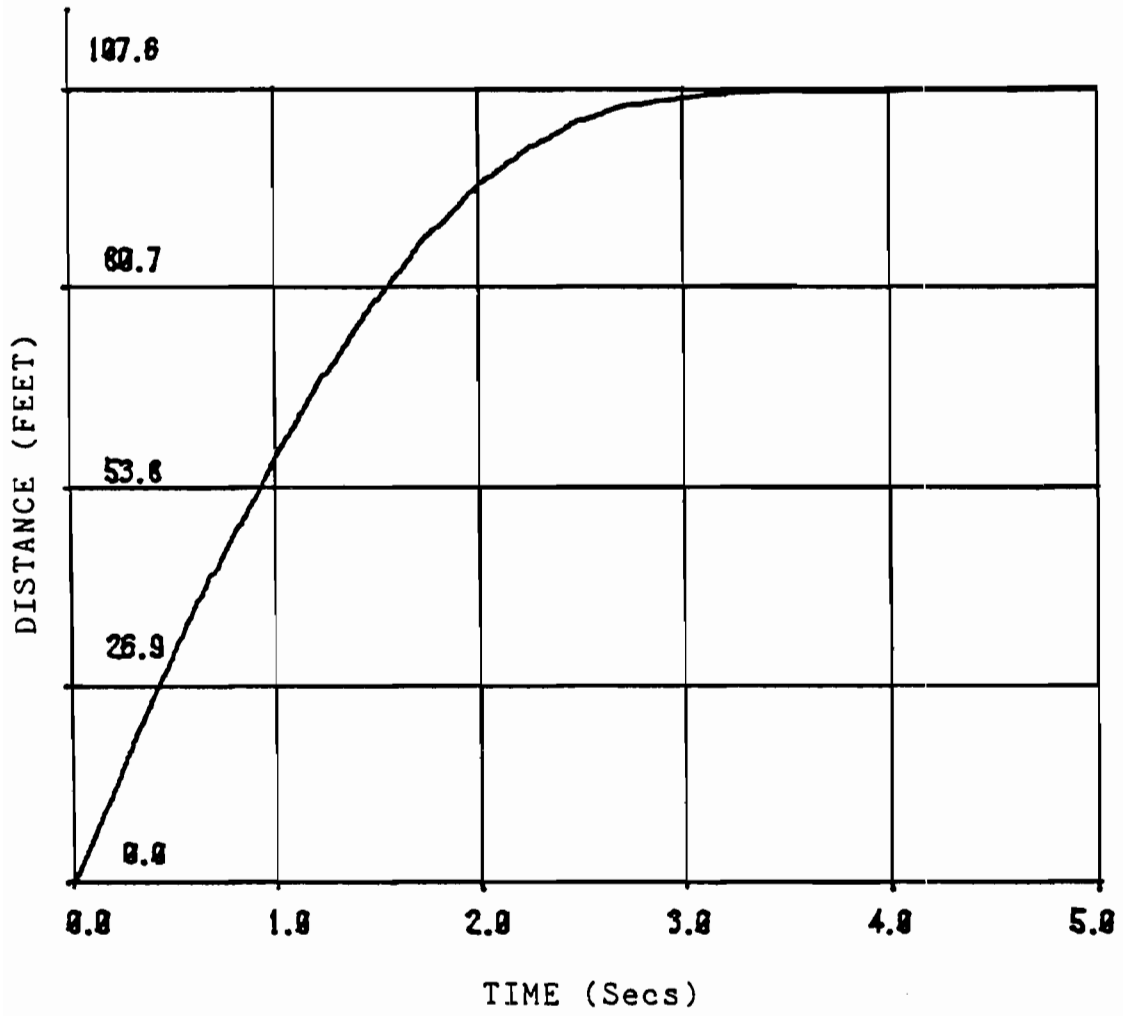


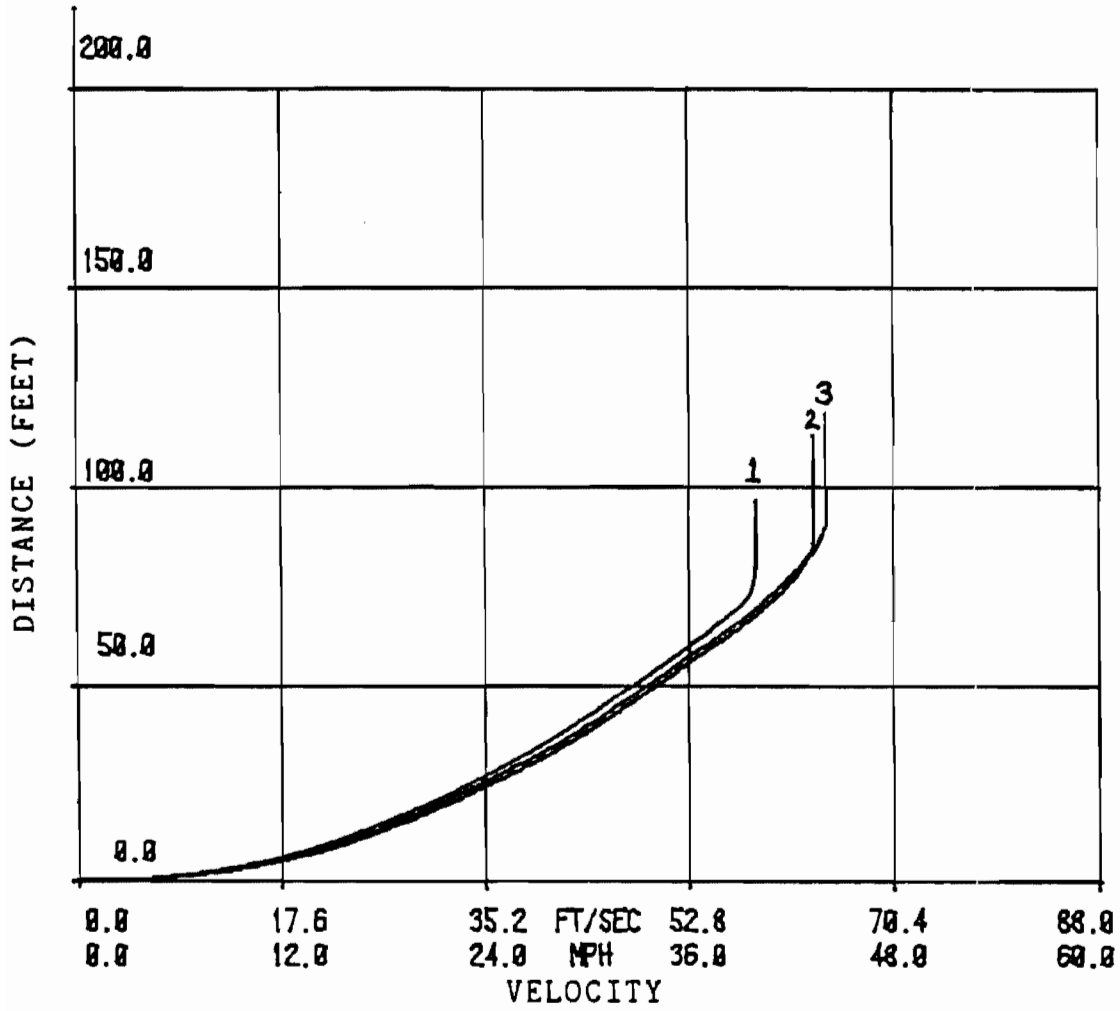
Figure 6-31. Distance vs. Time
 June 18, 1982 - Test Three
 Fifth-Wheel Data

total energy and, therefore, the initial velocity. This integration yields results which are generally lower than the previous results. Close examination of the fifth-wheel distance versus time data reveals points in the curve where the distance did not increase for a short period of time. This indicates that the Hall Effect switch at times did not detect the presence of a magnet passing by it. Eyewitness observations of the fifth-wheel indicate that the fifth-wheel began to bounce severely during the skids which could account for lost pulses. Therefore, the loss of accurate distance versus time data results. During the approach to the skid, the fifth-wheel did not bounce making the initial velocity measurement still valid. Work is currently under way which should correct the fifth-wheel device.

Table 6-2 includes the initial velocity as calculated by Equation (6-13) using the fifth-wheel as the distance data and the length of the skid marks left by the tires on the pavement. It also lists the distance as measured by the fifth-wheel and the distance calculated by the double integration of the deceleration versus time data.

Figure 6-32 is a plot of the distance versus velocity data obtained from the double and single integration of the adjusted deceleration versus time data using the higher recalibrated one-g value. All three curves from the testing done at test site two are contained on the same set of coordinates. The origin of these coordi-

JU188201
 DISTANCE (FEET)
 VS
 VELOCITY (FT/SEC-NPH)
 (ACCEL)



- 1 = Skid Test No. One
- 2 = Skid Test No. Two
- 3 = Skid Test No. Three

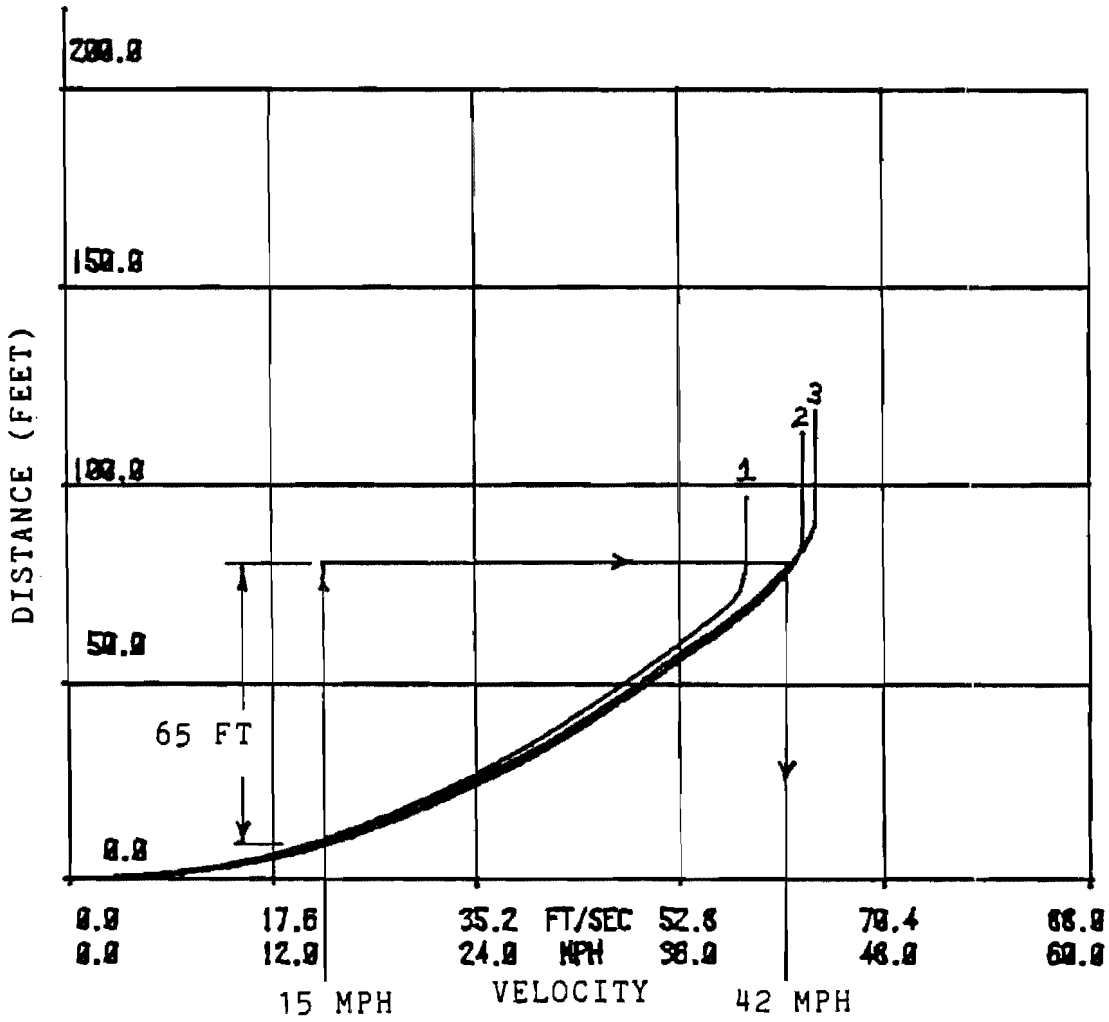
Figure 6-32. Distance vs. Velocity
 Test Site Two

nates is the point where the vehicle has stopped after the skid. From this plot, it can be seen that the distance versus velocity curves tend to fall along the same path. The three tests at site two were done at three different initial velocities so the curves do not end at the same point or velocity. By knowing the skid length of a vehicle which was involved in an accident being reconstructed at the same site, the initial velocity can be estimated. The length of the skid marks would be marked off on the distance scale and the point where the measurement intersects the distance versus velocity curve would indicate the minimum velocity at which the vehicle was travelling. If the velocity is beyond the range of the curve, the curve can be extended in a straight line as an estimate of distance versus velocity characteristics.

Figure 6-33 represents an example of the above procedure using Figure 6-32 as a data base. In a hypothetical example: if a vehicle's skid marks were 65 feet long and it was estimated that it was going 15 miles per hour at impact, the initial velocity can be estimated by adding 65 feet to the skid length which would result from a skid at 15 miles per hour. Using Figure 6-33, it is estimated that the vehicle was going a minimum of 42 miles per hour at the onset of the skid.

The results for the skid tests done at site one is tabulated in Table 6-3 and the distance versus velocity curves are contained in Figure 6-34.

JU188291
 DISTANCE (FEET)
 VS
 VELOCITY (FT/SEC-MPH)
 (ACCEL)



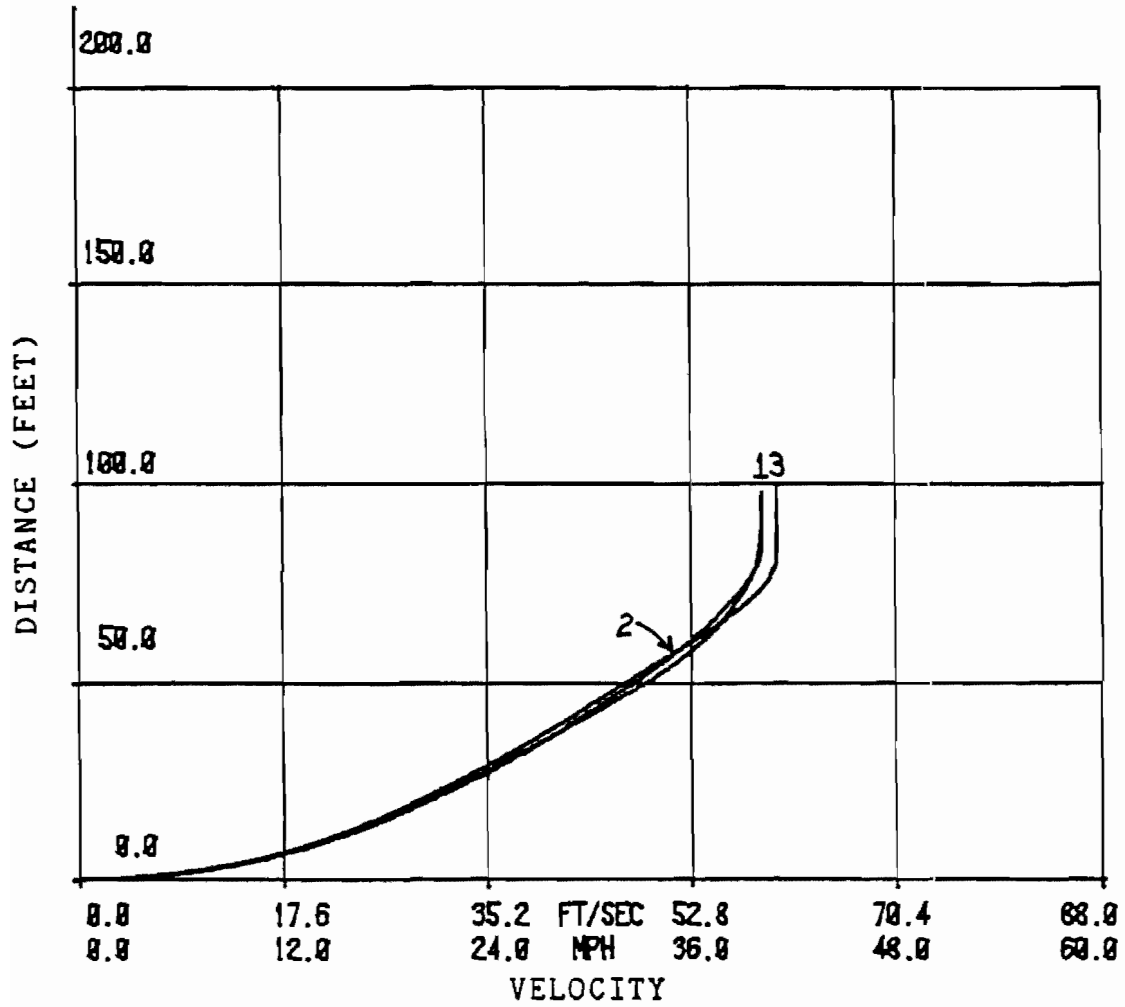
- 1 = Skid Test No. One
- 2 = Skid Test No. Two
- 3 = Skid Test No. Three

Figure 6-33. Distance vs. Velocity
 Test Site Two
 Example Velocity Estimation

TABLE 6-3
RESULTS OF SKID TESTS AT SITE ONE
JUNE 17, 1982

Description	Test Number		
	1	2	3
1. Initial Velocity (5th-Wh)	40 MPH	40 MPH	41 MPH
2. Initial Calibration Value (HEX)	CD	A4	96
3. Calibration Range Adjust	CD -C9	B3 - B0	C0 - BC
4. Velocity Range Using Calib. Range	40.13-40.86 MPH	40.21 - 40.9 MPH	41.06-41.09 MPH
5. Fifth-Wheel Distance	83.4 FT	86.2 FT	89.1 FT
6. Skid Length Measurement	70.5 FT	66.5 FT	76 FT
7. Initial Velocity Using 5th-Wheel Energy	36.09-36.45 MPH	36.85-37.16 MPH	38.08-38.49 MPH
8. Calculated Distance Using Double Integration of Decel. Data	98.00-99.95 FT	97.89-99.56 FT	99.27-101.4 FT

JU178281
 DISTANCE (FEET)
 VS
 VELOCITY (FT/SEC-MPH)
 (ACCEL)



- 1 = Skid Test No. One
- 2 = Skid Test No. Two
- 3 = Skid Test No. Three

Figure 6-34. Distance vs. Velocity
 Test Site One

Careful examination of the deceleration versus time data curves for all the tests reveals that there are differences in the characteristics of the coefficient of friction from one road surface to another. The tests done on relatively unused surfaces (test site one) show that the deceleration and coefficient of friction tend to remain relatively constant, while on a smooth, polished surface (test site two), the coefficient of friction tends to rise dramatically when the speed decreases. This could be explained by the fact that adhesion tends to play more of a role in the friction process at low speeds on smooth surfaces. Each surface must be evaluated separately for an accurate representation of the coefficient of friction.

CHAPTER VII

SUMMARY AND CURRENT WORK

As mentioned at the outset, the work presented herein represents only the beginning of a very extensive program of research. The progress to date has been quite good and represents a significant step in accomplishing our goals.

The analysis routines execute efficiently within the CAD environment and show close agreement with similar SMAC analyses and checks with known boundary conditions. The development of a graphic output device tailored to the needs of computer aided collision reconstruction will complete the development of a second generation of hardware.

Using a portable accelerometer mounted in a vehicle has proved to be a very accurate way to measure the coefficient of friction between a vehicle's tires and the road surface. With the accuracy of the fifth-wheel being within one mile per hour rounded down, the recalibrated accelerometer data is within two percent of the actual μ when an initial velocity of 40 miles per hour is used. The exact accuracy will depend on the accuracy of the fifth-wheel at a given speed. This method closely duplicates many of the unknown variables which were present at the time of the accident and therefore represents a poten-

tial significant improvement in simulation accuracy.

Current work is focused on the integration of the empirical data from the accelerometer into the MASS analysis routines. If instead of utilizing an analytical model of acceleration as it varies with speed, the measured data is used directly, then the trajectory analysis should be extremely accurate.

Continued development of both the instrumentation and hardware/software system is also progressing. For a much more detailed discussion of all work done to date, the reader is again encouraged to refer to references [3] to [8].

REFERENCES

1. J. F. Marquardt, "Vehicle and Occupant Factors that Determine Occupant Injury," SAE Paper 740303, 1974.
2. J. F. Wilson, "Two-Vehicle Collision Reconstruction: A Rational Computer-Aided Approach," Vehicle System Dynamics 2, 1973.
3. B. D. Olson, "A Modular Dynamic Simulation Approach to the Reconstruction of Automobile Accidents," Thesis (M.S. in M.E.), University of Texas, 1979.
4. J. E. Self, "Dynamic Simulation of Automobile Accidents," Thesis (M.S. in M.E.), University of Texas, 1979.
5. W. L. Kroeger, "A Graphic Input Device for a Modular Accident Reconstruction System," Thesis (M.S. in E.E.), University of Texas, 1981.
6. K. L. Dobbins, "An Operating System for a Modular Accident Simulation System," Thesis (M.S. in M.E.), University of Texas, 1982.
7. S. W. Reid, "Measurement of Automobile Tire-To-Road Coefficient of Friction with a Portable Transducer," Thesis (M.S. in M.E.), University of Texas, 1981.
8. R. L. Coke, "Measurement of Vehicle Tire-To-Road Coefficient of Friction With a Portable Microcomputerized Transducer," Thesis (M.S. in M.E.), University of Texas, 1982.
9. G. Grive, I.S. Jones, "Car Collisions--The Movement of Cars and Their Occupants in Accidents," Proc. Inst. Mech. Eng. Vol. 184, 1969-70.
10. R. R. McHenry, "Computer Program for Reconstruction of Highway Accidents," SAE Paper 730980, 1973.
11. F. P. Beer, E. R. Johnston, Jr., Vector Mechanics for Engineers: Dynamics, 2nd ed., McGraw-Hill, New York, 1972.
12. H. Reizes, The Mechanics of Vehicle Collisions, Charles C. Thomas, Springfield, Ill., 1973.

13. R. I. Emori, "Vehicle Mechanics of Intersection Collision Impact," SAE Paper 700177, January 1970.
14. W. Goldsmith, Impact, Edward Arnold, London, 1960.
15. R. M. Brach, "An Impact Moment Coefficient for Vehicle Collision Analysis," SAE Paper 770014, February, 1977.
16. R. P. Mason, D. W. Whitcomb, "The Estimation of Accident Impact Speed," Cornell Aeronautical Laboratory Report No. YB-3109-V-1, August, 1972.
17. K. L. Campbell, "Energy Basis for Collision Severity," SAE Paper 740564, 1974.
18. R. I. Emori, M. Tau, "Vehicle Trajectories After Intersection Collision Impact," SAE Paper 700176, January, 1970.
19. R. R. McHenry, "A Comparison of Results Obtained with Different Analytical Techniques for Reconstruction of Highway Accidents," SAE Paper 750893, 1975.
20. R. R. McHenry, "Development of a Computer Program to Aid the Investigation of Highway Accidents," Cornell Aeronautical Laboratory Report No. VJ-2979-V-1, December, 1971.
21. McHenry, Segal, Lynch, Henderson, "Mathematical Reconstruction of Highway Accidents," January 1973, NTIS No. 220150.
22. R. R. McHenry, J. P. Lynch, "CRASH2 User's Manual," Cornell Aeronautical Laboratory Report No. ZQ-5708-V-4, September, 1976.
23. M. E. James, Jr., H. E. Ross, Jr., "Improvement of Accident Simulation Model," Texas A & M Research Foundation Report No. RF-3258-1, November, 1976.
24. S. A. Lippmann, K. L. Oblizajek, "Lateral Forces of Passenger Tires and Effects on Vehicle Response During Dynamic Steering," SAE Paper 760033, February, 1976.
25. Otis Elevator Company, "Vehicle Lateral Control and Switching Project, Technology Review Study Progress Report, Otis Report - TTD VLACS-023, March, 1978.
26. D. L. Nordeen, "Analysis of Tire Lateral Forces and Interpretation of Experimental Tire Data," SAE Paper 670173, June, 1968.

27. Phelps, Pelz, Pottinger, Marshall, "The Mathematical Characteristics of Steady State, Low Slip Angle Force and Moment Data," SAE Paper 760031, February, 1976.
28. R. L. Wilson, "U. S. and Foreign Car Specifications," Motor Vehicle Manufacturers Association of the United States.
29. J. H. Dillard, "Measuring Pavement Slipperiness with a Pendulum Decelerometer," Highway Research Board, Bulletin 348, 1962, pp. 36-43.
30. Limpert, Rudolf, Motor Vehicle Accident Reconstruction and Cause Analysis, Michie, Charlottesville, Va, 1978.
31. W. E. Dillard and T. M. Allen, "Comparison of Several Methods of Measuring Road Surface Friction," Highway Research Board, Bulletin 219, January 1959, pp. 25-51.
32. F. P. Nichols, Jr., H. H. Dillard, and R. L. Alwood, "Skid Resistance Pavements in Virginia," Highway Research Board, Bulletin 139, 1956, pp. 35-59.
33. A. F. Marshall and W. Gartner, Jr., "Skid Characteristics of Florida Pavements Determined by Tapley Decelerometer and Actual Stopping Distances," Highway Research Board, Bulletin 348, 1962, pp. 1-17.
34. S. Mercer, "Locked Wheel Skid Performances of Various Tires on Clean, Dry Road Surfaces," Highway Research Board, Bulletin 186, 1958, pp. 8-25.
35. K. A. Grosch, "The Speed and Temperature Dependence of Rubber and its Bearing on the Skid Resistance of Tires," The Physics of Tire Traction, Theory, and Experiment (D. F. Hays and A. L. Brown, ED) Plenum, New York, 1974; Symposium held at General Motors Research Laboratories, Warren, Michigan, Oct 8-9, 1973, pp. 143-165.
36. K. C. Ludeme, D. F. Moore, R. Schonfeld, Williams and W. O. Yandell, "Tire Traction-The Role of the Pavement," The Physics of Tire Traction, Theory, and Experiment, (D. F. Hays and A. L. Brown, ED) Plenum, New York, 1974; Symposium held at General Motors Research Laboratories, Warren, Michigan, Oct 8-9, 1973, pp. 361-376.
37. W. E. DeVinney, "Factors Affecting Tire Traction," SAE Paper No. 670461, SAE Transactions, May 1967, pp. 1649-1656.

38. W. E. Davisson, "Basic Test Methods for Evaluating Tire Traction," SAE Paper No. 680136, SAE Transactions, January 1968, pp. 561-570.
39. W. O. Yandell, "The Relationship Between the Stress Saturation of Sliding Rubber and the Load Dependence of Road Tire Friction," The Physics of Tire Traction, Theory, and Experiment (D. F. Hays and A. L. Brown, ED) Plenum, New York, 1974; Symposium held at General Motors Research Laboratories, Warren, Michigan, Oct 8-9, 1973, pp. 311-323.
40. S. K. Clark, R. N. Kienle, H. B. Pacejka and R. F. Peterson, "Tire Traction-The Role of the Tire," The Physics of Tire Traction, Theory, and Experiment (D. F. Hays and A. L. Brown, ED) Plenum, New York, 1974; Symposium held at General Motors Research Laboratories, Warren, Michigan, Oct 8-9, 1973, pp. 361-376.
41. R. F. Peterson, C. F. Eckert, and C. I. Carr, "Tread Compound Effects in Tire Traction," The Physics of Tire Traction, Theory, and Experiment (D. F. Hays and A. L. Brown, Ed), Plenum, New York, 1974; Symposium held at the General Motors Research Laboratories, Warren Michigan, Oct 8-9, 1973, pp. 223-239.
42. A. M. White and H. O. Thompson, "Tests for Coefficients of Friction by Skidding Car Method on Wet and Dry Surfaces," Highway Research Board, Bulletin 186, 1958, pp. 26-34.
43. L. Segal, "Tire Traction on Dry Uncontaminated Surfaces," The Physics of Tire Traction, Theory and Experiment (D. F. Hays and A. L. Brown, Ed) Plenum, New York, 1974; Symposium held at the General Motors Research Laboratories, Warren Michigan, Oct 8-9, 1973, pp. 65-98.
44. V. E. Grough, "A Tire Engineer Looks Critically at Current Traction Physics," The Physics of Tire Traction, Theory, and Experiment (D. F. Hays and A. L. Brown, Ed) Plenum, New York, 1974; Symposium held at the General Motors Research Laboratories, Warren, Michigan, Oct 8-9, 1973, pp. 281-297.
45. W. E. Meyer, "Friction and Slipperiness," Highway Research Record, No. 214, 1968, pp. 13-17.
46. W. E. Meyer and H. W. Kummer, "Pavement Friction and Temperature Effects," Highway Research Board, Special Report 101, 1969, pp. 47-55.

47. R. Schonfeld, "Pavement Surface Texture Classification and Skid Resistance Photo Interpretation," The Physics of Tire Traction, Theory, and Experiment (D. F. Hays and A. L. Brown, Ed) Plenum, New York, 1974; Symposium held at the General Motors Research Laboratories, Warren, Michigan, Oct 8-9, 1973, pp. 325-338.
48. W. Close, "Locked Wheel Friction Tests on Wet Pavements," Highway Research Board, Bulletin 302, 1961, pp. 18-34.
49. E. Rabinowicz, Friction and Wear of Materials, John Wiley & Sons, New York, 1965.
50. "Review of Laboratory and Field Methods of Measuring Road Surface Friction," Report of Subcommittee E to the First International Skid Prevention Conference, Charlottesville, Virginia, September 8-12, 1958, Highway Research Board, Bulletin 219, 1959, pp. 52-55.
51. R. L. Calcote, "A Comparison of High-Speed Photography and Accelerometer Data Reducing Techniques," Experimental Mechanics, May 1977, pp. 167-171.
52. L. A. Leventhal, 8080A/8085 Assembly Language Programming, Osborne/McGraw Hill, Inc. Berkley, California, 1978.
53. R. J. Bibbero, Microprocessors in Instruments and Control, John Wiley & Sons, New York, 1977.
54. P. A. Stark, Introduction to Numerical Methods, The MacMillan Co., New York, N.Y., 1970.